ENZYMATIC REDUCTION OF NITRO COMPOUNDS TO AMINES WITH NITROREDUCTASES

A Dissertation
Presented to
The Academic Faculty

by

Jonathan T. Park

In Partial Fulfillment
of the Requirements for the Degree
Doctor of Philosophy in the
School of Chemical & Biomolecular Engineering

Georgia Institute of Technology
August 2014

ENZYMATIC REDUCTION OF NITRO COMPOUNDS TO AMINES WITH NITROREDUCTASES

Approved by:

Dr. Andreas S. Bommarius, Advisor
School of Chemical & Biomolecular Engineering
Georgia Institute of Technology

Dr. Christopher W. Jones
School of Chemical & Biomolecular Engineering
Georgia Institute of Technology

Dr. Julie A. Champion
School of Chemical & Biomolecular Engineering
Georgia Institute of Technology

Dr. Jim C. Spain
School of Civil and Environmental Engineering
Georgia Institute of Technology

Dr. Giovanni Gadda
Department of Chemistry
Georgia State University

Date Approved: June 10, 2014

To my grandparents.

초지일관

初志一贯

Be persistent and finish what you have set forth to accomplish.

ACKNOWLEDGEMENTS

I wish to thank my Advisor Professor Andreas Bommarius for all his guidance and encouragement over the years. Most importantly, for the freedom that he gave me to shape this thesis, and being patient with me throughout the years. I thank Prof. Julie Champion, Prof. Giovanni Gadda, Prof. Christopher Jones and Prof. Jim Spain for taking the time to be on my committee and providing me with valuable feedback.

I was very fortunate to have the opportunity to work with Prof. Anne-Frances Miller at the University of Kentucky, and her group members Ning and John. The wonderful discussions and occasional trips back and forth helped progress this project immensely. The Atlanta Flavin Group (AFM) has been a great source of insight for me. Prof. Dale Edmondson, Prof. Giovanni Gadda, Prof. Stefan Lutz, and all the students and Postdocs involved have presented me with an enormous amount of questions and discussion to direct my research.

I wish to thank many members of the Bommarius Lab that helped form me as a researcher and made the everyday life in the lab a pleasure. I thank Dr. Mélanie Hall for helping me start out in the lab, Dr. Janna Blum for training me on the HPLC and teaching me molecular biology skills, Ryan Clairmont for his help with NMR and MS work, visiting student Simeon Leupold for the extraordinary amount of work done during his short stay at GT, undergraduate researcher Kyle Ferguson for his efforts in the lab including the hydroxylamine synthesis work, Lizzette M. Gómez Ramos for her hard work and dedication. I enjoyed the company of many great colleagues. Past members: Drs. Tom Rogers, Yanto Yanto, Prabuddha Bandsal, Michael Abrahamson, and Russell

Vegh; thank you for all your help and inspiration in the lab. Current members: Dr. Bettina Bommarius, Dr. Minjeong Sohn, Dr. Mick Robbins, Michael Rood, Yuzhi Kang, Samantha Au, Marietou Paye, Aditi Sharma and Harrison Rose; the entertainment provided by all of you during my stay will be memorable.

I have two remarkable friends that I will never forget. I thank Jonathan "T" Rubin for being a great influence in research and being an even better friend. I could not have asked for a better lab-mate. Dun-Yen Kang, my roommate of nearly two years, for being the perfect roommate I saw more often at school. I enjoyed every moment of your presence, minus the terrible jokes.

My family has been truly supportive and trusting in me during my Ph.D. studies, and even before that. Thank you Mom, Dad, Minjoo and Meesun; the days spend with all of you are the best. My now extended family members (in-laws) have been nothing but kind to me and it is a joy to have every one of you in my life. I thank my beautiful wife Hyea. Without her understanding and sacrifices, I would not have been able to finish my degree at such a pace. Thank you Aaron, for simply being there smiling and hugging me when I arrive home, and calling me 아빠.

TABLE OF CONTENTS

Page

ACKNOWLEDGEMENTS iv

LIST OF TABLES xii

LIST OF FIGURES xiii

LIST OF SYMBOLS xvi

LIST OF ABBREVIATIONS xvii

SUMMARY xix

CHAPTERS

1 INTRODUCTION 1

1.1 Biocatalysis 1

1.2 Flavoenzymes 1

1.3 Nitroreductases 4

1.3.1 Literature survey of NR 5

1.3.2 NR applications 8

1.3.3 Nitrobenzene reduction and state of the art 11

1.4 Other flavoenzymes 13

1.4.1 Ene-reductases 13

1.4.2 NAD(P)H oxidases 15

1.5 NAD(P)H regeneration 18

1.6 Map of Dissertation 19

2 Reduction of Nitrobenzene with Nitroreductases 20

2.1 Introduction & Motivation 20

2.2 Materials & Methods 21
2.2.1 Enzymes and other materials 21
2.2.2 Protein Expression 21
2.2.3 Purification of Enzymes 22
2.2.4 Enzyme Assays 24
2.2.5 Gas chromatography (GC) 24
2.2.6 ^{15}N-NMR 25
2.2.7 High-performance liquid chromatography (HPLC) analysis 25
2.2.8 Liquid chomatography-mass spectroscopy (LC-MS) analysis 25
2.2.9 Synthesis of hydroxylamino compounds 26
2.3 Results & Discussion 26
2.3.1 Expression and purification of NRs 26
2.3.2 Spectral Characterization 28
2.3.3 Study of NRsalty and NRentcl-TRX 29
2.3.4 Product characterization through multiple analytical tools 30
2.3.5 Possibility of Amine Formation 34
2.4 Conclusion 37
3 Hammett correlation in biocatalytic nitroaromatic Reduction 39
3.1 Introduction & Motivation 39
3.2 Materials & Methods 40
3.2.1 Enzymes and Chemicals 40
3.2.2 Enzyme activity assays 40
3.2.3 Data analysis and fitting 41

3.3 Results & Discussion 42
3.3.1 NAD(P)H kinetics and preference 42
3.3.2 pH dependence of $\boldsymbol{kcat}$ and $\boldsymbol{kcat/KMS}$ 44
3.3.3 Specific activity of substituted nitroaromatics 45
3.3.4 Hammett Correlation 47
3.4 Conclusion 51
4 Enzymo-Chemical Synthesis of amines 52
4.1 Introduction & Motivation 52
4.2 Materials & Methods 53
4.2.1 Chemicals 53
4.2.2 Reducing agent screening 53
4.2.3 HPLC analysis 54
4.2.4 Enzymo-chemical reduction 54
4.2.5 Large Scale Synthesis 54
4.3 Results & Discussion 55
4.3.1 Sodium dithionite 55
4.3.2 Overall scheme of reduction 56
4.3.3 Screening reducing agents 57
4.3.4 Optimization of formamidine sulfinic acid (FSA) reduction conditions 57
4.3.5 Enzymo-chemical reduction 59
4.3.6 Scale-up of synthesis 60
4.4 Conclusion 62
5 Engineering towards Nitroreductase Functionality in Ene-reductase Scaffolds 63

5.1 Introduction & Motivation 63
5.2 Materials & Methods 64
5.2.1 Chemicals 64
5.2.2 Cloning 65
5.2.3 Protein expression and purification 65
5.2.4 Enzyme activity assays and data fitting 66
5.2.5 Product determination 67
5.2.6 Circular dichroism (CD) 67
5.2.7 Fluorescence study 67
5.3 Results & Discussion 67
5.3.1 Effect of C25G mutation for XenA 68
5.3.2 Analogous threonine to glycine mutation 69
5.3.3 Increasing the active site cavity 70
5.3.4 Iterative mutagenesis for activity improvement 74
5.3.5 Elimination of ER activity 74
5.3.6 Functional, kinetic and thermal characterization of variants 75
5.3.7 Nitroreductase vs. ene-reductase functionality 78
5.3.8 Universal application of mutations 80
5.4 Conclusion 81
6 NAD(P)H oxidase V (NoxV) from *Lactobacillus plantarum* displays enhanced operational stability even in absence of reducing agents 82
6.1 Introduction 82
6.2 Materials & Methods 84

6.2.1 Enzymes and other materials 84
6.2.2 Cloning 84
6.2.3 Site-directed mutagenesis 84
6.2.4 Overexpression 85
6.2.5 Purification 85
6.2.6 Enzyme assay and protein determination 86
6.2.7 pH activity 86
6.2.8 Temperature activity 87
6.2.9 Temperature stability 87
6.2.10 Kinetic parameters 87
6.2.11 Amplex Red Assay (H_2O_2 presence) 87
6.2.12 Total turnover number (TTN) 88
6.3 Results & Discussion 88
6.3.1 Cloning, expression, and purification 88
6.3.2 Enzyme activity and stability 90
6.3.3 Kinetic parameters 93
6.3.4 Water/H_2O_2 formation 95
6.3.5 Total turnover number (TTN) 95
6.3.6 Mutation for NADPH activity 99
6.3.7 Study of variants L179R and G178R/L179R 100
6.4 Conclusion 101
7 Recommendations and Conclusions 103
7.1 Recommendations 103

7.1.1 Enzymatic reduction of hydroxylamine 103
7.1.2 High-throughput colorimetric assay 106
7.1.3 Overcoming low solubility 108
7.2 Conclusions 109
Appendix A Enzyme Nomenclature 112
Appendix B Phylogenetic Tree 113
Appendix C Constructs & Primers 116
Appendix D NRmycsm Characterization 118
Appendix E Supplementary Information for Chapter 5 122
Appendix F Colorimetric assay methods 125
REFERENCES 126
VITA 143

LIST OF TABLES

Page

Table 1.1 Cost of nicotinamide cofactors and regeneration systems 18

Table 2.1 Comparison of amino-acid sequence identity/similarity 21

Table 2.2 Substrate Study for Nitro Reduction. 35

Table 3.1 Apparent kinetic parameters for NAD(P)H with fixed 2, 4-DNT 42

Table 3.2 Kinetic parameters for various substituted nitroaromatics 48

Table 4.1 Preliminary screen of reducing agents. 57

Table 5.1 Kinetics parameters of XenA wild-type (WT) and variant C25G 68

Table 5.2 Summary of ER and NR specific activity 73

Table 5.3 Kinetic characterization of KYE1 wild-type and variants. 76

Table 5.4 Thermal characterization of KYE1 wild-type and variants. 78

Table 6.1 Sequence identity and similarity comparison of NADH oxidases 90

Table 6.2 Table of purification of NoxV 90

Table 6.3 Comparison of TTN for NADH oxidases 97

Table 6.4 Cell lysate activity of mutants. 100

Table 6.5 Kinetic parameters of wild-type (WT) and mutant NAD(P)H oxidases 101

Table C.1 Construct information 116

Table C.2 Primer design for NoxV variants 116

Table C.3 ER to NR site-directed mutagenesis primer forward sequence 117

Table C.4 Primer design for NRentcl library 117

Table E.1 Growth conditions for KYE variants 122

Table E.2 Summary of KYE1 variants activity comparison 123

LIST OF FIGURES

Page

Figure 1.1 Structure of flavins 2

Figure 1.2 General mechanism of flavin redox chemistry 4

Figure 1.3 Schematic of two-electron reduction of nitro reduction 5

Figure 1.4 Crystal structure of NRentcl and NRmycsm 6

Figure 1.5 Applications of nitroreductases 8

Figure 1.6 Active pharmaceutical ingredients production from nitro precursors 10

Figure 1.7 Proposed reduction pathways of nitrobenzene to aniline 10

Figure 1.8 Schematic of asymmetric reduction of alkenes with EWGs 13

Figure 1.9 Crystal structure of OYE1 from *S. pastoris* 14

Figure 1.10 Schematic of O_2 reduction with either nox1 or nox2 16

Figure 1.11 Crystal structure of NADPH oxidase from *L. sanfranciscensis* 16

Figure 1.12 Overall Reactions Catalyzed by nox2 NAD(P)H Oxidases 17

Figure 1.13 NAD(P)H regeneration scheme with different enzymes. 19

Figure 2.1 SDS-PAGE with 12% gel of NRsalty and NRmycsm 27

Figure 2.2 Spectrum of FMN liberated from NRsalty and NRmycsm 27

Figure 2.3 Spectral studies of nitrobenzene and its derivatives 28

Figure 2.4 Nitrobenzene reduction catalyzed by NRentcl and NRsalty 30

Figure 2.5 ^{15}N-NMR scan of nitrobenzene-^{15}N reduced with NRsalty 32

Figure 2.6 LC-MS analysis of NRsalty product\ 33

Figure 2.7 Nitroaromatic substrates used for product distribution studies 34

Figure 2.8 Proposed fragmentation of nitrofurazone and its corresponding amine. 36

Figure 2.9 Updated reaction pathway of NB with NR..... 37

Figure 3.1 pH dependence of $\log(k_{cat}/K_M^S)$ and $\log(k_{cat})$ 43

Figure 3.2 Specific activity plotted according to the Hammett equation 46

Figure 3.3 Hammett plots for NRsalty and NRmycsm..... 49

Figure 4.1 Overall reduction scheme of the enzyme-chemical sequence..... 52

Figure 4.2 Proposed setups for combining the enzymatical and chemical reactions..... 56

Figure 4.3 Production of amine with FSA while varying the pH value 58

Figure 4.4 One-pot two-step reduction of 4-nitrobenzoic acid with NRsalty..... 60

Figure 4.5 ^{1}H-NMR spectra of 4-aminobenzoic acid in DMSO-d_6..... 61

Figure 4.6 HPLC chromatogram of purified 4-aminobenzoic acid 62

Figure 5.1 Specific activity dependence of XenA wild-type (WT) and variant C25G..... 68

Figure 5.2 Amino acid alignment of ERs compared to XenA C25G 69

Figure 5.3 Specific activity of YersER and KYE1 70

Figure 5.4 Substrate binding cavity comparison of OYE1, XenA and NRentcl 71

Figure 5.5 KYE1 crystal structure with mapped site-directed mutagenesis approach 71

Figure 5.6 Iterative mutagenesis to increase NR activity with 4-NBS as a substrate..... 73

Figure 5.7 Switch of activity from ER to NR. 75

Figure 5.8 Kinetics of KYE1 variants..... 76

Figure 5.9 Temperature dependent unfolding of KYE1 wild-type and variants 77

Figure 5.10 Evolutionary trade-off between ER and NR activity 79

Figure 5.11 Active sites of A) NerA, B) OPR-3, C) OYE-1, and D) XenA..... 80

Figure 6.1 Schematic conversion of ribitol to L-ribose NADH cofactor regeneration..... 83

Figure 6.2 SDS-PAGE (12% gel) analysis of NoxV 89

Figure 6.3 *L. plantarum* NoxV activity profile at different pH values 91

Figure 6.4 *L. plantarum* NoxV activity profile at various temperatures 92

Figure 6.5 T_{50}^{30} plot to study stability of *L. plantarum* NoxV 92

Figure 6.6 Michaelis-Menten kinetics to determine NoxV kinetic parameters 94

Figure 6.7 Hanes-Woolf plot to identify NAD^+ inhibition. 94

Figure 6.8 Total turnover number (TTN) analysis with different amounts of enzyme 96

Figure 7.1 Comparison of nitro, nitroso, hydroxylamine moieties. 104

Figure 7.2 Crystal structure of NRentcl 104

Figure 7.3 Proposed reaction scheme with a conjugated system of NRs and cytochrome enzymes (CYB5R and CYB5). 106

Figure 7.4 MBTH assay results 107

Figure B.1 NR phylogenetic tree 113

Figure B.2 ER phylogenetic tree 114

Figure B.3 Sequence alignment of ERs and NRs 115

Figure D.1 NRmycsm activity profile 119

Figure D.2 Thermal denaturation of NRmycsm 120

Figure E.1 Enzymatic production of 4-HABS from 4-NBS 124

LIST OF SYMBOLS

k_{cat}	Rate constant
k_{non}	non-catalyzed reaction rate constant
K_M^S	Michaelis constant of substrate (S)
$K_M^{NAD(P)H}$	Michaelis constant of NAD(P)H
σ	Hammett substituent constant
ρ	Hammett reaction constant
E_a	Activation energy
T_m	Melting temperature
ΔH_m	Enthalpy of melting

LIST OF ABBREVIATIONS

2, 4-DNT	2, 4-Dinitrotoluene
4-NNA	4-Nitro-1,8-naphthalic anhydride
4-NBS	4-Nitrobenzenesulfonamide
4-NBA	4-Nitrobenzoic acid
4-NBN	4-Nitrobenzonitrile
API	Active pharmaceutical ingredient
AFZ	Aminofurazone
ACS	ammonium cerium(IV) sulfate dehydrate
AN	Aniline
AYB	Azoxybenzene
BME	β-mercaptoethanol
CV	Column volulme
DTT	Dithiothreitol
ER	Ene-reductase
EWG	Electron-withdrawing group
FAD	Flavin adenine dinucleotide
FMN	Flavin mononucleotide
FDA	Food and Drug Administration
FSA	Formamidine sulfinic acid
FDH	Formate dehydrogenase
GDH	Glucose dehydrogenase

GTN	Glyceryl trinitrate
KIP	Ketoisophorone
MBTH	3-Methyl-2-benzothiazolinone hydrazone hydrochloride monohydrate
Nox	NAD(P)H oxidase
NADH	Reduced nicotinamide adenine dinucleotide
NADPH	Reduced nicotinamide adenine dinucleotide phosphate
NB	Nitrobenzene
NFZ	Nitrofurazone
NR	Nitroreductase
NOB	Nitrosobenzene
OYE	Old yellow enyzme
PCAF	Pentacyanoammineferroate sodium salt
PETN	Pentaerythritol tetranitrate
PHA	Phenylhydroxylamine
PDB	Protein Data Bank
SD	Sodium dithionite
TRX	Thioredoxin
TTN	Total turnover number
TAT	Triaminotoluene
TNT	Trinitrotoluene
QSAR	Quantitative structure–activity relationship
QSAR	Visual Molecular Dynamics

SUMMARY

Biocatalysis is nature's method of transforming organic compounds where enzymes are by far the most abundant natural catalyst for this task. Their major advantage lies in their selectivity and specificity, be it high *chemo*-, *regio*-, or *enantio*-selectivity or specificity. Such characteristics have propelled biocatalysis to complement and sometimes replace other catalytic routes for synthesizing chemicals, food ingredients, and active pharmaceutical ingredients (APIs). Enzymes that require the presence of a flavin cofactor for catalysis are called flavoenzymes. In this study, we utilize three different flavoenzymes for biocatalysis: mainly nitroreductases (NRs), but also ene-reductases (ERs) and NAD(P)H oxdiases (Noxs).

NRs are enzymes that catalyze the reduction of nitroaromatics to their corresponding nitroso, hydroxylamine, and, in limited cases, amine They have gathered interest in many scientific communities, and are currently actively researched bioremediation and prodrug activation. Here we attempt to utilize them for the purpose of synthesizing substituted aromatic amines that are found in a number of active pharmaceutical ingredients (APIs). As NRs described in the literature have varying product distribution ranges (from those that produce hydroxylamine to others that yield amine) several similar and different NRs were studied for their selectivity. Additionally, a quantitative structure–activity relationship (QSAR) was determined to characterize the substrate specificity of NRs.

To employ the use of flavoenzymes in synthesis, multiple *reaction*- and *protein*-engineering approaches were devised. One scheme was to establish an enzymo-chemical

synthesis where NRs were paired with reducing agents for a chemical reduction. Another method was to create a monomeric NR through directed evolution from ER scaffolds for future immobilization applications. Protein engineering techniques were also utilized on NADH oxidases which we characterized and developed for nicotinamide cofactor regeneration. As a whole, this dissertation expands our current understanding on NRs and demonstrates the possibility of using several flavoenzymes in the synthesis of organic molecules.

CHAPTER 1

INTRODUCTION

1.1 Biocatalysis

Biocatalysis is nature's method of transforming organic compounds.[1] Enzymes are by far the most abundant natural catalyst for this task. Their major advantage lies in their selectivity and specificity, be it high *chemo*-, *regio*-, or *enantio*-selectivity or specificity.[2] Additionally, they have supreme rate enhancement compared to the non-catalyzed reaction (k_{cat}/k_{non}) that can range from a 10^7 to 10^{19}-fold increase.[3,4] Enzymatic reactions can be conducted at near ambient temperatures and pressures, and are mostly run in aqueous medium. This can lead to lower energy costs, and render them environmentally benign compared to conventional chemical methods.[5] These advantages have propelled biocatalysis to complement and sometimes replace other catalytic routes in large-scale applications for synthesizing chemicals, food ingredients, and active pharmaceutical ingredients (APIs).[6]

1.2 Flavoenzymes

Flavins are yellow colored molecules that have an isoalloxazine ring as a basic structure (Figure 1.1). They were first discovered in 1879 from cow's milk as a bright yellow pigment.[7] It was initially termed lactochrome (named from where it was discovered), but is currently known as riboflavin (vitamin B_2) which is the precursor of all other flavins occurring in nature. Riboflavin itself is not the common form found in organisms, rather, it is found in two modified forms: flavin mononucleotide (FMN) and flavin adenine

dinucleotide (FAD) (Figure 1.1). These are mostly found as non-covalently bound enzyme cofactors in nature where the protein-ligand interaction primarily depends on the ribityl side-chain of the molecule.[8] Enzymes that require the presence of either form of flavin for catalysis are called flavoenzymes.

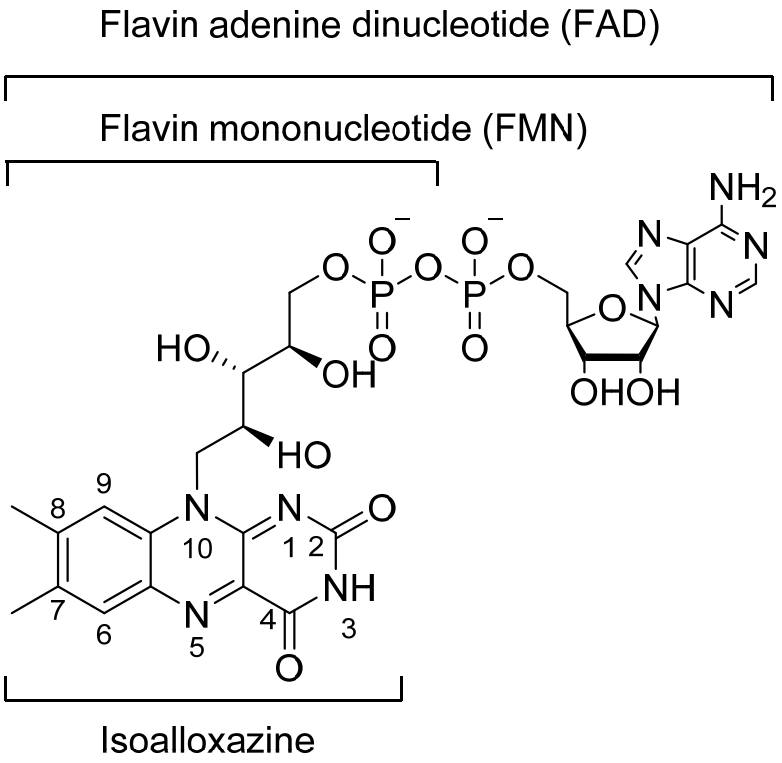

Figure 1.1 Structure of flavins

Flavoenzymes are versatile catalysts as they are capable of undergoing one- or two-electron transfers. Thus, the flavin can exist either as oxidized, one-electron reduced (semiquinone), or two-electron reduced states. As such, they can act as bridges to conjoin one- and two-electron redox reactions in biological systems, making them ubiquitous in nature.[9] Flavoenzyme catalyzed reactions require two-half reactions, where the flavin is

initially reduced then subsequently oxidized for complete turnover. Depending on the nature of the substrate involved in the reaction, flavoproteins have been divided into five major categories.[10,11]

A.1 *Transhydrogenases* – two-electron transfer from one organic molecule to another

A.2 *Dehydrogenase-oxidase* – molecular oxygen is the oxidizing substrate for two-electron transfer

A.3 *Dehydrogenase-monooxygenases* – one oxygen atom of O_2 is inserted to a substrate while the other is reduced to H_2O

A.4 *Dehydrogenase-electron transferase* – flavin is reduced with two-electrons, but is reoxidized with single-electron transfers

A.5 *Electron transferase* – one-electron transfer for both reduction and oxidation

The enzymes that are discussed in this thesis are transhydrogenases and dehydrogenase-oxidases. For detailed reviews of others, the reader is directed towards review articles such as "The chemical and biological versatility of riboflavin (Massey, 2000)" and "Formation and mode of action of flavoproteins (Merrill et al., 1981)".[8,12]

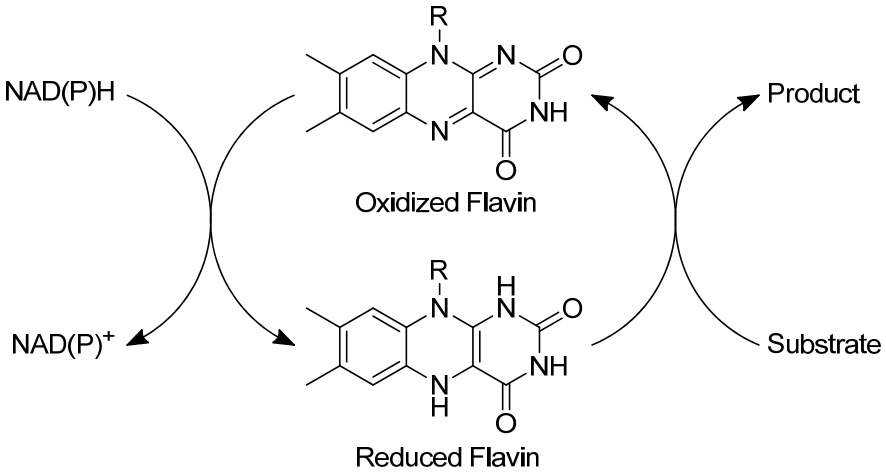

Figure 1.2 General mechanism of flavin redox chemistry

For both transhydrogenases and dehydrogenase-oxidases, the reductive-half reaction is a two-electron transfer. The primary electron donors are nicotinamide cofactors, namely NADH and NADPH (Figure 1.2). These pyridine nucleotides can reduce the flavin through hydride transfer.[13] Sequentially, the reduced flavin will in turn reduce a substrate. When this is an organic molecule, the enzyme is labeled a transhydrogenase, and when it is molecular oxygen the enzyme is termed a oxidase. These two types of reactivity are not completely exclusive, as there are transhydrogenases that are capable of reducing, at relatively slower rates, O_2 as well. In this dissertation, three different classes of flavoenzymes are studied: nitroreductases, ene-reductases and NAD(P)H oxidases.

1.3 Nitroreductases

Nitroreductases (NRs) are enzymes that catalyze the reduction of nitroaromatics to their corresponding nitroso, hydroxylamine, and, in limited cases, amine (Figure 1.3).

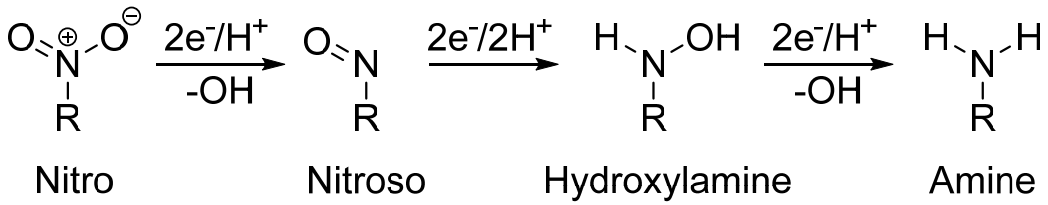

Figure 1.3 Schematic of two-electron reduction of nitro reduction to amine, with nitroso and hydroxylamine intermediates

1.3.1 Literature survey of NR

Depending on the nature of the first reduction step NRs can be categorized into two types. Oxygen-sensitive NRs (type II) catalyze a single electron transfer to produce the nitro anionic radical which can subsequently oxidize O_2 to produce superoxide radicals. There have been a few type II NRs found in *Escherichia coli* and *Clostridium* strains.[14-16] Current research on NRs is mostly focused on oxygen-insensitive (type I) NRs that perform a two-electron reduction of nitro to form nitroso. Isolated and characterized NRs include NfsA and NfsB from *E. coli* [17,18], NR from *Enterobacter cloacae* [19], NRSal (or Cnr) from *Salmonella typhimurium* [20], SnrA from *Salmonella typhimurium* [21], nitrobenzene nitroreductase (nbzA) from *Pseudomonas pseudoalcaligenes* [22], NAD(P)H:FMN oxidoreductase (FRase I) in *Vibrio fischeri* [18,23], RdxA from *Helicobacter pylori* [24], nbzA from *Pseudomonas putida* [25], PnrA and PnrB from *Pseudomonas putida* JLR11 [26], NitA and NitB from *Clostridium acetobutylicum* [27], GlNR1 (Fd-NR2) from *Giardia lamblia* [28], NfnB from *Mycobacterium smegmatis* [29], TbNTR from *Trypansoma brucei* [30], Ssap-NtrB from *Staphylococcus saprophyticus* [31], Frm2 from *Saccharomyces cerevisiae* [32], NR from *Streptomyces mirabilis* [33], MsAcg from *Mycobacterium smegmatis* [34], TcNr from *Taiwanofungus camphorates* [35], LmNTR

from *Leishmania major* [36], BaNTR1 from *Bacillus amyloliquefaciens* [37], and many others.

Type I NRs have previously been classified into two main groups, where the designation is based upon the different NRs that were identified in *E. coli* by Bryant et al.[38] NfsA (group A) is the major NR that uses exclusively NADPH as the electron donor, and NfsB (group B) is the minor NR that can use both NADH and NADPH for reduction.[17,18] However, the expansion in the family now makes it difficult to categorize all NRs in to these two groups.

As there are a vast number of NRs studied throughout the community, in this thesis we focus on the NfsB type NRs, namely NRsalty from *S. typhimurium* [20,39], NRentcl from *E. cloacae* [19,40] and NRmycsm from *M. smegmatis* [29] (futher explanation as to why these enzymes were selected are in Section 2.1, and discussion regarding the nomenclature is provided in Appendix A).

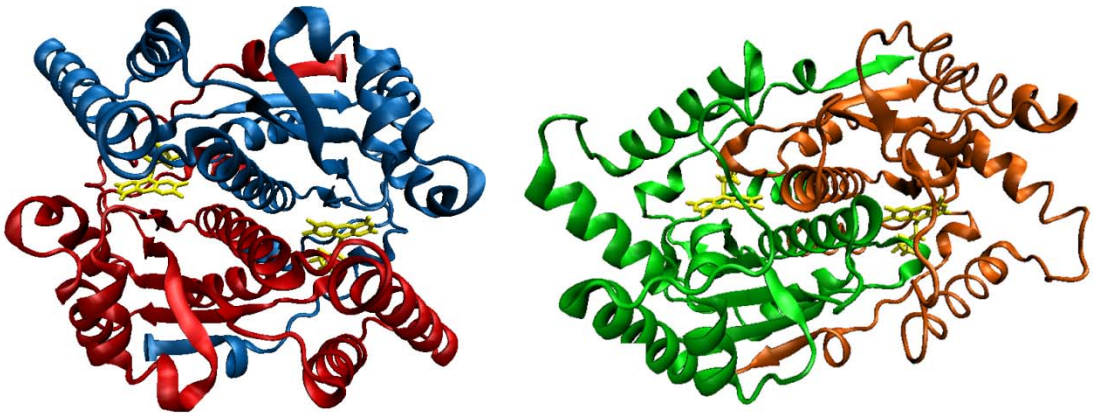

Figure 1.4 Crystal structure of NRentcl (left; PDB ID: IKQB) and NRmycsm (right; PDB ID: 2WZW). Image rendered with Visual molecular dynamics (VMD).[41]

The crystal structure of NRentcl and NRmycsm have previously been solved (there is none for NRsalty), and both have shown to be homodimeric enzymes with a flavin mononucleotide (FMN) prosthetic group for catalysis (Figure 1.4).[29,42] The FMN cofactor is non-covalently bound at the dimer interface, where there are two symmetric, but independent, active sites constructed with residues from both monomeric subunits. These structures are very similar to that of NfsB from *E.coli* [43,44], NADH oxidase in *Thermus thermophilus* [45], flavin reductase P (FRP) in *Vibrio harveyi* [46], FRase I from *Vibrio fischeri* [47]. As discussed previously, these enzymes do not prefer one nicotinamide cofactor over the other. This is mainly because there is no binding domain, such as the Rossmann fold, for NAD(P)H backbone interaction.

Overall the NRs undergo a bi-bi ping-pong mechanism, where both the reduced nicotinamide co-substrate and substrate take turns binding at the *re* face of the flavin.[40,42] However, despite the many mutational [48-52] and computational studies [53] conducted on NRs, there are still many unknown details regarding the mechanism. The presence of any catalytically active residues has yet to be identified, and the mechanism of nitro reduction has yet to be elucidated. These are some of the questions that are partially addressed in this thesis.

Additionally, other than the enzymes discussed above, there are some that can reduce non-aromatic nitro groups. The substrates can be xenobiotic nitro esters such as glycerol trinitrate (GTN) and pentaerythritol tetranitrate (PETN), or nitro alkenes that are conjugated with an aromatic ring such as nitro styrenes as substrates. The well-known ones include glycerol trinitrate reductase (NerA) from *Agrobacterium radiobacter* [54] and

pentaerythritol tetranitrate (PETN) reductase from *Enterobacter cloacae* [55]. Both are members of the old yellow enzyme (OYE) family, and will be discussed in Section 1.4.1.

1.3.2 NR applications

NRs have gathered interest in many scientific communities, and currently there are two major active fields where they are being studied.

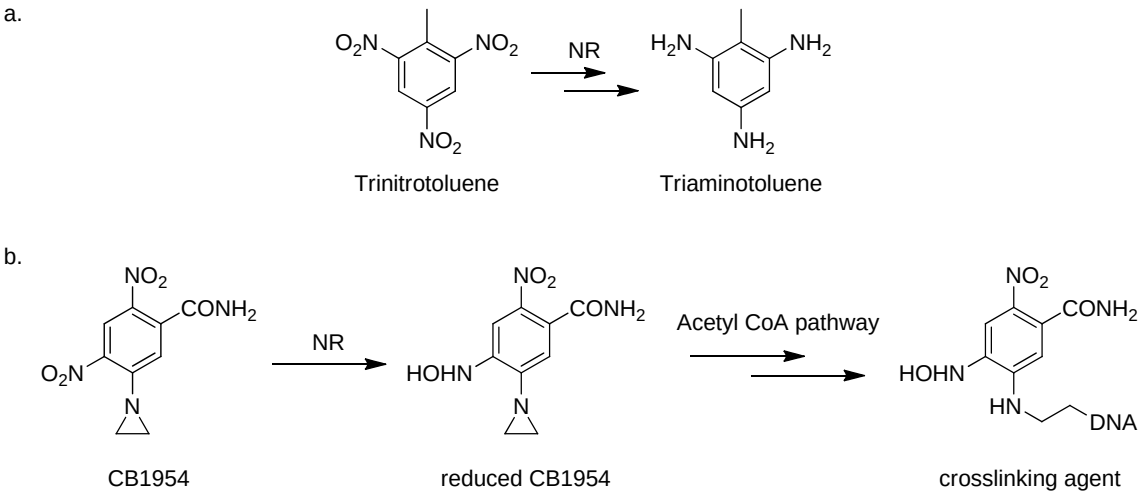

Figure 1.5 a) Bioremediation of trinitrotoluene (TNT) to triaminotoluene (TAT). b) Prodrug (CB1954) activation *in vivo* to create a DNA crosslinking agent

The first is for bioremediation where possible degradation of xenobiotic nitroaromatics, such as trinitrotoluene (TNT) and picric acid, has received the most attention (Figure 1.5a). Nitroaromatic compounds are used to synthesize dyes and explosives and can be produced by nitration and incomplete combustion of fossil fuels.[56] The anthropogenic nature of these compounds makes it difficult for nature to degrade. Also, the presence of an uncontrolled reduction can possibly yield a nitroso and/or hydroxylamine compound, which is more toxic than the original compound.[56,57] Microorganisms that degrade nitroaromatics have been discovered such as *Pseudomonas pseudoalcaligenes* [58],

Mycobacterium [59], *Rhodobacter capsulatus* [60], *Escherichia coli* [61,62], *Saccharomyces sp.* ZS-A1 [63], *Candida* sp. AN-L14 [63], *Klebsiella* sp. [64], *Pseudomonas aeruginosa* [65], *Pseudomonas putida* KP-T202 [66], *Irpex lacteus* [67], *Yarrowia lipolytica* [68], *Cellulomonas* sp. ES6 [69], *Fusarium oxysporum* [70], and *Raoultella terrigena* HB [71]. However, the specific enzymes responsible for the multiple reactions involved in the reduction of these xenobiotics often have yet to be characterized and understood completely.

The second is the coupled use of NRs with prodrugs to activate them for medical applications, namely antibody-directed enzyme prodrug therapy (ADEPT) [72-74], gene-directed enzyme pro-drug therapy (GDEPT) [75-77] and virus-directed enzyme pro-drug therapy (VDEPT)[78,79]. In these therapies, the enzymes with specific functions of interest are delivered to the medication site and coupled with a prodrug. This prodrug that originally is inactive when first delivered will become activated through the enzyme to complete its medicinal purpose (Figure 1.5b). A procedure with NRs will involve the enzyme to activate a prodrug by reducing aromatic nitro groups to hydroxylamines which will then crosslink to DNA and cause cell death. Such applications are envisioned for the treatment of cancer.

Further, in this study, the application of NRs will be investigated for active pharmaceutical ingredient (API) syntheses which involve the reduction of aromatic nitro groups to amines. Substituted aromatic amines can be found in a number of API syntheses as intermediates or final products. Some examples include sildenafil, the antibiotic linezolid and the HIV protease inhibitor amprenavir (Figure 1.6).[80]

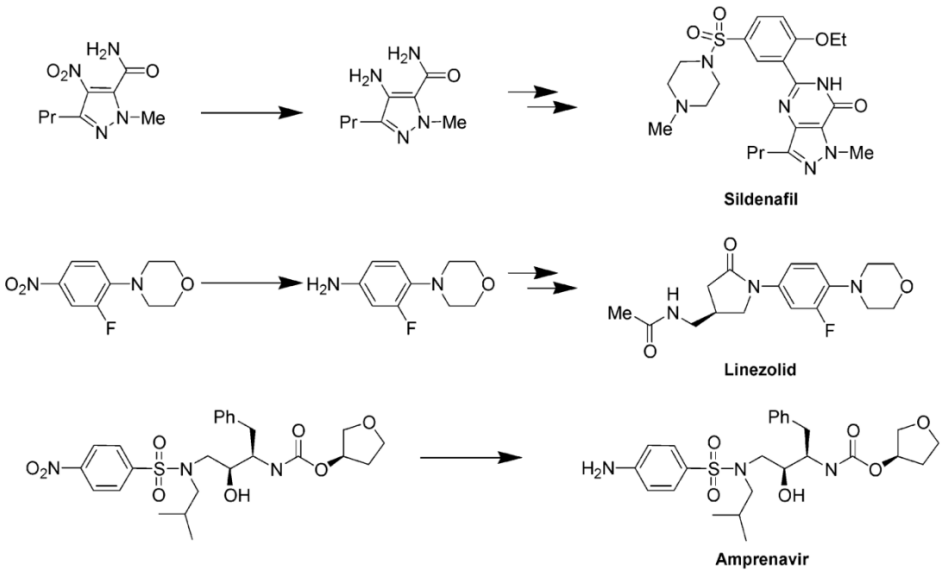

Figure 1.6 Active pharmaceutical ingredients (APIs) with aromatic amine production from nitro precursors. Figure adapted from Hoogenraad et al.[80]

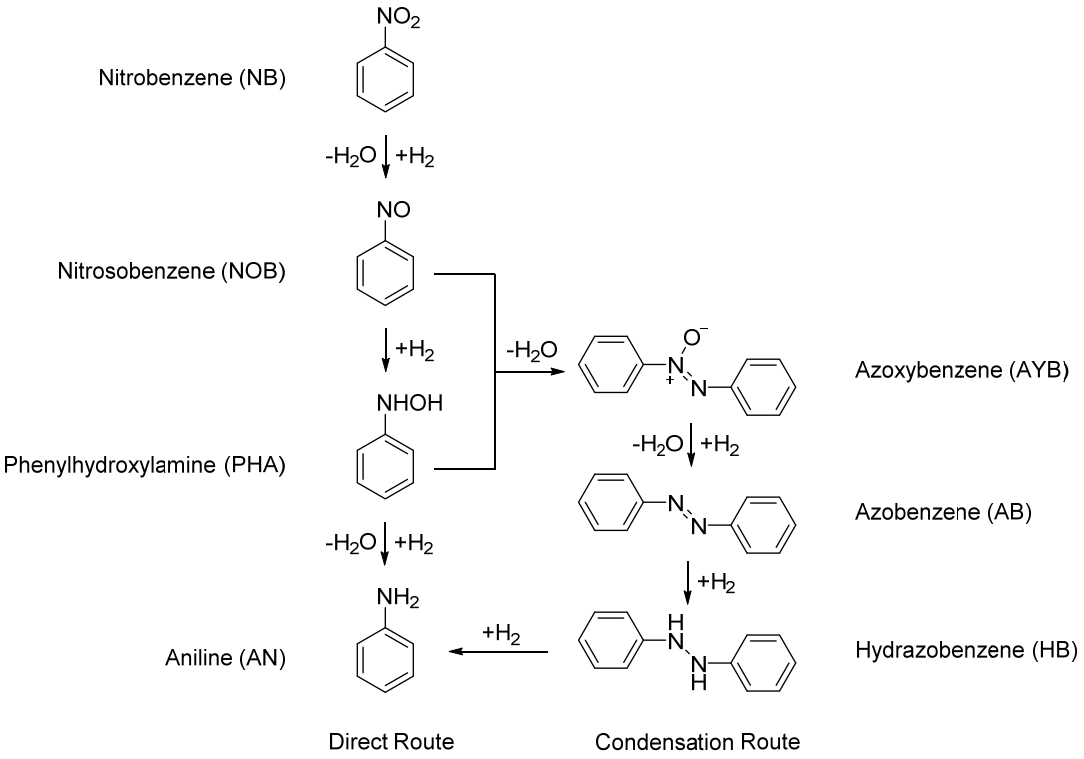

Figure 1.7 Proposed reduction pathways of nitrobenzene to aniline through i) the direct route and ii) condensation route by Fritz Haber.[81] Figure adapted and modified from Corma et al.[82]

1.3.3 Nitrobenzene reduction and state of the art

The nature of nitrobenzene reduction is complex compared to the simple one-step reaction typically depicted in organic chemistry text books.[83,84] The difficulties are well documented: Fritz Haber demonstrated the formation of several intermediates and side-products on electrode surfaces as early as 1898 (Figure 1.7).[81,85] Most notably, nitroso- and hydroxylamines were formed as intermediates from the direct pathway of producing amines, while the condensation pathway of intermediates yielded azoxy-, azo-, and hydrazobenzene as side-products.

Conventional organic syntheses for aromatic amines involve catalytic hydrogenation of nitro precursors with hydrogen gas and noble metal catalysts such as palladium, platinum and rhodium.[86] Two main aspects, namely chemoselectivity and sustainability, are currently being addressed for further improvement of these technologies. The traditional methods are very effective for nitro reduction, but frequently lack chemoselectivity and catalyze additional side-reactions.[82,87,88] In particular, catalytic hydrogenation can lead to the reduction of functional groups such as carbonyls and unsaturated carbon bonds [88,89] or dehalogenation of substituted nitroaromatics, i.e. the release of HCl, HBr or HI.[90,91] Such limitations have been overcome to some extent through catalyst modification by alloying or poisoning with metal oxides. Although these alterations have shown to improve selectivity they also lead to a decrease in activity.[92] Transfer hydrogenation is seen as an attractive alternative that also exhibits better selectivity. This method is considered advantageous as it utilizes reducing agents such as sodium dithionite, iron, tin, or zinc in ammonium chloride or ammonium formate instead of hydrogen gas.[92-94] Literature examples include the use of

rhodium, palladium, ruthenium, copper and cobalt complexes as catalysts.[89,95-98] However, the use of precious metals in both techniques has raised concern due to their scarcity and high costs.[99] For improved sustainability, recent advances in the heterogeneous catalysis field have focused on utilizing abundant materials such as iron and nickel. Examples include the use of Fe_2O_3- based particles in water-THF [98], $Fe(BF_4)_2 \cdot 6H_2O$ with mono- and bidentate phosphines [93], and silica gel supported Ni-catalysts [99].

Overall, there have been significant advances not only to address the selective production of amine from nitro precursors but also to limit side-reactions occurring on additional substituents. Further, many technologies have been developed to address the sustainability of heterogeneous catalytic methods by avoiding the use of metals as catalysts. However, the use of these technologies is still less than straight forward when utilizing these procedures on complex molecules, such as those found in the pharmaceutical industry. High-throughput systems have been developed to find optimal conditions for each target molecule and these studies have confirmed that these conditions can differ drastically from molecule to molecule.[80]

Biocatalytic reduction of nitro arenes is considered as an alternative pathway for the production of amines in relatively mild conditions which will be favorable in terms of energy costs. Further, the use of an enzymatic route is touted for the use in latter stages of a synthesis where the presence of multiple functional groups will require the use of an extremely chemoselective catalyst. Moreover, the Food and Drug Administration (FDA) has strict regulations against heavy metal contamination in pharmaceuticals.[100,101] Therefore, an approach centered on a biocatalytic route is sought for the reduction of nitro to amine.

1.4 Other flavoenzymes

The main enzyme of interest is the NR in this dissertation. However, there are additional projects that involve the use of flavoenzymes that are introduced here.

1.4.1 Ene-reductases

Ene-reductases (ERs), or enoate reductases, are enzymes capable of reducing α, β unsaturated carbon-carbon double bonds with adjacent electron-withdrawing groups such as aldehydes, ketones, carboxylic acids, esters, nitriles, and nitro groups (Figure 1.8).[102,103] Their biggest utility lies in their ability to create up to two chiral centers while reducing an alkene substrate.

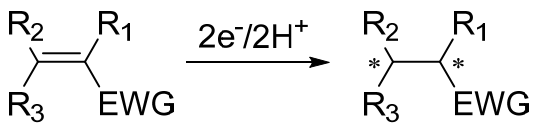

EWG = aldehyde, ketone, nitrile, carboxylic acid, ester, nitro

Figure 1.8 Schematic of asymmetric reduction of alkenes with adjacent electron-withdrawing groups (EWG)

The old yellow enzyme (OYE) family is well known class of flavoenzymes that can reduce activated C=C bonds at the expense of nicotinamide cofactors. Enzymes in this family include OYE1 from *Saccharomyces pastoris* [104,105], OYE2 and OYE3 from *Saccharomyces cerevisiae* [106,107], morphinone reductase (MR) from *Pseudomonas putida* [108], pentaerythritol tetranitrate (PETN) reductase from *Enterobacter cloacae* [55], *N*-ethylmaleimide reductase (NemA) from *Escherichia coli* [109], glycerol trinitrate reductase (NerA) from *Agrobacterium radiobacter* [54], xenobiotic reductase A (XenA) from

Pseudomonas putida [110], xenobiotic reductase B (XenB) from *Pseudomonas fluorescens* [110], TcOYE from *Trypanosoma cruzi* [111], 12-oxophytodienoate reductases (OPR1-3) from *Arabidopsis thaliana* and *Lycopersicon esculentum* [112,113], YqjM from *Bacillus subtilis* [114], SYE1-4 from *Shewanella oneidensis* [115], KYE1 from *Kluyveromyces lactis* [116], YersER from *Yersinia bercovieri* [116], NCR from *Zymomonas mobilis* [117], TOYE from *Thermoanaerobacter pseudethanolicus* E39 [118], and others. There have been suggestions that OYEs are implicated in the antioxidant defense system, but their physiological role has yet to be determined.[103,114,119]

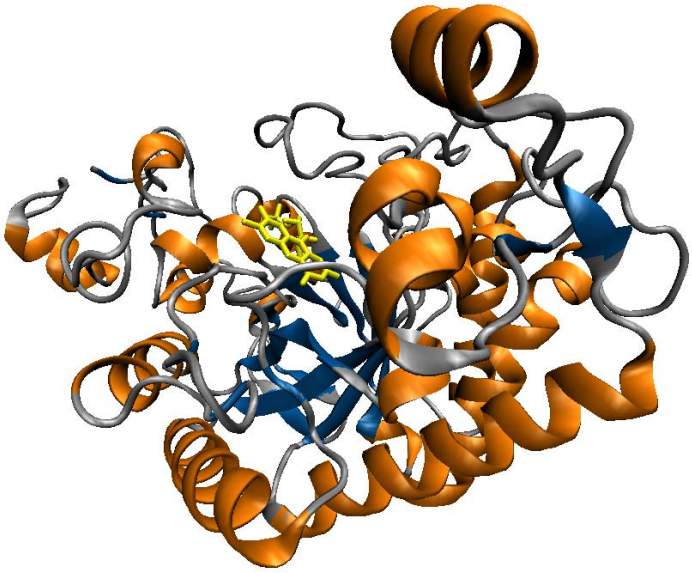

Figure 1.9 Crystal structure of OYE1 from *Saccromyces pastoris* (PDB ID: 1OYB) colored according to secondary structure; α-helices (orange) and β-sheets (blue). Image rendered with VMD.[41]

OYEs have a TIM barrel fold, also known as a $(\alpha\beta)_8$ fold, which is derived from the name of triosephosphate isomerase (TIM), the first enzyme crystallized with such a structure.[120] Eight α-helices and parallel β-sheets alternate to form a central barrel comprised of β-strands, which is surrounded by an outer barrel of α-helices. The active

site is located at the C-terminal end of the β-barrel, where the FMN cofactor is bound (Figure 1.9).

Similar to NRs, substrate reduction happens through a bi-bi-ping-pong mechanism.[121] ERs from the OYE family, in most cases, prefer NADPH as the electron source. The hydride of the NADPH is transferred to the N5 position of the flavin to be reduced in the reductive half-reaction. Subsequently, in the oxidative half-reaction, the hydride is transferred to the β-carbon and is followed by a proton addition to the α-carbon. Compared to the catalytic hydrogenation methods which commonly undergo a *syn*-addition, biocatalytic ones undergo an *anti*-addition of hydrogens.[122-124] Considering OYE1 as an example, His-191 and Asn-194 (which can be His in some OYEs) are known to be important for substrate binding as they hydrogen bond with the carbonyl oxygen.[125] Tyr-196 has been shown to be the proton donor, but can be replaced with water as well.[126]

1.4.2 NAD(P)H oxidases

NAD(P)H oxidases (Noxs) are enzymes that catalyze the oxidation of NAD(P)H to $NAD(P)^+$, while reducing molecular oxygen. They can be divided into two groups depending on the extent of O_2 reduction. nox1 NAD(P)H oxidases are ones that catalyze a two-electron transfer to produce hydrogen peroxide, while nox2 catalyzes a four-electron transfer to yield water (Figure 1.10).[127,128] As H_2O_2 can deactivate enzymes, water producing nox2 have more potential to be useful in the context of biocatalysis. Therefore, here in this review only nox2 enzymes will be discussed.

$$NAD(P)H + O_2 + H^+ \xrightarrow{nox1} NAD(P)+ + H_2O_2$$

$$2NAD(P)H + O_2 + 2H^+ \xrightarrow{nox2} 2NAD(P)+ + 2H_2O$$

Figure 1.10 Schematic of molecular oxygen reduction with either two-electron (nox1) or four-electron (nox2) reduction

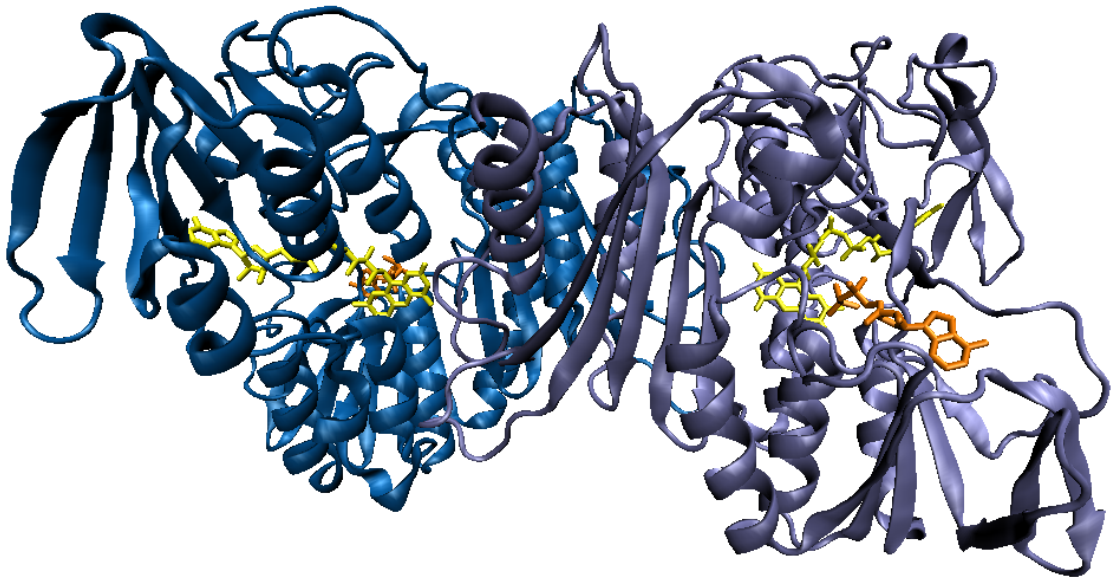

Figure 1.11 Crystal structure of NADPH oxidase from *Lactobacillus sanfranciscensis* (PDB ID: 2CDU) colored by subunit and ligands; FAD (yellow) and adenosine diphosphate (ADP; blue). The ADP binding site is where NAD(P)H will potentially bind for catalysis. Image rendered with VMD.[41]

Water-forming Noxs have been shown to be active as homodimers where each monomer has a bound flavin adenine dinucleotide (FAD) cofactor.[129,130] Known nox2 enzymes include ones from *Streptococcus mutans* [131], *Enterococcus faecalis* [132], *Lactobacillus sanfranciscensis* [128], *Lactobacillus brevis* [133], *Lactococcus lactis* [134]. The

structure is a Rossmann fold, which is common for enzymes that take NAD(P)H as a substrate.[135] All previously discovered nox2 NAD(P)H oxidases have a conserved cysteine residue that is catalytically active.[133,134,136,137] This is supported by the fact that a Nox with a cysteine mutated to serine produced H_2O_2 instead of water.[138-140] During catalysis, the thiol (–SH) or thiolate ($–S^-$) is oxidized to sulfenic acid (–SOH) and reduced back to the thiol/ate as a part of the NAD(P)H reduction mechanism (Figure 1.12).[130] During this redox cycle the cysteine can also be overoxidized, producing a sulfinic ($–SO_2H$) and then a sulfonic acid ($–SO_3H$), irreversibly, and thereby deactivating the enzyme.[141,142] This is the presumed cause of turnover-limited operational stability of nox2 proteins.[139,143] Overoxidation of this cysteine residue can be decelerated by employing exogenous reducing agents such as dithiothreitol (DTT) or β-mercaptoethanol (BME)[143]; thus, extending the useful active enzyme lifetime and its total turnover number (TTN), a measure of operational stability.

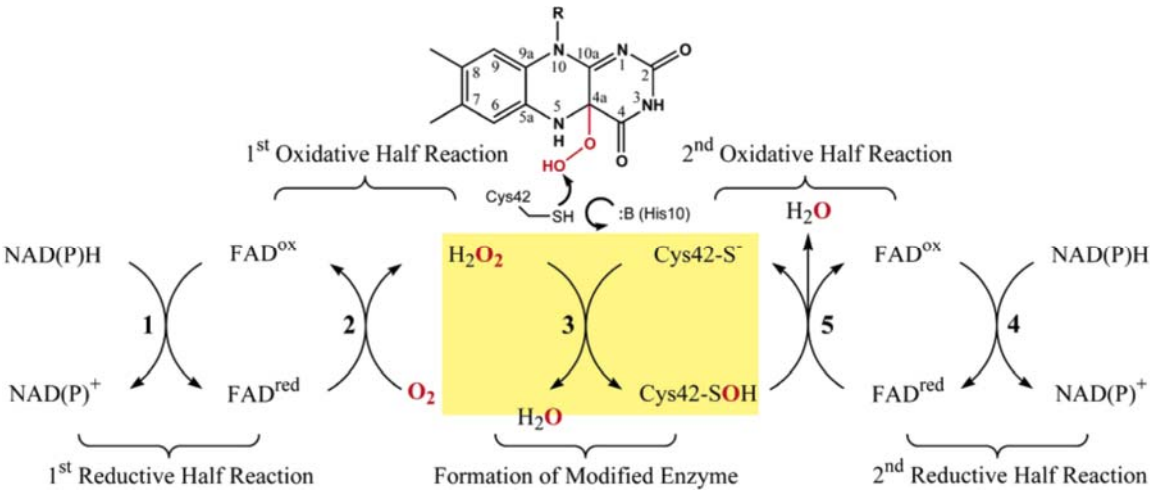

Figure 1.12 Overall Reactions Catalyzed by nox2 NAD(P)H Oxidases. Scheme is adapted from Lountos et al.[130]

1.5 NAD(P)H regeneration

As noted previously, oxidoreductases such as NRs and ERs consume NAD(P)H as coenzymes. However, high costs make it difficult to use them in stoichiometric quantities (Table 1.1). Therefore, an *in situ* regeneration system needs to be implemented for sustainability. Several methods have been investigated including chemical, electrochemical, photochemical, and enzymatic approaches (for detailed reviews on these methods see "Regeneration of Nicotinamide Coenzymes: Principles and Applications for the Synthesis of Chiral Compounds (Weckbecker et al. 2010)".[144,145] Among these, the enzymatic method is known to have the highest selectivity and total turnover number (TTN; the moles of product produced by each mole of catalyst over its lifetime).[146]

Table 1.1 Cost of nicotinamide cofactors [147] and regeneration systems[148]

Compound	Price ($/mol)
NADH	3,580
NADPH	96,530
$HCOONH_3$	0.2
Glucose	0.2
Acetone	0.25
$(NH_3)_3PO_3$	0.87

There are several enzymes that are useful for reduction of oxidized nicotinamide cofactors. These include the enzymes formate dehydrogenase (FDH) [149-151], glucose dehydrogenase (GDH) [152,153], glucose-6-phosphate dehydrogenase (G6PDH) [154,155], alcohol dehydrogenase (ADH) [156-159] and phosphite dehydrogenase (PTDH) [160,161] (Figure 1.13). Among these, GDH will be used in this thesis to establish the NAD(P)H recycling system due to its high specific activity and stability.[144,145]

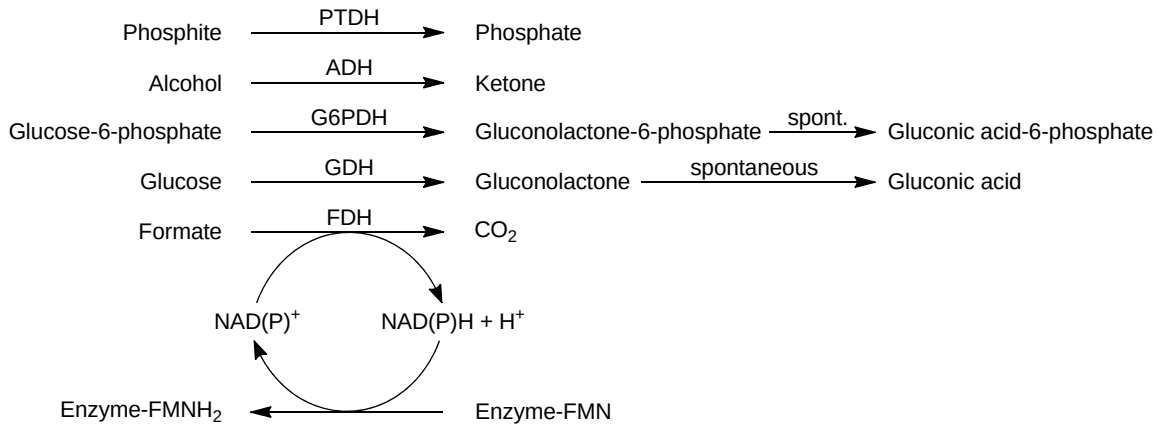

Figure 1.13 NAD(P)H regeneration scheme with different enzymes.

1.6 Map of Dissertation

This thesis studies various applications of flavoenzymes for organic synthesis. Chapter 2 discusses the reduction of nitrobenzene with NRs and the product distribution. Chapter 3 investigates the substrate specificity of NRs and characterizes the reactivity in relation to the substrate structure. Chapter 4 employs NRs in conjunction with reducing agents, namely formamidine sulfinic acid (FSA) for the enzymo-chemical synthesis of aromatic amines. Chapter 5 is a study that utilizes protein engineering to create a NR from a monomeric ER scaffold. Chapter 6 characterizes of an NADH oxidase for a stable cofactor regeneration system. Chapter 7 summarizes the main findings in each chapter and discusses recommendations for future research.

CHAPTER 2

REDUCTION OF NITROBENZENE WITH NITROREDUCTASES

2.1 Introduction & Motivation

Nitroreductases (NRs) have been identified and partially characterized for its nitrobenzene reduction pathway. The product distribution of NRs described in the literature can be categorized into two groups based upon the extent of reduction. In extensively studied NRs, including those from *E. coli* (NRescco) and *Enterobacter cloacae* (NRentcl), it is reported that the hydroxylamine is produced as the major product from nitroaromatics.[40,162] More recently, Yanto et al. studied NRsal (NRsalty in this article) from *Salmonella typhimurium*, showing a 6% yield of aniline from nitrobenzene reduction. Other side-products included the intermediates nitroso and hydroxylamine in small quantities along with the condensation product of the nitroso and hydroxylamine states, azoxybenzene at a 70% yield.[39] Another example of an NR producing an amine was found in NRmycsm from *Mycobacterium smegmatis*, where Manina et al. were able to reduce the antituberculosis drug BTZ043 to the corresponding amine, BTZ045, however, with unknown yield and volumetric productivity.[29]

This difference in product distribution becomes more intriguing when considering the high amino acid similarity that NRsalty has compared to NRescco and NRentcl (Table 2.1). To investigate the reason for this variance the reported reaction conditions for NRsalty and NRentcl were investigated and compared to see if this dictated the final reduction state. Additionally, NfnB from *M. smegmatis* (NRmycsm), which is very different in sequence homology and produces the amine, was included in these studies to understand what factors contribute to the final product distribution (Table 2.1).

Table 2.1 Comparison of amino-acid sequence identity/similarity. Uniprot accession numbers: NRsalty (P15888), NRentcl (Q01234), NRescco (P38489), NRmycsm (A0R6D0)

%	NRsalty	NRentcl	NRescco	NRmycsm
NRsalty	-	89/92	89/91	6/15
NRentcl	89/92	-	88/90	6/13
NRescco	89/91	88/90	-	6/13
NRmycsm	6/15	6/13	6/13	-

2.2 Materials & Methods

2.2.1 Enzymes and other materials

The gene of *nrentcl* from *E. cloacae* was a kind gift from Dr. Anne-Frances Miller (University of Kentucky). *nrmycsm* from *Mycobacterium smegmatis* was a generous gift from Dr. Giovanna Riccardi at the Università degli Studi di Pavia. NADH and NADPH were obtained from Amresco (Solon, OH) and EMD chemicals (Gibbstown, NJ), respectively. Phenylhydroxylamine was a kind gift from Dr. Jim Spain (Georgia Tech). Other hydroxylamines were synthesized according to Section 2.2.9. Nitrobenzene (unlabeled and ^{15}N-labeled), nitrosobenzene, aniline (unlabeled and ^{15}N-labeled), azoxybenzene, deuterated solvents (acetonitrile-d_3), and other general chemicals were purchased from Sigma-Aldrich (St. Louis, MO).

2.2.2 Protein Expression

The genes *nrsalty* and *nrmycsm* were expressed in pET-28a vectors, and *nrentcl* was expressed in pET-32a with a thioredoxin (TRX)-tag for increased solubility of the protein (for additional construct information see Appendix C). Plasmids were transformed into BL21(DE3) cells for expression. 1 L cultures were inoculated using 1% (v/v) overnight precultures with appropriate antibiotics (30 $\mu g.mL^{-1}$ of kanamycin for pET-28a, and 50 $\mu g.mL^{-1}$ of ampicillin for pET-32a), and grown at 37 °C. When OD600 reached 0.5~0.7

protein expression was induced with 1 mM isopropyl β-D-1-thiogalactopyranoside (IPTG). After induction, cultures of NRsalty and NRentcl-TRX were expressed at 37 °C for 8 h and 4 h, respectively, and NRmycsm was expressed overnight (~16 h) at 28 °C. Cells were harvested with a Beckman floor centrifuge at 4050 g for 10 min. Pellets were either directly used for purification or stored at -80 °C.

2.2.3 Purification of Enzymes

Purification was performed at 4 °C or on an ice bath, and centrifugation steps were carried out with a Sorvall RC5Bplus centrifuge at 26940 g for 30 min. NRsalty was purified according to a previous study with modifications.[39] Cell pellets were resuspended in 20 mL of 50 mM Tris-Cl pH 7.5 (buffer A) and sonicated at 14 W for 30 s nine times with 30 s breaks in between. Lysed cells were centrifuged, and saturated ammonium sulfate solution was added to the clarified lysate to a final concentration of 40%. The sample was equilibrated with constant mixing for an hour and then centrifuged. Additional saturated ammonium sulfate solution was added to the supernatant to a final concentration of 70%. After one hour of equilibration the sample was centrifuged, and the pellet was resuspended with 5 mL of buffer A. Next, the sample was dialyzed against 500 mL of buffer A for 2 h and then transferred into fresh buffer and further dialyzed for another 2 h. The protein was filtered through 0.8 and 0.2 μm membrane microfilters in series. Filtered protein solution was injected on to an ÄKTAexplorer™ (GE Healthcare Life Sciences; Piscataway, NJ) equipped with a HiPrep 16/10 DEAE anionic exchange column, pre-equilibrated with buffer A. Gradient separation was performed from 10 to 30% using buffer A with 1 M NaCl (buffer B) over 15 column volumes (CVs). Fractions were collected, assayed for activity, and concentrated to less than 2 mL with 3 kDa

molecular weight cutoff (MWCO) Nanosep® centrifugal devices (Pall; Port Washington, NY). FMN was exogenously added to a final concentration of 0.2 mM and incubated for 1 h. The FMN supplemented enzyme solution was injected on a HiPrep 16/60 Sephacryl S-300 column and eluted with an isocratic flow of buffer A with 150 mM NaCl.

Purification of NRmycsm and NRentcl-TRX was carried out with standard his-tag affinity chromatography. Cell pellets were resuspended in 20 mL of 50 mM sodium phosphate, 300 mM NaCl, and 20 mM imidazole at pH 8.0. Cell slurry was sonicated at 14 W for 30 s nine times with 30 s breaks in between. Lysed cells were centrifuged, and the resulting supernatant was incubated with exogenous FMN with a final concentration of 0.2 mM for 1 h. The sample was bound to 2 mL of Ni-NTA resin with gentle rocking at 4 °C for 45 min, and then purified with column chromatography. The resin was washed with five column volumes (CVs) of 50 mM sodium phosphate (pH 8.0), 300 mM NaCl, and 50 mM imidazole two times. Afterwards, the protein was eluted with 0.5 CVs of 50 mM sodium phosphate (pH 8.0), 300 mM NaCl and 250 mM imidazole eight times.

Active fractions were determined and stored at -20 °C with 50% (v/v) glycerol. Protein concentration was determined through the Bradford assay [163], and purity was analyzed through sodium dodecyl sulfate polyacrylamide gel electrophoresis (SDS-PAGE).

FMN occupancy was determined according to the method published by Chapman and Reid.[164] A 5 to 10 μM enzyme solution was heated for 10 min at 90 °C. The precipitated protein was centrifuged for 10 min at 13000 rpm. The absorbance spectra of liberated FMN in the supernatant were scanned, and the concentration was determined with an extinction coefficient at 446 nm, ε_{446}, of 12,200 $M^{-1}.cm^{-1}$.

2.2.4 Enzyme Assays

Spectrophotometric studies were performed on a Beckman Coulter DU 800 UV/Vis spectrophotometer (Pasadena, CA). Spectral scans of substrates were taken at a concentration of 100 μM from a range of 200 to 800 nm. When studying the effect of oxygen, anaerobicity was achieved by bubbling buffer with nitrogen gas and preparing samples in a glove bag (Glas-Col; Terre Haute, IN) also purged with nitrogen.

Nitrobenzene reduction was performed with 100 μM nitrobenzene, 5 $U.mL^{-1}$ glucose dehydrogenase (GDH), 10 μM NAD^+, 10 mM dextrose, and 1 μM NR in 100 mM PIPES buffer with 50 mM KCl (pH 7.0). The change in wavelength absorbencies was monitored for 90 min, with an interval of 10 min. Additional conversion assays for product identification were carried out with identical conditions with the exception of using 50 mM Tris-Cl (pH 7.5) instead of a PIPES buffer at a 1 mL scale. The products were extracted with 0.5 mL of ethyl acetate and either analyzed on GC or further dried over a gentle stream of argon gas, and resuspended in water:acetonitrile (50:50) for HPLC and LC-MS analysis.

2.2.5 Gas chromatography (GC)

GC-FID analysis was performed on a Shimadzu GC-2010 with a Shimadzu SHRX5 column (15 m, 0.25 mm, 0.25 μm). Temperature program: injector and detector temperature at 300 °C; split ratio 25:1; start at 80 °C, hold 5 min, 10 $°C.min^{-1}$ to 290 °C, hold 5 min. Retention time: nitrosobenzene 1.4, aniline 2.0 min, min, nitrobenzene 3.5 min phenylhydroxylamine 5.9 min, azoxybenzene 15.3 min.

2.2.6 ^{15}N-NMR

Enzymatic reduction of ^{15}N-labeled nitrobenzene was scaled up to 200 mL. The reaction was carried out with conditions identical to the spectrophotometric assays, with the exception of using 50 mM Tris-Cl (pH 7.5) as the buffer. The reaction was continued for 6 h, and the product was extracted with ethyl acetate three times (100, 50, and 20 mL). The extract was dried with anhydrous magnesium sulfate ($MgSO_4$), filtered, and concentrated to 1 mL through rotary evaporation. The reaction product was dissolved in acetonitrile-d_3, for NMR. ^{15}N-NMR spectra was recorded on a Bruker Avance III HD-500 at 50.70 MHz using inverse gated proton decoupling, with the assistance of Dr. Gelbaum from the Georgia Tech NMR center.

2.2.7 High-performance liquid chromatography (HPLC) analysis

Analysis was conducted with a Shimadzu LC-20AT pump (Kyoto, Japan), Phenomenex Luna® 5 μM C18 100 Å 250 x 4.6 mm (Torrance, California), and SPD-M20A prominence diode array detector (PDA). Separation was achieved with an isocratic flow of acetonitrile and water. Flow compositions and detection wavelengths are summarized in Table 2.2. Samples were prepared by diluting with acetonitrile and centrifuging for 5 min before sampling.

2.2.8 Liquid chomatography-mass spectroscopy (LC-MS) analysis

Analysis was performed with an Agilent 6320 Ion Trap LC-MS system (Santa Clara, CA) with Electrospray Ionization (ESI). Separation was achieved on an Agilent ZORBAX SB-C18 5 μM 150 x 0.5 mm capillary HPLC column with an isocratic flow of water:acetonitrile (50:50) at a flow rate of 0.1 mL.min^{-1}.

2.2.9 Synthesis of hydroxylamino compounds

Hydroxylamine standards 4-(hydroxyamino)benzoic acid and 4-(hydroxyamino)benzene sulfonamide were synthesized from their parent nitro compounds according to previously published methods by Bauer et al.[165] 1-Nitroso-3-(trifluoromethyl)benzene was oxidized from 3-aminobenzotrifluoride using *m*-chloroperoxybenzoic acid according to previously published methods.[166,167] *N*-Hydroxy-3-(trifluoromethyl)-benzenamine was obtained from reduction of the nitroso derivative with ascorbic acid.[166,168]

2.3 Results & Discussion

2.3.1 Expression and purification of NRs

NRsalty purification was modified for a larger-scale production. Size-exclusion chromatography (SEC) was added as a last step to eliminate impurities. Both NRentcl-TRX and NRmycsm were purified with a His-tag Ni-NTA system. For *nrmycsm*, in addition to the N-terminal his-tag, the stop codon was eliminated to add a his-tag at the C-terminus (performed by the Riccardi group), to facilitate purification. This may help achieve that goal, but the effect towards the enzyme activity or stability is unknown. NRmycsm was found to express better at lower temperature (~28 °C) than the traditional 37 °C. As the earlier elutions contained slight impurities, experiments were carried out with the latter fractions (Figure 2.1).

All three NRs utilize FMN as a cofactor. As the cofactor is essential for catalysis, the occupancy (ratio of FMN/enzyme) was determined by denaturing the enzyme, eliminating the aggregated protein, and measuring the absorbance spectrum of free FMN. NRsalty had an occupancy of 0.68 while NRmycsm had 0.54.

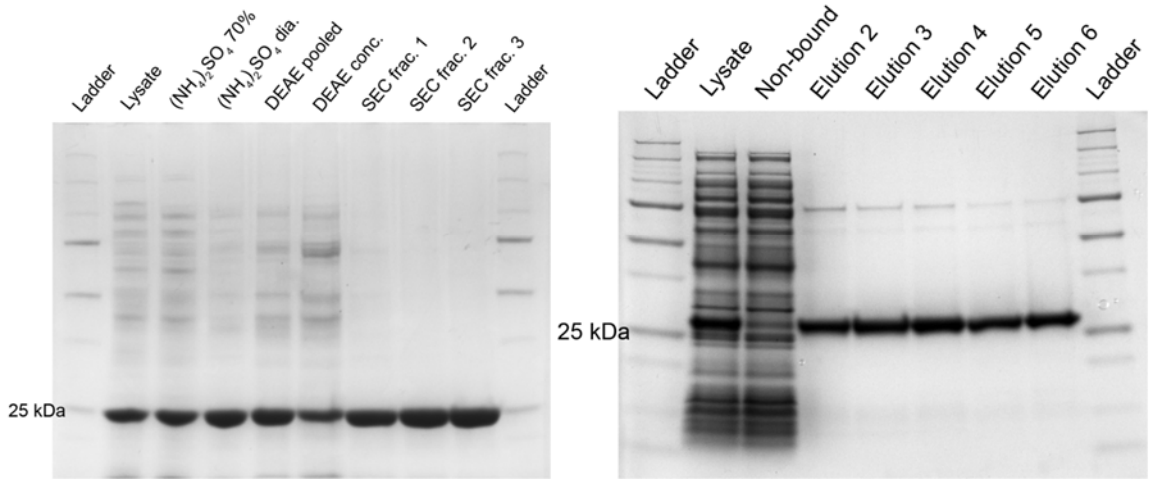

Figure 2.1 SDS-PAGE with 12% gel of a) NRsalty (left) and b) NRmycsm (right) to confirm protein purity. Lysate: clarified lysate; $(NH_4)_2SO_4$ 70%: supernatant from centrifuged sample with 70% ammonium sulfate; $(NH_4)_2SO_4$ dia.: ammonium sulfate precipitated protein pellet resuspended and dialyzed against 50 mM Tris-Cl (pH 7.5); DEAE pooled: fractions collected from HiPrep 16/10 DEAE column; DEAE conc.: combined DEAE sample concentrated with Nanosep® centrifugal devices; SEC frac. 1-3: fractions collected from HiPrep 16/60 S-300 column; Non-bound: cell lysate that did not bind to Ni-NTA; Elution 2-6: fractions eluted from Ni-NTA column.

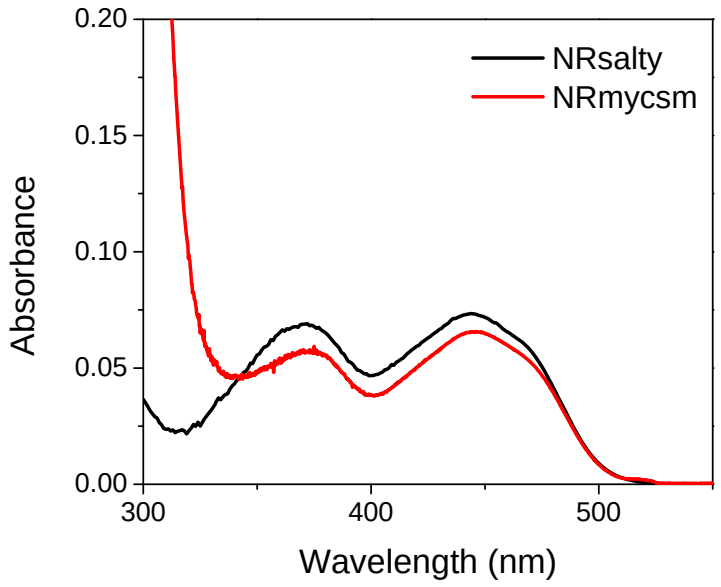

Figure 2.2 Spectrum of FMN liberated from NRsalty and NRmycsm

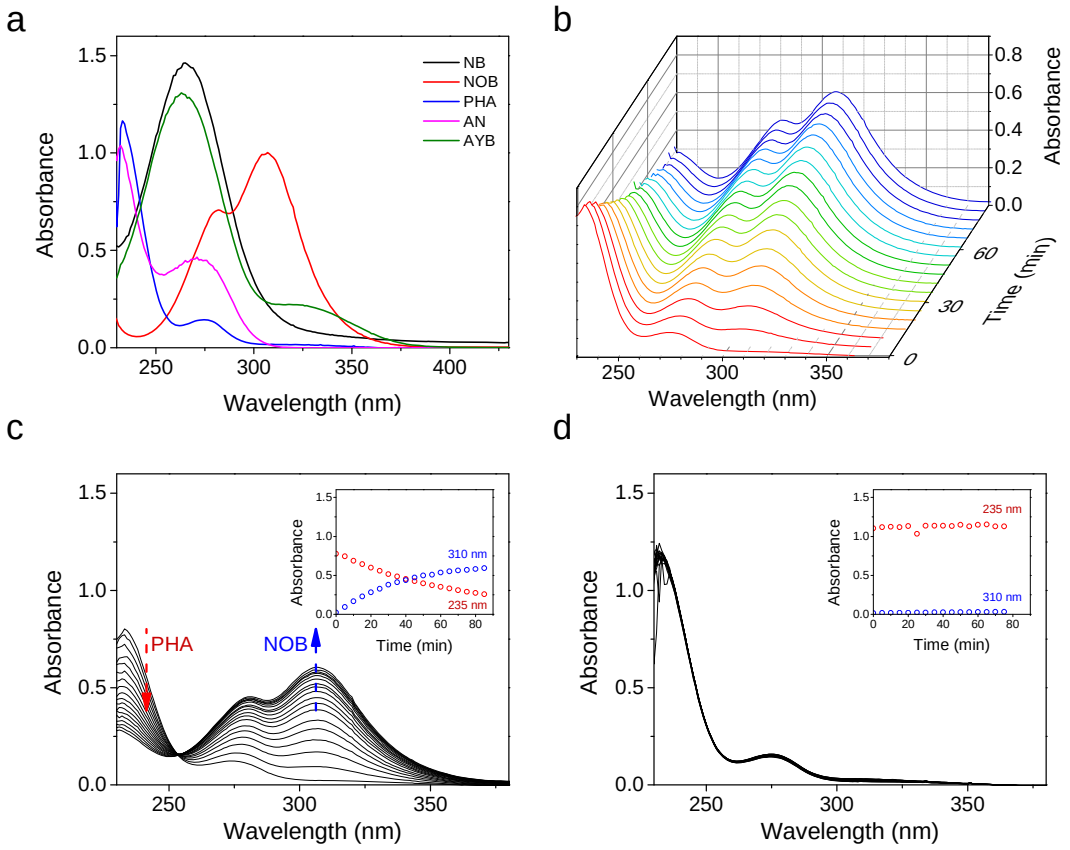

Figure 2.3 Spectral studies of nitrobenzene and its derivatives; (a) spectral characterization of standards at 0.1 mM; (b) instability of PHA; oxidation of PHA in (c) aerobic and (d) anaerobic conditions.

2.3.2 Spectral Characterization

Spectral characteristics of nitrobenzene and its reduced states were recorded and compared (Figure 2.3a). Although it is difficult to differentiate phenylhydroxylamine (PHA) and aniline (AN), nitrobenzene (NB) and nitrosobenzene (NOB) were easily discernible from both with a λ_{max} of 268 and 310 nm, respectively. When measuring the spectrum of PHA, it was found to be unstable, and to change rapidly over time. By observing the resulting spectrum, it was suspected that the PHA was converting to NOB

(Figure 2.3b, c). This hypothesis was supported with literature examples that PHA could oxidize to NOB in the presence of molecular oxygen.[169,170] An attempt to create a PHA solution anaerobically was made by purging the buffer with N_2 before adding the substrate inside an anaerobic glove bag, also purged with nitrogen gas. The stability of PHA was monitored spectrophotometrically, and was shown to be stable over the course of an hour (Figure 2.3d). Further experiments were performed in the presence and absence of O_2, where azoxybenzene was formed in aerobic conditions (data not shown).

2.3.3 Study of NRsalty and NRentcl-TRX

The reduction of NB with NRentcl-TRX was performed as previously reported and the product formation was compared to that of NRsalty[40]. For both enzymes, the characteristic peak of NOB at 310 nm was undetectable as an intermediate on the spectrophotometer. The absence of a NOB signal indicates that the first reduction step is rate-limiting, and the subsequent reduction from NOB to PHA happens instantaneously.[40] Further, this second reduction step can occur solely with the cofactor NAD(P)H, but the presence of NR increases the rate of reaction, confirming that NOB is a substrate for NRs (data not shown). As previously reported reaction conditions varied (e.g. buffer salts and additives), the reduction was repeated while varying the reaction components to see if the selectivity was affected. However, no discernible difference was observed on the spectrophotometer, and the reason for nitrosobenzene detection from NRsalty[39] was

unclear from these experiments. As the characteristic absorbencies were similar for PHA and AN, it was determined that a spectrophotometric assay alone was insufficient to draw a conclusion on the final redox state, necessitating an alternative analytical tool for product analysis.

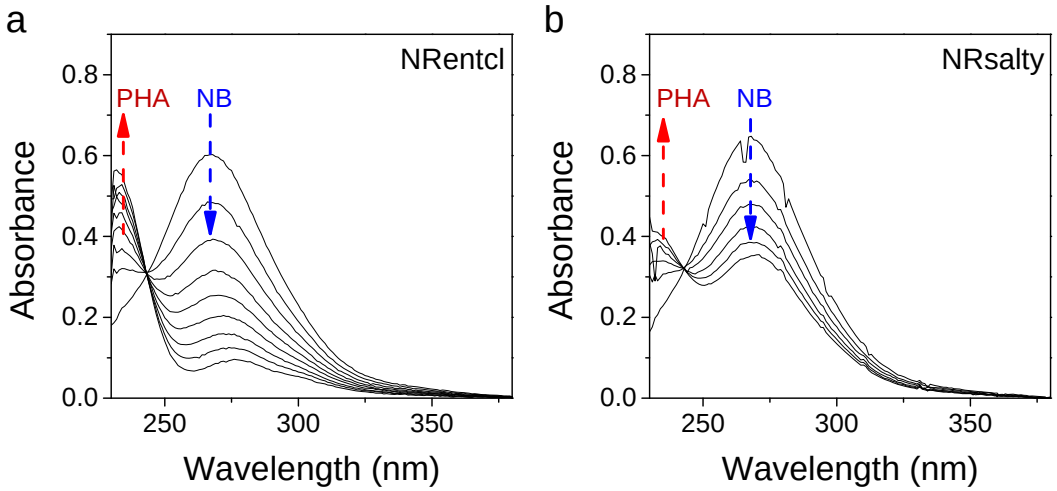

Figure 2.4 Nitrobenzene reduction monitored on the spectrophotometer, catalyzed by a) NRentcl and b) NRsalty with 100 µM nitrobenzene, 5 U.mL^{-1} glucose dehydrogenase (GDH), 10 µM NAD^{+}, 10 mM dextrose, and 1 µM NR in 100 mM PIPES buffer with 50 mM KCl (pH 7.0) at 25 °C

2.3.4 Product characterization through multiple analytical tools

To overcome the shortcomings of the spectrophotometer assay, gas chromatography with a flame ionization detector (GC-FID) was selected to separate and detect PHA and AN. However, this method was found to be problematic for PHA. When analyzing PHA standards, the chromatograms showed significant amounts of NOB and AN, as well as AYB. Due to the uncertainty of whether the sample or analytical tool was the cause for such a phenomenon, an attempt was made to avoid using PHA as the starting substrate. NOB, which is the higher oxidation state of PHA, was selected as the starting substrate,

and an NADH recycling system was implemented with the premise that NADH alone will be able to reduce the NOB to PHA and provide a clean substrate to start with. Surprisingly, all runs, including the negative control with no NR, showed similar levels of amine formation. Such observations lead to the hypothesis that the analytical tool, rather than the substrate, was causing the false positive signal of amine. This thought is further supported by the fact that hydroxylamines are known to be unstable in the presence of oxygen and at elevated temperatures.[170,171] It is speculated that during injection two molecules of hydroxylamine will undergo disproportionation to form NOB and AN as the oxidized and reduced product. To confirm the hypothesis that aniline was being formed through the GC instrument alternative analytical tools such as HPLC, LC-MS and NMR were selected to characterize the product distribution.

^{15}N-NMR was initially considered as a method to monitor the reaction in real-time. However, this proved to be non-trivial due to low substrate solubility and slow signal acquisition times. Alternatively, an enzymatic reduction of NB was performed anaerobically, extracted, and the resulting product was analyzed through ^{15}N-NMR (Figure 2.5). The scans showed that the major product was PHA (δ = -243.56 ppm), with trace amounts of AYB (δ = -52.65, -52.96, -57.51, and -57.74 ppm). The formation of AYB is a common side-product that can be formed during the work-up of the sample when it is exposed to oxygen.[172] Comparison with a standard solution of AN (δ = -325.10) confirmed that there was no amine production from the enzymatic reaction. Further studies with ^{1}H-NMR supported the fact that it was indeed PHA being produced from the enzymatic reduction (data not shown). This is also in agreement with the recent

findings of Pitsawong et al., in which the NRentcl was shown to produce exclusively the hydroxylamine equivalent of 4-nitrobenzoate.[173]

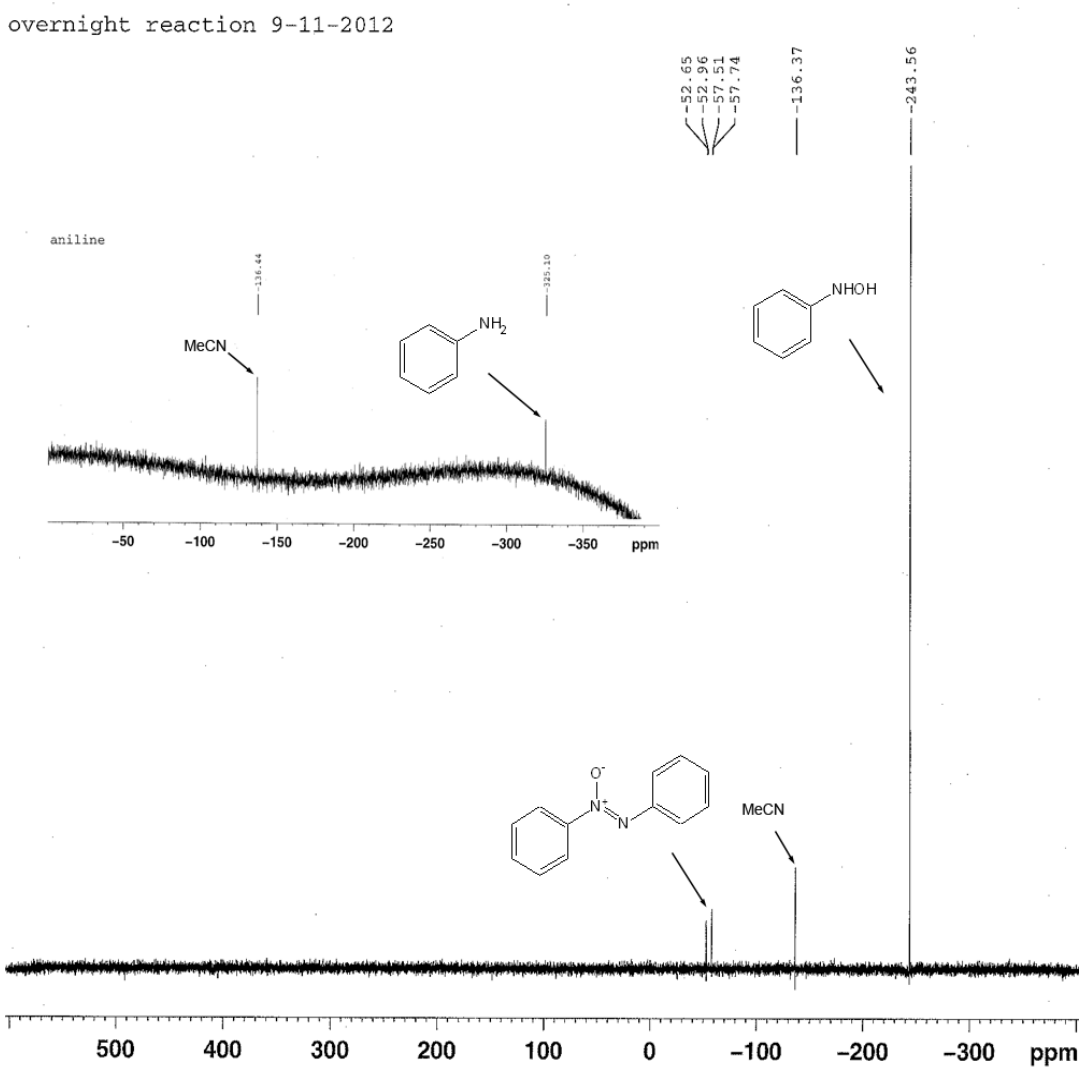

Figure 2.5 ^{15}N-NMR scan of nitrobenzene-^{15}N reduced with NRsalty, and AN standard

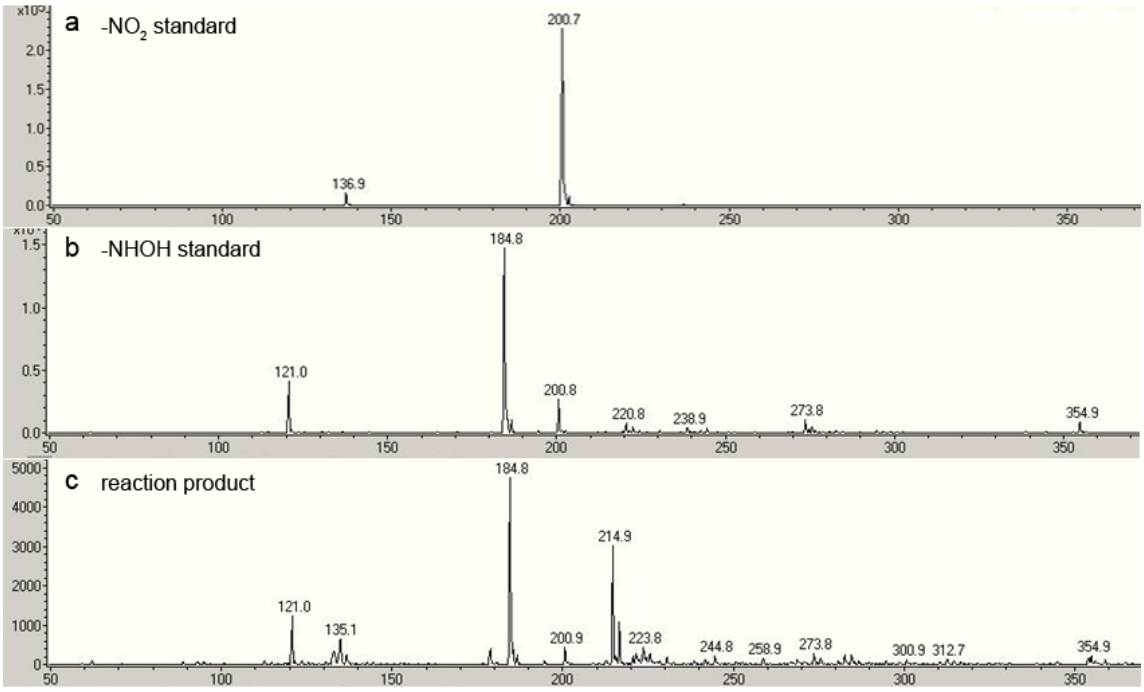

Figure 2.6 LC-MS analysis of NRsalty product. 1 mM 4- nitrobenzenesulfonamide (4-NBS), 5 U.mL^{-1} glucose dehydrogenase (GDH), 10 μM NAD^{+}, 10 mM dextrose, and 1 μM NR in 50 mM Tris-Cl (pH 7.5).

HPLC and LC-MS were implemented to develop a more practical analytical tool for the different nitroaromatics and its derivatives. Unsubstituted NB and its reduced forms are difficult to analyze on HPLC and LC-MS for the following reasons: i) AN is very basic, and cannot be retained on regular C18 columns, and ii) MS detection through Electrospray ionization (ESI) requires the target molecule to have ionization sites for protonation or deprotonation, where NB and its derivatives lack these characteristics. To overcome these issues 4-nitrobenzene sulfonamide (4-NBS) and 4-nitrobenzoic acid (4-NBA) were selected and synthesized as model substrates for these studies. Reduction of these substrates with NR yielded the hydroxylamines as the product both on HPLC and LC-MS (Figure 2.6), corroborating the findings on ^{15}N-NMR.

2.3.5 Possibility of Amine Formation

As previously discussed, most NRs have been shown to reduce nitroaromatics to hydroxylamines as final products. There are a couple of exceptions including NRmycsm from *M. smegmatis* and NR from *Streptomyces mirabils* DUT001 (NRstrmi). In the first example, *M. smegmatis* was found to be immune against the anti-tuberculosis benzothiazinone drug, BTZ043 (**9**). This resistance was identified to be caused by NRmycsm, which was capable of reducing the nitro drug to the corresponding amine, BTZ045, as the major product, rendering it inactive.[29] In the second example, Yang et al. showed that the soil bacterium *Streptomyces mirabils* DUT001 was able to reduce 4-nitro-1,8-naphthalic anhydride (4-NNA) to its corresponding amine and identified a NRstmi that was responsible for this transformation.[33,174]

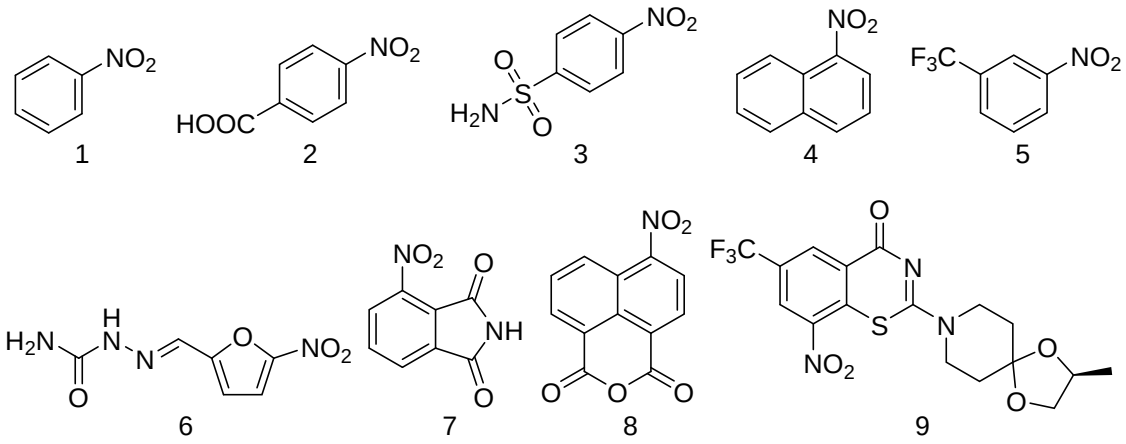

Figure 2.7 Nitroaromatic substrates used for product distribution studies

Based upon these examples, two hypotheses were estabilished: i) specific enzymes are able to reduce nitroaromatics to the amine, and/or ii) there are certain characteristics and attributes a substrate must have in order to be reduced to the amine.

To test these hypotheses, NRsalty and NRmycsm were utilized for the reduction of different nitroaromatics (Figure 2.7). To use minimal cofactor and drive the thermodynamic equilibrium for these reactions, an NADH recycling system using glucose dehydrogenase (GDH) was implemented. After an overnight reaction, the product was analyzed *via* HPLC and LC-MS.

Table 2.2 Substrate Study for Nitro Reduction.

	Name	Product	Analytical tools[a]	Detection
1	nitrobenzene	-NHOH	HPLC (40%)	235 & 265 nm
2	4-nitrobenzoic acid	-NHOH	HPLC (30%)	280 nm
3	4-nitrobenzenesulfonamide	-NHOH	HPLC (30%)	260 nm
			LC-MS (50%)	(-)-mode
4	1-nitronaphthalene	-NHOH	HPLC (40%)	215 nm
5	3-nitrobenzotrifluoride	-NHOH	HPLC (50%)	245 nm
6	nitrofurazone	-NHOH/-NH_2	HPLC (15%)	260 & 300 nm
			LC-MS (20%)	(+)-mode
7	3-nitrophthalimide	-NHOH	HPLC (30%)	230 nm
			LC-MS (50%)	(+)-mode
8	4-nitro-1,8-naphthalic anhydride	-NHOH/-NH_2	HPLC (50%)	270 & 345 nm
			LC-MS (50%)	(+)-mode

[a]percent of acetonitrile for the mobile phase with the make-up solvent as water

For most substrates both enzymes generated results similar to previous findings; the nitroaromatics were reduced to the hydroxylamine. 3-Nitrobenzotrifluoride was studied to see if the trifluoromethyl (–CF_3) substituent on BTZ043 (**9**) is responsible for amine production. Comparison of the enzymatic product and chemically synthesized standards showed that the corresponding hydroxylamine, *N*-hydroxy-3-(trifluoromethyl)-benzenamine, was produced. This implies that the –CF_3 substituent alone is insufficient, and the conjugated ring system of BTZ043 is necessary for the reduction to amine.

Interestingly, 4-NNA (**8**), the only substrate shown to be reduced to the amine with a single enzyme among the ones tested, showed to produce the amine, albeit in very

small quantities. Hypothesizing that bulkier substrates with more aromaticity are favorable for reduction, 1-nitronaphthalene (**4**) was studied but only yielded hydroxylamine.

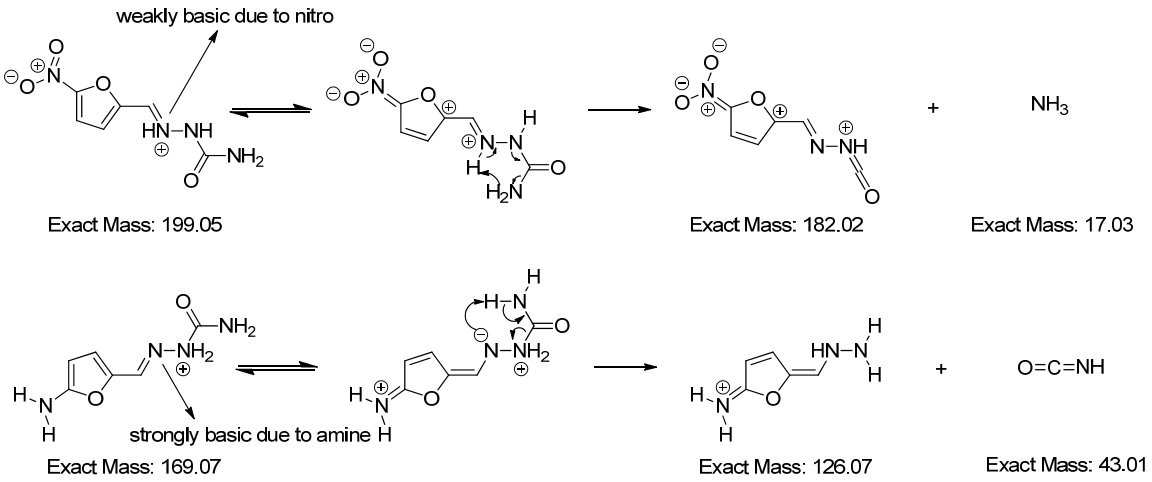

Figure 2.8 Proposed fragmentation of nitrofurazone and its corresponding amine.

Additionally, reduction of nitrofurazone (NFZ, **6**), while mostly resulting in the hydroxylamine, also produced a minute amount of aminofurazone (AFZ). To confirm the formation of AFZ both the substrate and product were analyzed using Mass spectrometry (MS) fragmentation and the resulting fragmentation patterns were compared. The major fragmentation masses for nitro- and aminofurazone were 182 and 126, respectively. The mass difference of the major fragment can be explained by comparing the change in resonance effect by the redox state (Figure 2.8). It is presumed that the electron-withdrawing effect of NFZ will make the imine nitrogen of the semicarbazone weakly basic, promoting rearrangement to release ammonia. AFZ will have the opposite outcome

since the amine group is electron-donating. This will cause the compound to rearrange and lose isocyanic acid, and the hydrazine will be detected.

2.4 Conclusion

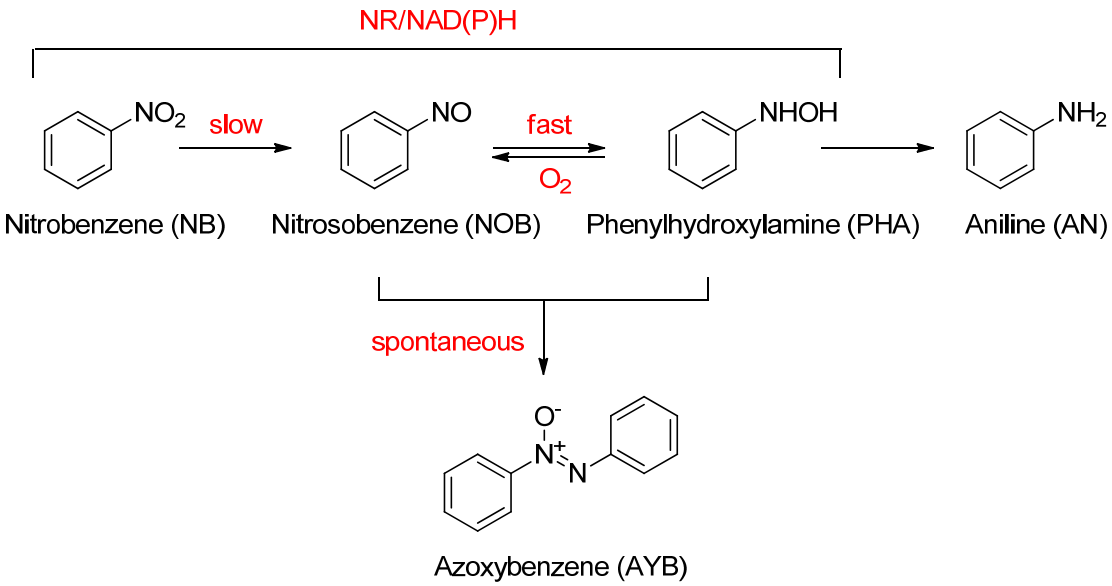

Figure 2.9 Updated reaction pathway of NB with NR.

The reaction pathway for NRsalty was found to be similar to that of previously published NRs (Figure 2.9).[40] The first reduction step from nitro to nitroso is relatively slow compared to the second step of nitroso to hydroxylamine. Molecular oxygen was identified as the cause for PHA oxidation to NOB, leading to the production of AYB. This side-reaction could be prevented effectively by performing the reactions anaerobically. Also, it was confirmed through ^{15}N-NMR and HPLC that the enzymatic product from NB was PHA, not AN. Previous detection of AN was an artifact of the GC analysis where the unstable PHA chemically reacted to form several products, among

them the amine. For analytical purposes, subsequent studies in this thesis were carried out with either 4-nitrobenzoic acid (4-NBA) or 4-nitrobenzenesulfonamide (4-NBS)

The reason for limited examples of amine production was investigated to define whether it was dependent on the enzyme and/or substrate. Reduction of an array of nitro substrates with NRsalty and NRmycsm suggested that the selectivity is unlikely to be dictated by the enzyme alone. Rather, there seems to be a relation with substrate features. A systematic approach with derivatives of BTZ043 may help understand the exact characteristics necessary to produce the amine.

CHAPTER 3

HAMMETT CORRELATION IN BIOCATALYTIC NITROAROMATIC REDUCTION

3.1 Introduction & Motivation

As discussed in Section 1.3.2, enzymatic reduction of nitro aromatics has been focused in the field of bioremediation. For such applications the molecule of interest commonly has multiple nitro groups on the benzene ring such as trinitrotoluene (TNT). Therefore, information available in the literature focuses on such compounds. There have been some instances where a large scope of substrates were studied, one example being the work of McCormick et al.[175]. However, these studies were in the context of cell free extract and only compared the reaction rate at one given condition, making it difficult to infer these results directly to single enzymes. Hence, a systematic approach, such as a quantitative structure–activity relationship (QSAR), will be immensely helpful in understanding and characterizing the substrate specificity of NRs.

In this study, the kinetic properties of previously discussed NRs, NRsalty from *Salmonella typhimurium* and NRmycsm from *Mycobacterium smegmatis*, were investigated. Additionally, the substrate specificity of both enzymes were explored over a broad range of substituted nitro compounds and characterized according to QSAR relationships. Overall, the target of this study was two-fold: gain better understanding of the mechanism and establish a criterion for potential target selection.

3.2 Materials & Methods

3.2.1 Enzymes and Chemicals

Enzymes were expressed and purified as described previously (Chapter 2). All chemicals such as substituted nitro compounds and salts used for buffers were obtained from Sigma-Aldrich (St. Louis, MO).

3.2.2 Enzyme activity assays

Initial specific activity measurements were conducted on a DU 800 spectrophotometer (Beckman Coulter; Brea, CA). Studies were performed with 0.1 μM enzyme, 0.5 mM NADH, and 0.1 mM nitro substrate at 25 °C. Oxidation of the cofactor NADH was monitored at 370 nm (ε_{370} = 2,660 $M^{-1}.cm^{-1}$).[176]

To determine the apparent NAD(P)H Michaelis-Menten kinetic parameters, k_{cat} and $K_M^{NAD(P)H}$, 2,4-dinitrotoluene (2,4-DNT) was used as a model substrate. A range from 0.013 to 0.5 mM and 0.05 to 2 mM was used for NADH and NADPH, respectively. When studying NRsalty, a range from 12.5 μM to 12 mM was studied for each substituted nitro compound depending on its solubility with 0.5 mM NADH. A baseline rate of NAD(P)H consumption was measured prior to addition of nitrosubstrate in order to account for NAD(P)H oxidation activity. For NRmycsm, a microtiter plate (MTP) assay was used with a Synergy H4 Multi-Mode Plate Reader (BioTek; Winooski, VT) in 96-well plates. Substrate concentrations ranging from 0.01 mM to 4 mM were studied to measure the kinetic parameters.

pH dependence of the enzyme kinetics were investigated by using 4-nitrobenzene sulfonamide (4-NBS) as a model substrate for NRsalty, and using 4-nitrobenzonitrile (4-

NBN) for NRmycsm. Buffers used for these studies were 50 mM citrate (pH 5-6), Bis-Tris-Cl (pH 6-6.5), Tris-Cl (pH 7-9), carbonate (pH 9-10).

3.2.3 Data analysis and fitting

Data were fit with OriginPro (v 9.0.0) software (OriginLab; Northampton, MA). Kinetic data for NAD(P)H and nitro substrates were fit according to the Michelis-Menten equation (Equation 3.1) where one substrate was varied while the other was fixed.[177] v is the reaction rate, $[E]_0$ is the enzyme concentration and $[S]$ is the varied substrate concentration. Equation (3.1) simplifies to equation (3.2) when the substrate concentration is much lower than K_M^S. The pH dependencies of steady-state kinetic parameters were fit with either equation (3.3), which describes a curve with unit slope on both sides of a plateau, or equation (3.4), which is simplified from equation (3.3) and applicable when the curve is present in the acidic region and the plateau is in the basic. $K_{a,1}$ and $K_{a,2}$ are the dissociation constants of the functional groups that are important for catalysis. Y is k_{cat} or k_{cat}/K_M^S, and C is the pH-independent value of the kinetic parameter of interest.

$$v = \frac{k_{cat}[E]_0[S]}{K_M^S + [S]} \tag{3.1}$$

$$v = \frac{k_{cat}}{K_M^S}[E]_0[S] \qquad when\ K_M^S \gg [S] \tag{3.2}$$

$$\log Y = \log \frac{C}{1 + \left(\frac{10^{-\mathrm{pH}}}{10^{-\mathrm{p}K_{a,1}}}\right) + \left(\frac{10^{-\mathrm{p}K_{a,2}}}{10^{-\mathrm{pH}}}\right)} \tag{3.3}$$

$$\log Y = \log \frac{C}{1 + \left(\frac{10^{-\mathrm{pH}}}{10^{-\mathrm{p}K_{a,1}}}\right)} \tag{3.4}$$

3.3 Results & Discussion

3.3.1 NAD(P)H kinetics and preference

A study was conducted to characterize each enzyme's preference for the nicotinamide co-substrate (for pH and activity profiles of NRmycsm see Appendix D). Kinetic parameters of the co-substrate NAD(P)H were obtained with 2,4-dinitrotoluene (2,4-DNT) as a fixed substrate, and fit according to the Michaelis-Menten equation (Table 3.1). NRsalty displayed a high k_{cat} when utilizing NADPH compared to NADH. However, the K_M^{NADPH} value (189 μM) was much larger compared to K_M^{NADH} value (39.3 μM). Further comparison of k_{cat}/K_M^{NADPH} and k_{cat}/K_M^{NADH} indicated that NADH is preferred as the co-substrate. For NRmycsm there was no preference between NADH and NADPH. Based on these findings subsequent substrate studies were carried out with NADH at 0.5 mM.

Table 3.1 Apparent kinetic parameters for NAD(P)H with 2, 4-DNT as a fixed substrate (not saturating conditions for 2, 4-DNT)

	NADH			NADPH		
	k_{cat} (s^{-1})	K_M^{NADH} (μM)	k_{cat}/K_M^{NADH} ($\mu M.s^{-1}$)	k_{cat} (s^{-1})	K_M^{NADPH} (μM)	k_{cat}/K_M^{NADPH} ($\mu M.s^{-1}$)
NRsalty	57 ± 2	39 ± 6	1.45 ± 0.23	104 ± 4	189 ± 23	0.55 ± 0.07
NRmycsm	23 ± 1	118 ± 15	0.12 ± 0.03	24 ± 1	95 ± 13	0.25 ± 0.04

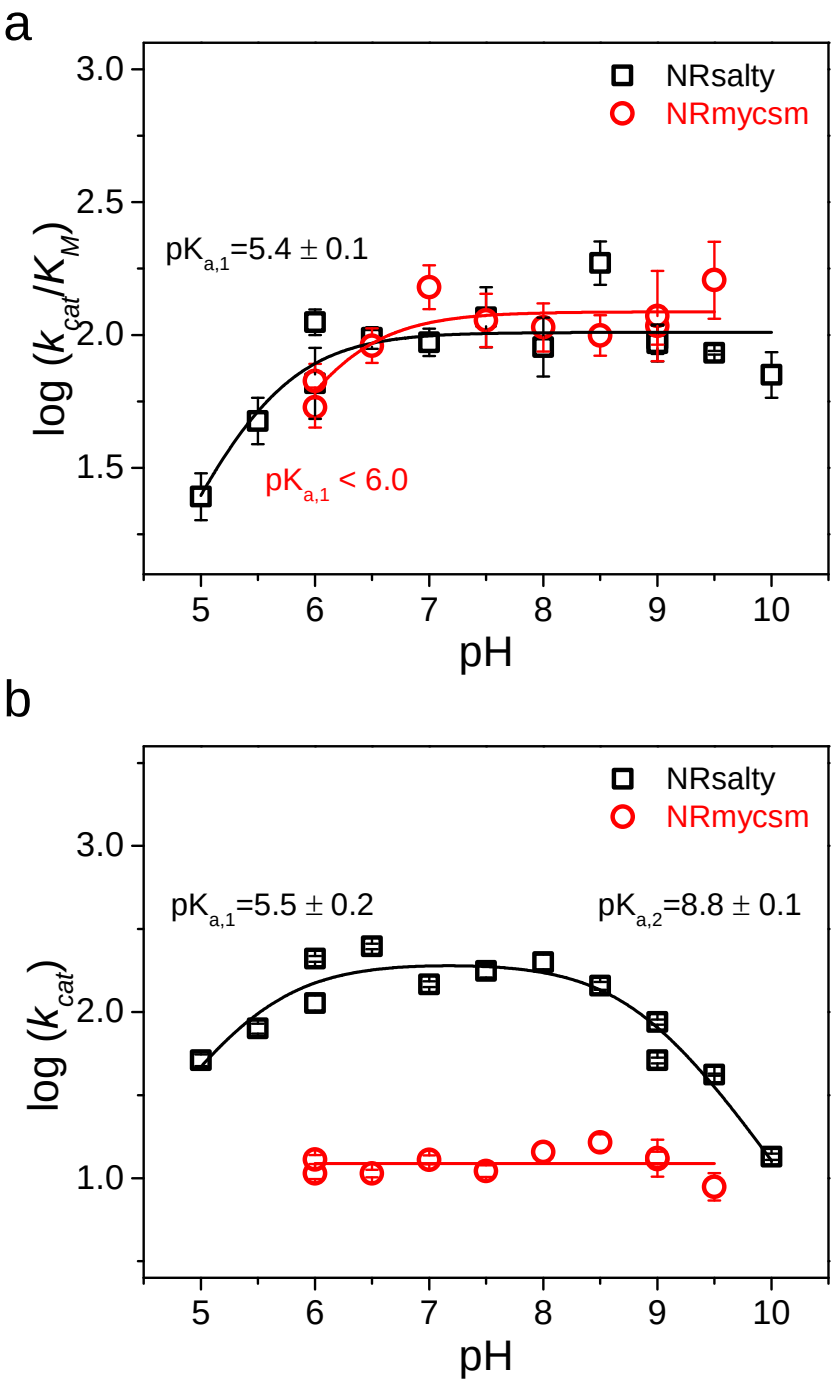

Figure 3.1 pH dependence of $\log(k_{cat}/K_M^S)$ and $\log(k_{cat})$ for NRsalty (black) and NRmycsm (red) with model substrates of 4-NBS and 4-NBN, respectively. Data were fit with equations (3.3) and (3.4).

3.3.2 pH dependence of k_{cat} and k_{cat}/K_M^S

The effect of pH on the steady-state kinetic parameters was determined for both NRsalty and NRmycsm (Figure 3.1). For NRsalty both k_{cat} and k_{cat}/K_M^{4-NBS} decrease in the acidic region and shows more less an identical p$K_{a,1}$ of 5.5. This phenomenon indicates that either there is a deprotonated residue that is important for a catalytic step occurring between substrate binding up through the first-irreversible step or that the enzyme is unstable at lower pH. A homology structure of NRsalty was designed using ESyPred3D[178] with NRentcl (PDB ID: 1KQC) [42], which shares an identity of 88.9%, as a template. This structure was searched for histidine (pK_a = 6.1), glutamate (pK_a = 4.1) and aspartate (pK_a = 4.1) as possible candidates for the deprotonated residue. Interestingly Glu165 and His128 were found to exist in close proximity (4.5 and 6.5 Å) to the substrate binding site. Glu165 is conserved throughout NRs from *E. cloacae*, *E. coli* and *S. typhimurium* and its amine backbone has been proposed to serve as a hydrogen bond donor for the N5 position of the flavin (3.1 Å) according to previously published three-dimensional structures.[42,44] The structure of NRmycsm (PDB ID: 2WZW)[29] was also examined as it exhibits a p$K_{a,1}$ < 6.0 for k_{cat}/K_M^{4-NBN}. However, none of the three residues (His, Glu and Asp) were found within 10 Å of the active site. This lack of such residues suggests that if both enzymes have identical catalytic mechanisms the observed decrease in k_{cat} and k_{cat}/K_M^{4-NBS} and k_{cat}/K_M^{4-NBN} is likely due to pH instability.

NRsalty had an additional p$K_{a,2}$ of 8.8 ± 0.1 in the basic region of the k_{cat} values. The pK_a from NRsalty can be indicative of a residue necessary for catalysis or it can be from the deprotonation of the substrate 4-nitrobenzenesulfonamide (4-NBS) as the substrate has a sulfonamide moiety (pK_a = 9.48).[179] This sulfonamide group does not

participate in the reaction, but the change in charge can easily change the transition state stabilization pattern. Compared to NRsalty that displays a basic pK_a, the k_{cat} of NRmycsm is independent of pH throughout the studied region. The the lack of a pK_a can be interpreted as a difference in the rate-limiting step between the enzymes. For example, NRsalty will be exhibiting the pK_a because the chemical step is partially rate-limiting, whereas NRmycsm will be pH independent because a there is a step slower than catalysis, such as product release, which is fully rate limiting. To investigate whether the pK_a is from the substrate or enzyme two sets of approaches can be proposed. The first is measuring the k_{cat} of NRsalty with a different but similar substrate that has no difference in protonation state at basic pH to identify if the pK_a comes from the substrate. The second way to identify the source of the pK_a is to identify residues in the active site that could contribute to the pK_a at 8.8 and mutate it to a different, but similar, amino acid in order to shift the pKa. Within 5 Å of the substrate binding site only one residue, Lys14, is a candidate, and mutating this residue to an Arg should help verify if this residue is catalytically active. Additionally, further studies with stopped-flow kinetics are required to identify rate-limiting steps at each pH for a more in depth understanding of the mechanism.

3.3.3 Specific activity of substituted nitroaromatics

To study the substrate spectrum of NRs kinetic assays to monitor NAD(P)H oxidation were performed with UV-visible spectroscopy at 370 nm (ε_{370} = 2,660 $M^{-1}.cm^{-1}$), rather than 340 nm (ε_{340} = 6,220 $M^{-1}.cm^{-1}$). This was done to i) avoid absorbance overlap from the nitroaromatic substrates, and ii) accommodate higher NAD(P)H concentrations. Preliminary specific activity measurements were performed with 0.5 mM NADH and 0.1

mM substrate. Initial specific activity studies included a variety of nitrobenzenes with electron-donating and withdrawing substituents at the *meta*- and *para*-positions. Substrates with *ortho*-substitutions were excluded as steric effects could lead to complications. The NADH oxidase activities were measured by monitoring the NAD(P)H oxidation in the absence of nitro substrates, and subtracted as background activity (less than 3% activity compared to slowest nitro substrate). This measure was taken to correct for the presence of molecular oxygen which is an additional substrate that can consume the cofactor, as these experiments were conducted under aerobic conditions.

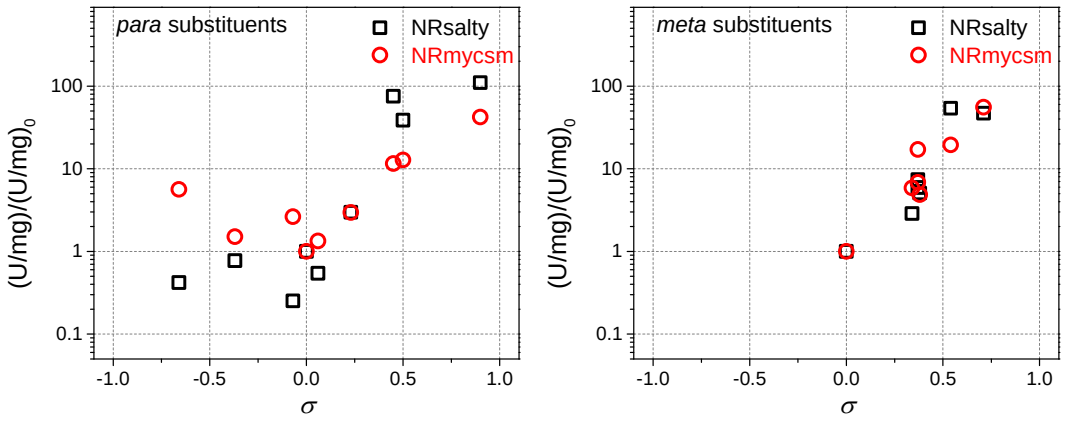

Figure 3.2 Specific activity of NRsalty and NRmycsm plotted according to the Hammett equation

For both enzymes, it was observed that substrates with stronger electron-withdrawing groups had higher specific activity, which is in agreement with previously published literature.[56,175,180] These observations were investigated for any potential quantitative structure-activity relationships (QSAR) by separating the substrates according to the substituent position relative to the nitro group, *meta*- and *para*-, and

plotting the results according to their Hammett substituent constants and relative specific activities (Figure 3.2).[181,182] Regardless of the substituent position, it was clear that the activities had a QSAR which lead to the hypothesis that the kinetic parameters, namely k_{cat} and k_{cat}/K_M^S, can be characterized with the Hammett correlation.

3.3.4 Hammett Correlation

The Hammett equation was developed to explain the effect of a substituent on reaction rates and equilibrium constants as a linear free-energy relationship.[183] This was developed using ionization of benzoic acids as a model system, where Hammett himself studied many benzoic acid derivatives to measure the effect of the different substituents.[184] The relationship was described through the following equation,

$$\log\frac{k}{k_0} = \sigma\rho \qquad (3.5)$$

where k is the reaction rate with a substituent, and k_0 is the value of the unsubstituted moiety. The Hammett substituent constant, σ, captures inductive and resonance effects within the substrate whereas the Hammett reaction constant, ρ, represents the nature of the reaction. A positive ρ indicates that a negative charge is created or a positive charge is lost in the transition state. The opposite holds when ρ is negative, and when there is no change in charge ρ will be zero.

To characterize the NRs according to the Hammett relationship, kinetic parameters were developed with various *para*-substituted nitroaromatics according to the Michaelis-Menten model (Table 3.2). These measurements were taken at pH 7.5 where the enzyme kinetics is independent of pH. For NRsalty, it was impossible to elucidate k_{cat} and K_M^S in certain cases as the activity did not reach saturation before encountering solubility limits. Instead, k_{cat}/K_M^S was measured from the linear increase of activity with

increasing substrate concentration, where the Michaelis-Menten model simplifies to equation (3.2).

Table 3.2 Kinetic parameters for various substituted nitroaromatics

NRsalty

Substituent	Sigma (σ)	k_{cat} (s^{-1})	K_M^S (mM^{-1})	k_{cat}/K_M^S ($s^{-1}.mM^{-1}$)
-H	0	-	-	1.7 ± 0.1
$-COO^-$	0	5.8 ± 0.3	1.13 ± 0.11	5.1 ± 0.6
-Cl	0.23	-	-	5.2 ± 0.2
$-COOCH_3$	0.45	-	-	84.5 ± 6.8
$-COCH_3$	0.5	166 ± 25	0.99 ± 0.28	167 ± 54
$-SO_2NH_2$	0.6	182 ± 11	1.68 ± 0.29	108 ± 20
-CN	0.66	290 ± 13	1.22 ± 0.10	238 ± 22
$-SO_3CH_3$	0.9	275 ± 22	0.74 ± 0.17	373 ± 90

NRmycsm

Substituent	Sigma (σ)	k_{cat} (s^{-1})	K_M^S (mM^{-1})	k_{cat}/K_M^S ($s^{-1}.mM^{-1}$)
-H	0	3.4 ± 0.4	2.82 ± 0.61	1.2 ± 0.3
-Cl	0.23	4.5 ± 0.5	0.39 ± 0.14	11 ± 4
$-COOCH_3$	0.45	9.0 ± 0.3	0.12 ± 0.01	75 ± 7
$-SO_2NH_2$	0.6	17.2 ± 0.9	0.19 ± 0.02	91 ± 13
-CN	0.66	16.0 ± 1.0	0.14 ± 0.03	111 ± 22
$-SO_3CH_3$	0.9	19.1 ± 0.8	0.12 ± 0.01	165 ± 18

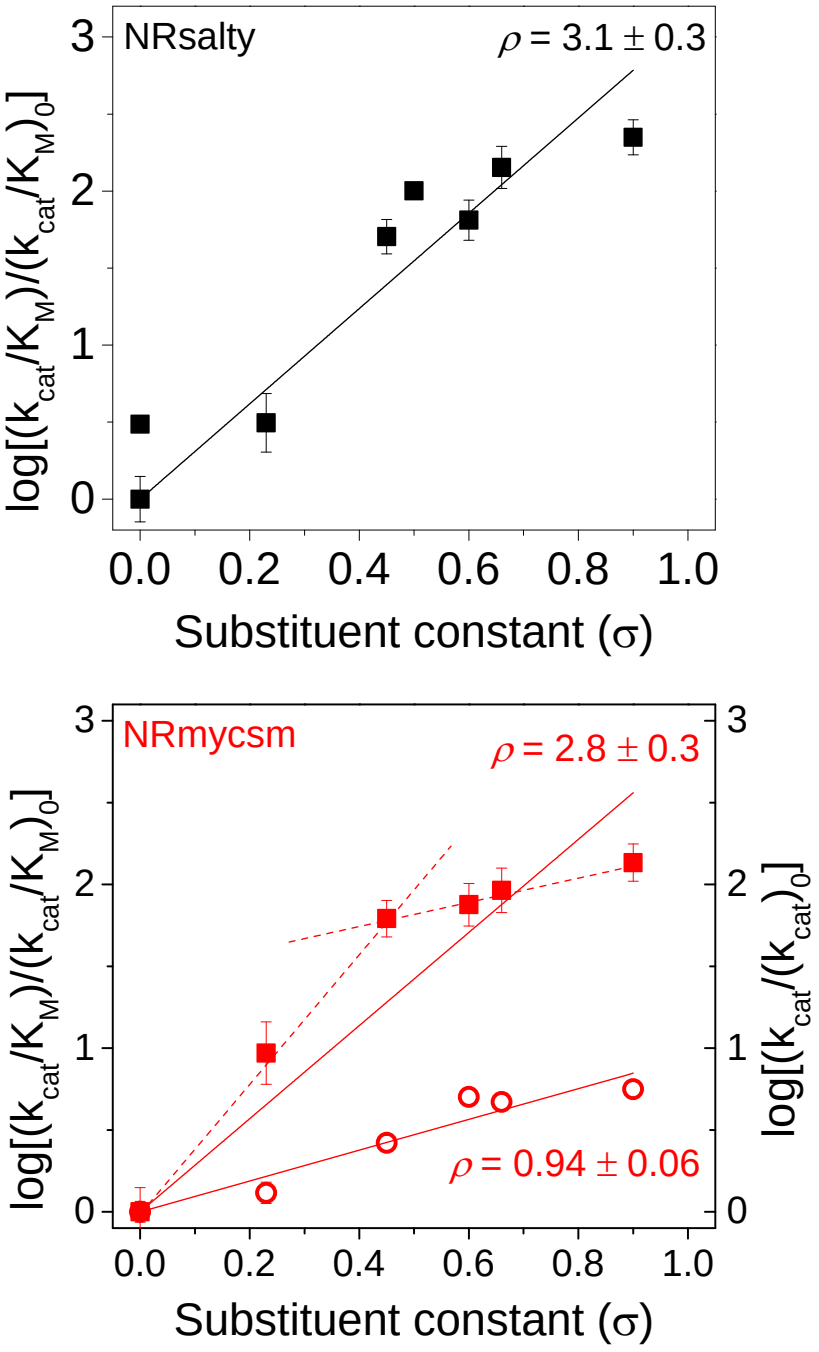

Figure 3.3 Hammett plots for a) NRsalty and b) NRmycsm.
(■ and ■): $\log[(k_{cat}/K_M^S)/\ (k_{cat}/K_M^S)_0]$; (○): $\log[(k_{cat})/\ (k_{cat})_0]$

When plotting the kinetic data as a function of the Hammett equation, both enzymes showed to have a Hammett reaction constant, ρ, of roughly 3 for their $\log[(k_{cat}/K_M^S) / (k_{cat}/K_M^S)_0]$ relationship. These comparable ρ values indicate that the characteristic of the transition states produced by the two different enzymes is nonetheless similar. However, it can also be argued that there is a change in the substituent effect ρ for NRmycsm. Here, two linear regressions can be plotted with $\sigma =$ 0.45 as the transition point where the nature of either substrate binding or the first irreversible-step in overall steady-state kinetics changes. Although it is unknown what part of catalysis is being affected, there is a possibility that this phenomenon can be related with steric effects of the lower σ substrates which are generally smaller in size. The hypothesis will be that initially the substituents improve binding drastically, but this improvement becomes insignificant once the substrate becomes bulkier. Notably, the K_M^S value of the unsubstituted nitrobenzene is much higher compared to those with substituents. For higher σ substrates the increase would then be a result of transition state stabilization of the first irreversible-step. To rule out substrate binding as the cause for this transition point, additional experiments to study the substrate binding affinity (K_d). Such experiments will include measuring the substrate kinetic rates while varying inhibitor concentration or monitoring the flavin fluorescence quenching while varying the substrate concentration.

Overall, the Hammett correlation supports our hypothesis that electron-withdrawing groups stabilize the transition state formed by the enzymes. This implies that the transition state involves accumulation of excess electron density. Therefore,

when selecting substrates for reduction, it is important to note that those with a larger σ can be expected to be better substrates.

3.4 Conclusion

In summary, the pH dependencies of NRsalty and NRmycsm revealed that there is an acidic pK_a that is important for a phenomenon occurring before the first irreversible-step. However, the lack of a similar residue in both substrates suggests that it may be due to enzyme instability at acidic pH values. Further, the absence of a basic pK_a for NRmycsm indicates that product release may be rate-limiting. Both NRsalty and NRmycsm exhibit better catalytic reduction of substrates with electron-withdrawing substituents *para*- to the nitro group. This phenomenon was analyzed via the Hammett equation wherein NRsalty showed a linear increase of $\log[(k_{cat}/K_M^S) / (k_{cat}/K_M^S)_0]$, but NRmycsm showed a possible change in either substrate binding or transition-state stabilization. Additional studies on NRmycsm are necessary to understand each catalytic step independently to test the hypothesis: at low σ the substrate binding is affected and substantially improves k_{cat}/K_M^S, whereas at high σ the extent of transition state stabilization of the first irreversible-step by electron-withdrawing groups dictates k_{cat}/K_M^S. However, these studies were not pursued as they were beyond the scope of this thesis.

CHAPTER 4

ENZYMO-CHEMICAL SYNTHESIS OF AMINES

4.1 Introduction & Motivation

As discussed in Chapter 2 many of the currently studied NRs produce the hydroxylamine as the final product. As the pharmaceutically interesting compounds are amines, it is necessary to develop a way to further reduce the hydroxylamine. One method to achieve this goal is to pair enzymatic reduction with chemical reduction. Examples of combined enzymatic and chemical synthesis include deracimisation of D, L-amino acids using amine-boranes and L-amino oxidase, chiral alcohol synthesis with palladium and alcohol dehydrogenase, and synthesis of asymmetrically branched *N*-glycans with glycosyltransferases from chemically synthesized glycan precursors.[185-187] In all these cases, the enzymatic step follows the chemical ones (and usually introduces the chirality); therefore, the processes are termed chemoenzymatic processes. Here, a system was designed to utilize NRs in conjunction with simple reducing agents for a sequence of enzymatic reductions followed by a chemical reduction; this sequence therefore is termed enzymo-chemical reduction (Figure 4.1).

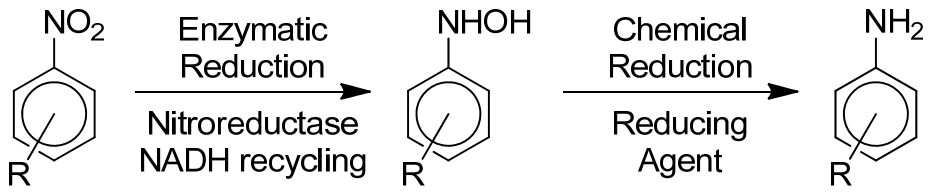

Figure 4.1 Overall reduction scheme of the enzyme-chemical sequence from nitro to amino aromatics

4.2 Materials & Methods

4.2.1 Chemicals

Substrate and product standards such as 4-nitrobenzoic acid, 4-nitrobenzene sulfonamide, 4-aminobenzoic acid, and sulfanilamide, and reducing agents including sodium dithionite (sodium hydrosulfite), formamidine sulfinic acid (thiourea dioxide), amine-borane, and sodium cyanoborohydride were purchased from Sigma-Aldrich (St. Louis, MO).

Sodium 4-nitrobenzoate was prepared by dissolving 4-nitrobenzoic acid in ethyl acetate. The dissolved compound was precipitated as a sodium salt with the addition of a 10 N NaOH solution. The resulting crystals were filtered, washed with additional ethyl acetate and vacuum dried.

All other material is discussed in section 2.2.1.

4.2.2 Reducing agent screening

Reducing agents sodium dithionite (SD), formamidine sulfinic acid (FSA), ammonia borane, sodium cyanoborohydride, and sodium formate were incubated with either 1 mM of 4-(hydroxyamino)benzoic acid or 4-(hydroxyamino)benzene sulfonamide at a final starting concentration of 5 mM. After 5 h of incubation the reaction mixtures were analyzed using HPLC. For SD and FSA, experiments were repeated anaerobically in a Coy anaerobic chamber (Grasslake, MI). FSA reduction temperature dependence was studied by varying the incubation temperature at 25, 37, 60, 80 °C. The reaction was continued for 5 h, then diluted with an equal volume of acetonitrile and analyzed through HPLC.

4.2.3 HPLC analysis

4-Nitrobenzoic acid and 4-nitrobenzene sulfonamide, and their reduced states were analyzed using HPLC (Shimadzu; Kyoto, Japan). Analysis was conducted with a Shimadzu LC-20AT pump, Phenomenex Luna® 5 μM C18 100 Å 250 x 4.6 mm, and SPD-M20A prominence diode array detector (PDA). Separation was achieved with an isocratic flow of water:acetonitrile (70:30) at a flow rate of 1 $mL.min^{-1}$. Retention times: 4-(hydroxyamino)benzoic acid 3.65 min, 4-aminobenzoic acid 4.26 min, 4-nitrobenzoic acid 15.5 min monitored at 280 nm; 4-(hydroxyamino)benzenesulfonamide 3.33 min, 4-sulfanilamide 3.66 min, 4-nitrobenzenesulfonamide 9.34 min monitored at 260 nm.

4.2.4 Enzymo-chemical reduction

Nitroreductase from *Salmonella typhimurium* (NRsalty) was purified as discussed previously (Section 2.2.3). Enzymatic reduction was performed at a 1 mL scale with a final concentration of 1 mM substrate (pre-dissolved as 200 mM in DMSO), 1 μM NRsalty, 2.5 $U.mL^{-1}$ glucose dehydrogenase (GDH), 10 mM dextrose, and 0.1 mM NAD^+. After 1 h, chemical reduction was initiated by an addition of 5 mM FSA and 1 M HCl, and incubated at 60 °C. The reaction mixture was diluted in half with HPLC acetonitrile, centrifuged at 13793 g for 5 mins, and then analyzed using HPLC.

4.2.5 Large Scale Synthesis

75 mM Sodium 4-nitrobenzoate (1.42 g, 7.5 mmol) was dissolved and reduced in 100 mL of 100 mM NaP_i buffer with a GDH recycling system (250 mM dextrose, 1 mM NAD^+, 10 $U.mL^{-1}$ GDH), and 5 μM of NRsalty for 6 h. The resulting hydroxylamine was further reduced with the direct addition of HCl and FSA to a final concentration of 1 M and 250 mM, respectively, and incubated at 60 °C for 12 h. The reaction product was extracted

three times with ethyl acetate (50, 25, and 10 mL), dried over $MgSO_4$, and filtered. The product was recovered through rotary evaporation with a final mass of 0.94 g.

4-amino-benzoic acid: ^{1}H NMR (400 MHz, DMSO-d_6): δ 12.00 (s, 1H, OH), 7.58 (d, 2H, J = 8.8 Hz, CH), 6.51 (d, 2H, J = 8.8 Hz, CH), 5.87 (s, 2H, NH).

4.3 Results & Discussion

4.3.1 Sodium dithionite

Sodium dithionite (SD) was selected as the initial reducing agent as Powell et al. showed that it can be used to reduce *N*-nitrosotetrahydroisoquinoline to its corresponding amine.[188] Preliminary experiments were conducted by reducing 4-(hydroxyamino)-benzoic acid while varying the amount of SD. HPLC analysis of the reaction showed that the addition of SD converted –NHOH to $–NH_2$. However, about 60% of the starting material converted to side-products in the reaction. These side-products were presumed to be charged and hydrophobic based on their HPLC elution times and immiscibility in organic solvents. One possible side-product can be the sulfamic acid that has been proposed to form from an aromatic hydroxylamine.[189] Additionally, as dithionite is known to react with molecular oxygen to create radicals, there is concern that this will be the cause of side-product formation. To avoid such complications, experiments were repeated in anaerobic conditions, but no significant difference was detected in the product distribution (data not shown).

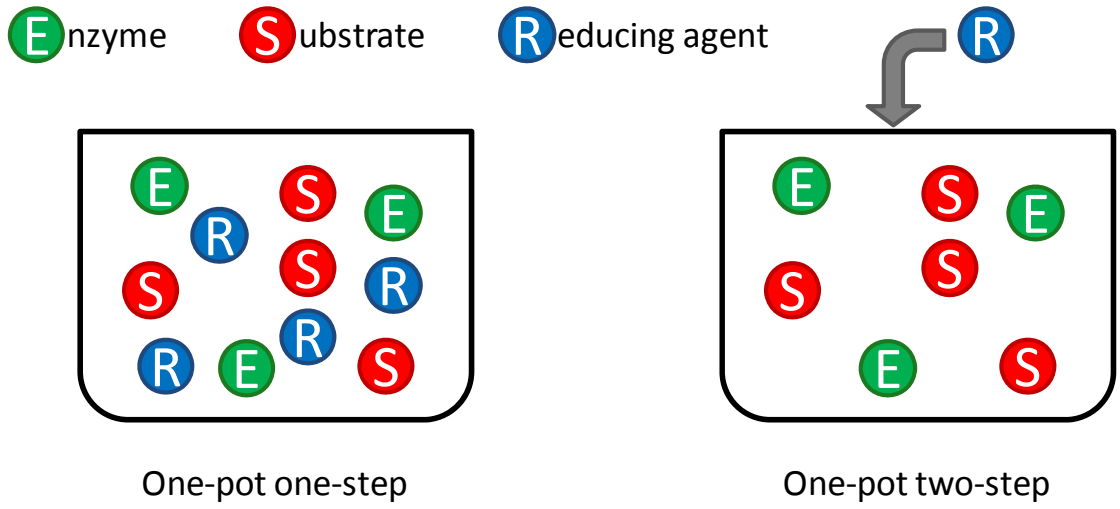

Figure 4.2 Proposed setups for combining the enzymatical and chemical reactions

4.3.2 Overall scheme of reduction

To investigate feasibility of combining the enzyme and chemical reactions, two setups were proposed for amine production (Figure 4.2). The first was a single-batch reaction where all components were combined from the beginning. The second was a two-step synthesis where the enzymatic reduction with NR takes place, followed by the addition of the reducing agent to complete the production of amine. Here, the first approach failed to effectively convert the nitro substrate to the hydroxylamine, limiting the overall conversion (less than 20% conversion). This can be understood in conjunction with the fact that SD is known to create radicals that can deactivate enzyme by reacting with the flavin cofactor.[190] Moreover, SD can react with the nitro substrate to create a radical-anion which in turn produces superoxide from oxygen, opening up additional possibilities to deactivate the enzyme.[191,192] In the second system, full conversion of the nitro to hydroxylamine was achieved, but subsequent reduction with SD still suffered from

selectivity limitations. Concerns regarding the product selectivity and SD oxygen sensitivity lead to a continued search for reducing agents.

4.3.3 Screening reducing agents

Additional reducing agents were screened based upon previous literature examples of imine and oxime reduction. These included formamidine sulfinic acid (FSA) [193], amine-borane [194], and sodium cyanoborohydride [195]. They were tested for the chemical reduction of hydroxylamine (Table 4.1). FSA was able to reduce to the amine with a yield of roughly 30%. However, ammonia-borane and sodium cyanoborohydride showed no reactivity towards the hydroxylamine.

Table 4.1 Preliminary screen of reducing agents.

Reducing Agent	Formula	Amine yield (%)
Sodium Dithionite	$Na_2S_2O_4$	36
Formamidine sulfinic acid	$NH_2C(=NH)SO_2H$	31
Ammonia-borane	BH_3NH_3	0
Sodium cyanoborohydride	$NaBH_3CN$	0

4.3.4 Optimization of formamidine sulfinic acid (FSA) reduction conditions

The redox potential of a reducing agent is known to be dependent on the temperature and pH of the solution. Previous studies with FSA have shown that its redox potential becomes increasingly negative with increasing temperature and decreasing pH.[196] To investigate whether this influences the conversion, different temperatures and pH values were studied to find optimal conditions for the chemical reduction.

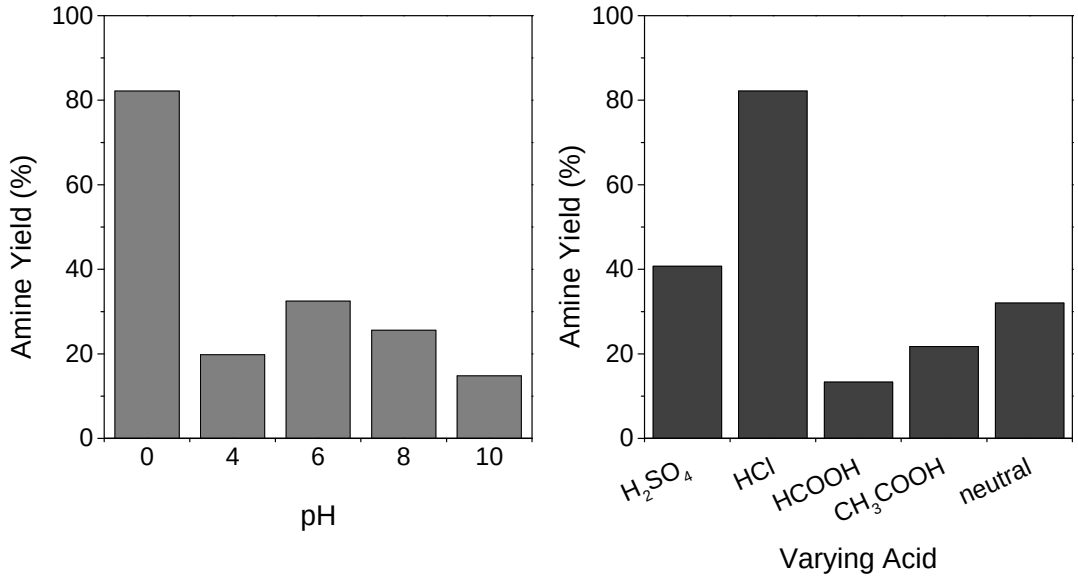

Figure 4.3 Production of amine with FSA while varying the pH value (50 mM buffer) and acid type (1 M) at 60 °C

Temperatures of 25, 37, 60 and 80 °C were tested; largest amounts of amine were observed at 60 and 80 °C. Although FSA has been shown to reduce nitroaromatics to amines under basic conditions, the selectivity is lost as carbonyl groups will be reduced to alcohols.[193,197-199] Additionally, basic conditions are unfavorable for liquid-liquid extraction of certain substrates that have pK_a values less than 12, as they would be charged under basic conditions and thus not extract into the organic phase. Therefore, the pH study was limited to neutral and acidic conditions. Solutions with a pH value of 0, 4, 6, 8, and 10 were tested, and the most acidic condition was found to work best (Figure 4.3). To understand if the type of acid had a significant impact several different types were screened at a constant concentration of 1 M. Among those, only HCl had a significant impact on the amine yield (Figure 4.3). The results for formic acid and acetic acid are not surprising as both have higher pK_a values (3.75 and 4.75, respectively) than

HCl (pK_a = -7). At 1M concentration formic and acetic acid solutions will result in overall pH values of 1.9 and 2.4. However, it is intriguing that the comparably strong acid H_2SO_4 (pK_a = -6.62) did not exhibit high yields. A speculative reasoning can be placed based on the fact that sulfuric acid is an oxidizing acid, which can interfere with the reducing mechanism. The possibility of aromatic nitro reduction with FSA was examined to ensure that the complete reaction would not occur under acidic conditions and higher temperatures (i.e. to confirm that the enzyme reduction was still necessary). The nitro group was unaffected during reductions indicating that the hydroxylamine is selectively reduced in acidic conditions (data not shown). Based on these results subsequent chemical reduction with FSA was carried out with the addition of 1 M HCl, and incubation at 60 °C.

4.3.5 Enzymo-chemical reduction

Enzymo-chemical reduction of 4-nitrobenzoic acid was achieved as a one-pot two-step synthesis with NRsalty and FSA (Figure 4.4). Without the addition of FSA, there was no amine found in the reaction. When reduction with FSA was initiated, the amount of hydroxylamine immediately decreasing while the final product was confirmed as 4-aminobenzoic acid through HPLC, and the non-isolated yield after 6 h was 82%.

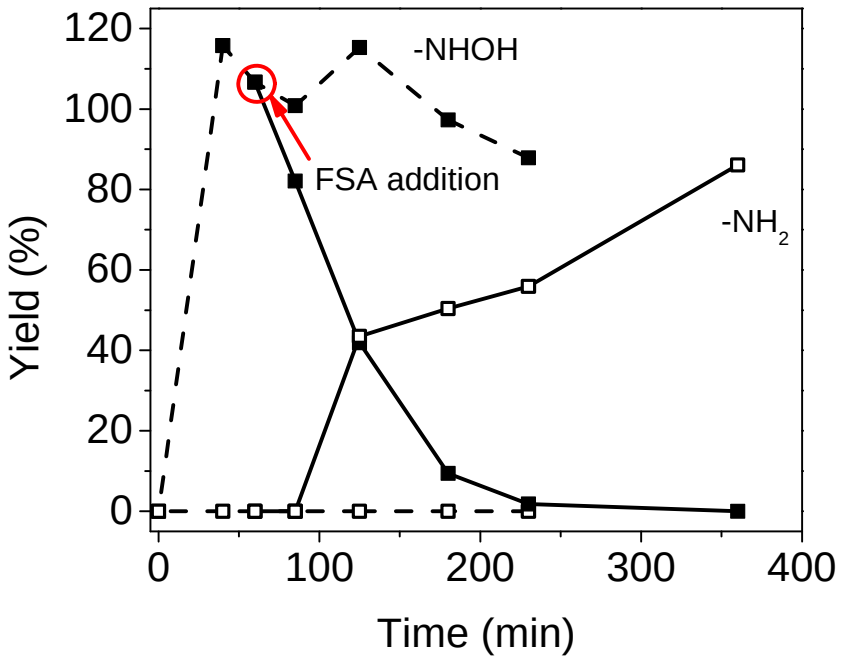

Figure 4.4 One-pot two-step reduction of 4-nitrobenzoic acid with NRsalty reduction to –NHOH and addition of FSA at 60 mins; (■): -NHOH; (□): -NH2; solid line: after addition of FSA; dotted line: control experiment (no addition of FSA after 60 mins); conditions: 60 °C, pH 0, [FSA] 5 mM, relative molarity [FSA]/[NHOH] = 5.

4.3.6 Scale-up of synthesis

Enzymo-chemical reduction was scaled up to a gram scale, where the reduction was carried out at a 100 mL reaction volume. 4-Nitrobenzoic acid was converted to its sodium salt and used as the starting substrate. The higher solubility of the sodium salt greatly increased the substrate availability in aqueous solution. 1.42 g of sodium 4-benzoic acid was reduced with 5 μM NRsalty in the presence of a GDH recycling system. The reaction was monitored via HPLC and when conversion of the nitro substrate to hydroxylamine was complete the chemical reaction was initiated with the addition of FSA and HCl. After overnight incubation at 60 °C the product was extracted with ethyl acetate and dried with $MgSO_4$. Solid crystals were obtained through rotary evaporation and analysis of the

isolated dry product was performed via ^{1}H-NMR (Figure 4.5) and HPLC (Figure 4.6). Comparison with 4-aminobenzoic acid authentic standards revealed that the product was indeed the amine. Most importantly, the appearance of the NH protons was notable from the NMR spectrum. A total mass of 0.94 g was obtained from the reaction. Excluding a minor amount of residual ethyl acetate (1.3 % w/w) the isolateed yield was 90.2%.

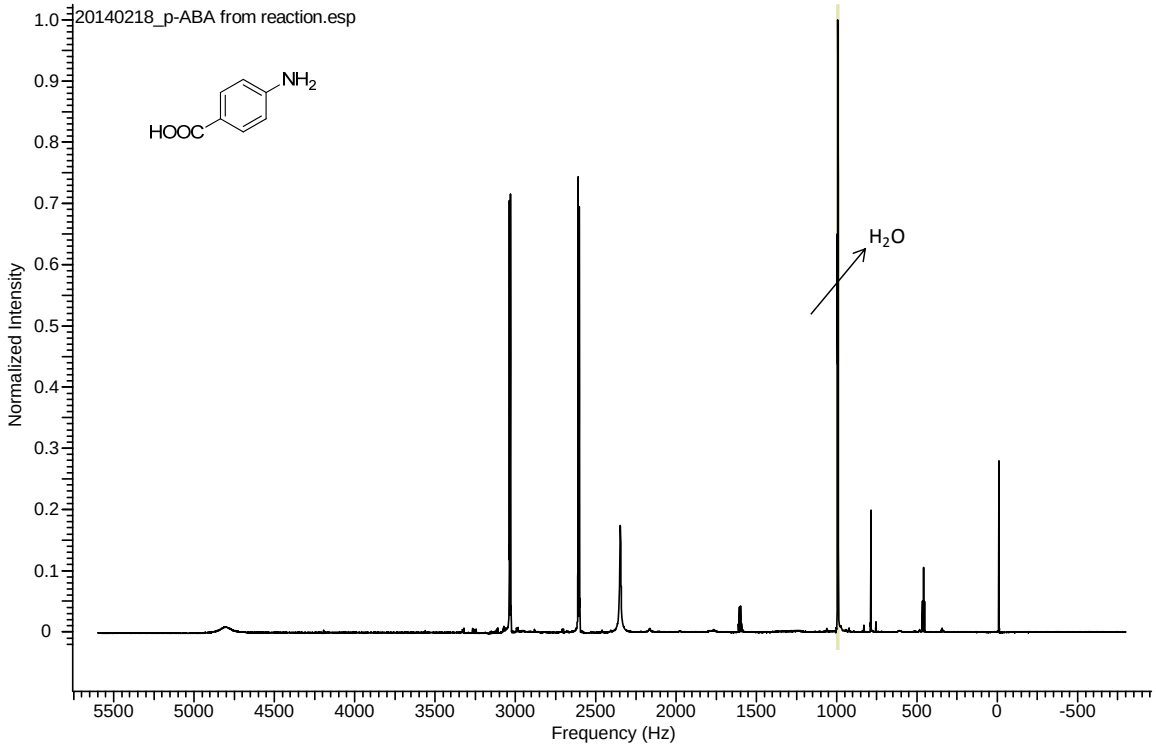

Figure 4.5 ^{1}H-NMR spectra of 4-aminobenzoic acid in DMSO-d_6

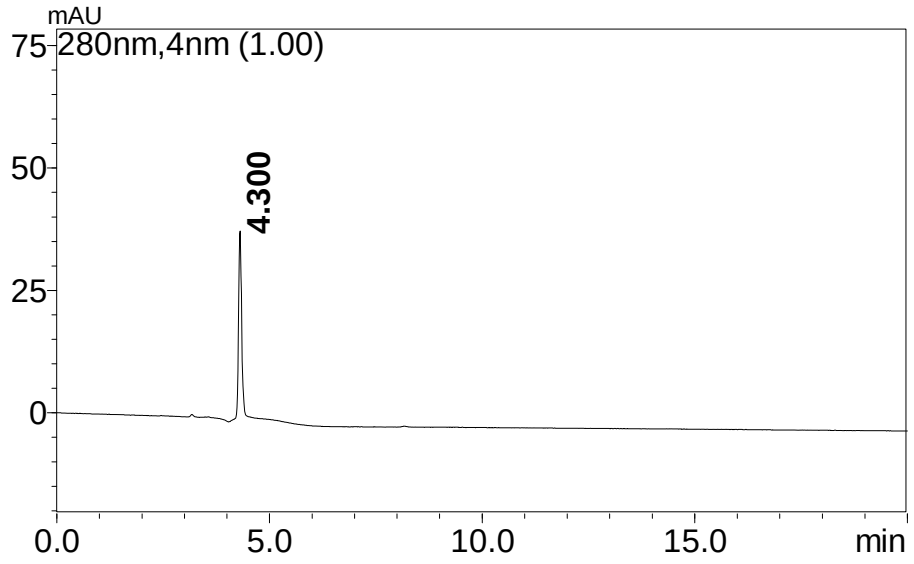

Figure 4.6 HPLC chromatogram of purified 4-aminobenzoic acid

4.4 Conclusion

In summary, this study has identified sodium dithionite (SD) and formamidine sulfinic acid (FSA) as effective reducing agents for the reduction of hydroxylamines to the corresponding amines. Further optimization of reduction with FSA in acidic conditions and elevated temperatures demonstrated an amine production with high yield (>80%). Importantly, the acidic conditions helped preserve the selective hydroxylamine reduction, whereas in basic conditions the carbonyl groups can possibly reduce to alcohols.[197,199] A one-pot two-step enzyme chemical reduction was conceived and proven to work as anticipated. Scale-up was attempted with sodium 4-nitobenzoate as a substrate, and from here, 90.2% was recovered as the 4-aminobenzoic acid.

CHAPTER 5

ENGINEERING TOWARDS NITROREDUCTASE FUNCTIONALITY IN ENE-REDUCTASE SCAFFOLDS

5.1 Introduction & Motivation

As previously discussed in Chapter 1, both nitroreductases (NRs) and ene-reductases (ERs) utilize flavin mononucleotide (FMN) as a cofactor, but catalyze distinct reactions. NRs are capable of reducing nitroaromatics to their corresponding hydroxylamines, and in rare cases the amine, while ERs are widely used to reduce alkenes with adjacent electron withdrawing groups such as aldehydes, ketones, esters, carboxylic acids and nitriles.[102,103,200]

A pronounced difference in these enzymes lies in their distinct structures. NRs are homodimeric enzymes that have the FMN cofactor bound at the interface, where the active site is composed of residues from both monomers.[42,43]_ENREF_52 In comparison, ERs have a TIM barrel structure that can either exist as monomers, dimers, and other multi-oligomeric states.[200,201]_ENREF_51 The FMN cofactor is bound at the C-terminal of the barrel, which forms an active site, independently for each monomer.

Interestingly, the functionality of these enzymes is known to overlap to some extent. NR from *Salmonella typhimurium* is known to reduce α, β-carbon double bonds with adjacent nitro groups, whereas OYE1 from *Saccharomyces pastorianus*, pentaerythritol tetranitrate (PETN) reductase from *Enterobacter cloacae* and xenobiotic reductase A (XenA) from *Pseudomonas putida* have been shown to reduce explosives

such as trinitrotoluene (TNT) through nitro reduction.[39,202] However, the reason for this cross-selectivity has yet to be understood.

Previously, Yanto et al. has shown that nitrobenzene conversion of xenobiotic reductase A (XenA) from *Pseudomonas putida* is higher when mutating cysteine at position 25 to glycine (C25G).[203] This was chosen as a starting point to investigate the possibility of increasing NR functionality in ER scaffolds. The overall hypothesis for this work was that ER or NR functionality can be determined by a few active site residues such as C25G, and, thus, that variants of active site residues can lead to a switch in functionality.

In this study, ERs KYE1 from *Kluyveromyces lactis* and YersER from *Yersinia bercovieri* are selected as model enzymes due to their high similarities to OYE1 and PETN reductase, respectively (for sequence similarities see Appendix B).[116] Introduction of NR functionality into these enzymes is attempted through site-directed and iterative mutagenesis. The study focuses on two main goals: scientifically, we desire a better understanding of the governing factors in functional selectivity and from an engineering perspective, utilization of the monomeric scaffold is targeted for future applications where such a tertiary structure is beneficial.

5.2 Materials & Methods

5.2.1 Chemicals

Ene-substrates ketoisophorone and 2-cyclohexen-1-one were purchased from Sigma-Aldrich (St. Louis, MO) and TCI America (Portland, OR) respectively. All other compounds were discussed in section 2.2.1.

5.2.2 Cloning

Recombinant plasmid construction of KYE1 from *Kluyveromyces lactis*, YersER from *Yersinia bercovieri* and xenobiotic reductase A (XenA) from *Pseudomonas putida* has been described in previous studies and are summarized in Appendix C.[116,203,204] Site-directed mutations were introduced through overlap extension polymerase chain reaction (OE-PCR). Oligonucleotide synthesis and DNA sequencing were done through Eurofins-MWG|Operon (Huntsville, AL). Primer sequences are described in Table C.**3**.

5.2.3 Protein expression and purification

XenA wild-type and the C25G variant were expressed and purified according to previously published methods with modifications.[203] A HiPrep 16/10 QFF column (GE healthcare; Fairfield, CT) was used in place of the HiTrap Q XL, with a 50 mM NaP_i buffer (pH 7.5) instead of Bis-Tris as the mobile phase. The concentration of NaCl was increased from 0 to 500 mM over 20 column volumes (CVs) for protein elution. Subsequent steps were performed as published.[203] KYE1 and YersER were also expressed and purified according to previously published literature with an additional 1 h incubation with exogenous FMN prior to binding the protein to the Ni-NTA resin.[116] Variants were transformed into BL21(DE3) competent cells. For the variants of KYE1 and YersER, different temperatures and isopropyl β-D-1-thiogalactopyranoside (IPTG) concentrations were used (Appendix E). Gene expression was induced with IPTG between an OD_{600} of 0.5 and 0.7. Expression times were 4 h at 37 °C, 8 h at 30 °C, and overnight at 18 °C.

Protein concentration was determined through the Bradford assay, and purity was analyzed through sodium dodecyl sulfate polyacrylamide gel electrophoresis (SDS-PAGE).[163] FMN occupancy was measured as described before (Section 2.2.3). Active fractions were buffer exchanged using a PD-10 Desalting Column (GE Healthcare; Fairfield, CT) to 50 mM NaP_i, 150 mM NaCl buffer (pH 8.0). Enzymes were stored at -20 °C after addition of glycerol to 50% (v/v).

5.2.4 Enzyme activity assays and data fitting

Enzyme activity was determined by monitoring the oxidation of NADPH using UV-Visible spectrometry with a DU 800 spectrophotometer (Beckman Coulter; Brea, CA). For ene-reductase activity assays, ketoisophorone (KIP) and 2-cyclohexen-1-one were selected as model compounds. Reactions were conducted in 50 mM NaP_i buffer (pH 7.5) with 0.2 mM NADPH, 10 mM substrate, and 0.5 μM enzyme at 25 °C. NADPH oxidation was monitored at 340 nm (ε_{340} = 6,220 $M^{-1}.cm^{-1}$). Nitroreductase activity was monitored with a specific activity assay described before with modifications (Section 2.2.4). Reactions were conducted in a 50 mM NaP_i buffer (pH 7.5) with 0.5 mM NADPH, 0.5 mM 4-nitrobenzenesulfonamide (4-NBS), and 0.5 μM enzyme at 25 °C. NADPH oxidation was monitored at 370 nm with an extinction coefficient, ε, of 2,660 $M^{-1}.cm^{-1}$.[176] All measurements were performed in triplicates.

Assays to determine k_{cat}, K_M^{NADPH} and K_M^S were performed on the DU 800 spectrophotometer (Beckman Coulter; Brea, CA). Reaction rates for NADPH were determined from 6 to 500 μM NADPH with 1 mM 4-NBS and 0.5 μM enzyme. Substrate kinetics was measured with 0.3 mM NADPH and 4-NBS ranging from 15 to 1250 μM.

The data were fit according to the Michaelis-Menten equation (Equation 3.1) using OriginPro (v 9.0.0) software (OriginLab; Northampton, MA).

5.2.5 Product determination

Overnight enzymatic reactions were performed with the following conditions: 1 mM substrate, 10 mM of dextrose, 0.1 mM $NADP^+$, 2.4 $U.mL^{-1}$ of GDH and 1 μM enzyme. For 4-NBS conversion studies, the reaction was quenched with an equal volume of acetonitrile, and the sample was centrifuged at 13,000 g for 2 min. The supernatant was analyzed via HPLC with methods described previously (Section 4.2.3).

5.2.6 Circular dichroism (CD)

Circular dichroism (CD) measurements were performed on Olis Multiscan (Bogart, GA). Protein ellipticity was monitored at either 220 or 230 nm, depending on the variant, from 20 to 80 °C with a ramp of 1 $°C.min^{-1}$. Data were normalized to represent the folded fraction of protein, and fit to a van't Hoff equation using a two-state model.

5.2.7 Fluorescence study

Fluorescence of the FMN bound enzymes was measured on a Synergy H4 Multi-Mode Plate Reader (BioTek; Winooski, VT). Wild-type and variants were diluted to 6 μM and aliquoted into 96-well plates. Excitation spectra were recorded from 300 to 580 nm with an emission wavelength of 600 nm. Emission spectra were measured from 450 to 700 nm with excitation at 430 nm. Recorded spectra were normalized according to FMN absorbance measurements.

5.3 Results & Discussion

5.3.1 Effect of C25G mutation for XenA

The increase in conversion observed with XenA C25G by Yanto et al. could be from either activity or stability improvements. To understand the effect of the mutation, both enzymes were purified and studied for their activity towards 4-nitrobenzenesulfonamide (4-NBS) as a substrate. Steady-state Michaelis-Menten kinetics showed that the C25G variant had a higher k_{cat} value of 8.9 s^{-1}, but also a larger K_M^{4-NBS} value of 820 µM compared to wild-type XenA. Overall, the k_{cat}/K_M^{4-NBS} increased by an order of magnitude with the C25G variant (Table 5.1, Figure 5.1). This finding confirmed that the higher conversion is most likely a result from increased activity, thus investigating stability changes as well were unnecessary.

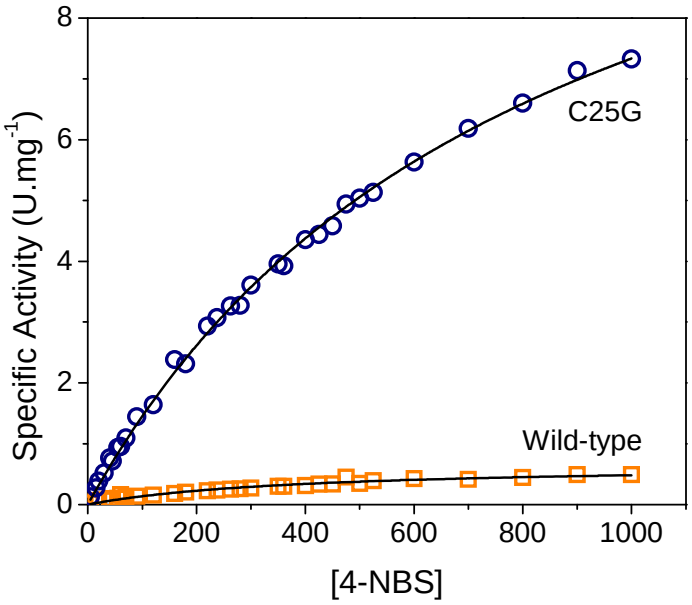

Figure 5.1 Specific activity dependence of XenA wild-type (WT) and variant C25G on 4-nitrobenzenesulfonamide (4-NBS) as a substrate at 25 °C

Table 5.1 Kinetics parameters of XenA wild-type (WT) and variant C25G

Enzyme	k_{cat} (s^{-1})	K_M^{4-NBS} (µM)	k_{cat}/K_M^{4-NBS} ($s^{-1}.mM^{-1}$)

XenA WT	0.44 ± 0.03	388 ± 55	1.1 ± 0.2
XenA C25G	8.9 ± 0.2	820 ± 31	11 ± 1

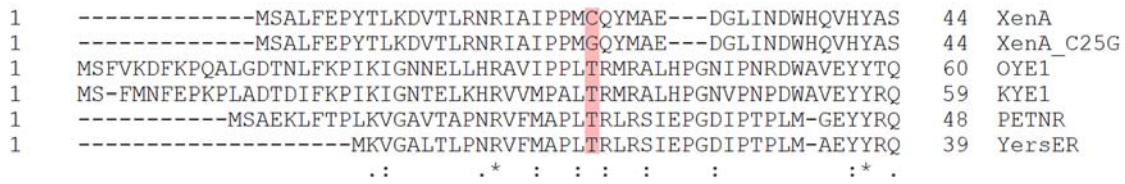

Figure 5.2 Amino acid alignment of ERs compared to XenA C25G. For sequence information see Appendix B.

5.3.2 Analogous threonine to glycine mutation

Analysis of the XenA crystal structure (PDB ID: 3L68) indicated that distance between C25 and the N5 of FMN is 3.9 Å.[205,206] In addition, amino acid sequence comparison of XenA to the ene-reductases OYE1, KYE1, PETN reductase and YersER revealed that these enzymes all have a threonine residue in place of a cysteine at the corresponding position (Figure 5.2). Increased activities observed from the C25G variant, lead to the hypothesis that mutating the analogous threonine to glycine (position T27 for YersER, and T37 for KYE1) will yield similar increase in NR activity. This mutation appeared promising given that NRs also have a glycine residue located in front of the N5 position of the flavin.[42-44] It has been previously speculated that the glycine residue is necessary, as anything larger could intrude the space of the flavin active site.[42]

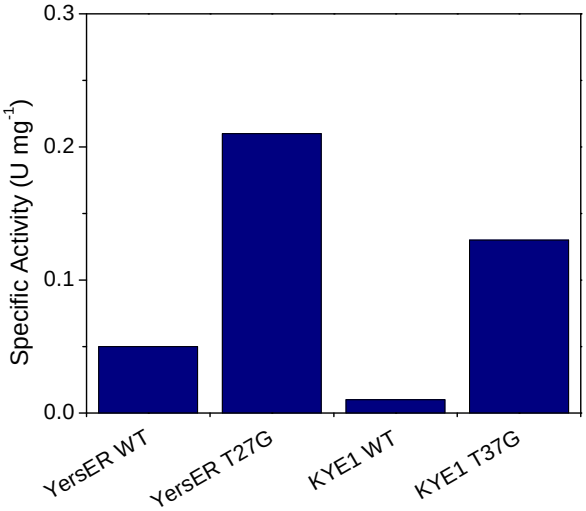

Figure 5.3 Specific activity of YersER and KYE1 wild-type (WT) and Thr to Gly variants. Reactions conducted in 50 mM NaP_i buffer (pH 7.5) with 0.5 mM NADPH, 0.5 mM 4-nitrobenzenesulfonamide (4-NBS), and 0.5 μM enzyme at 25 °C

Variants YersER T27G and KYE1 T37G were created through overlap-extension PCR, expressed, purified and studied to compare activity towards 4-NBS. Although both mutations showed a slight increase in NR activity, the magnitude was insufficient to conclude that this single mutation will solely be responsible for altering the specificity from ER to NR (Figure 5.3).

5.3.3 Increasing the active site cavity

Available OYE1, XenA and NRentcl crystal structures were scrutinized to find an alternative approach.[42,206,207] Comparison of the binding pocket cavity revealed that the FMN in OYE1 was secluded within the structure compared to XenA, which has the cofactor visible from the environment (Figure 5.4). The fact that the binding pockets of NRs are also fairly large and exposed led to the hypothesis that the enzyme functionality could be altered by increasing the entrance size and the binding pocket cavity volume.

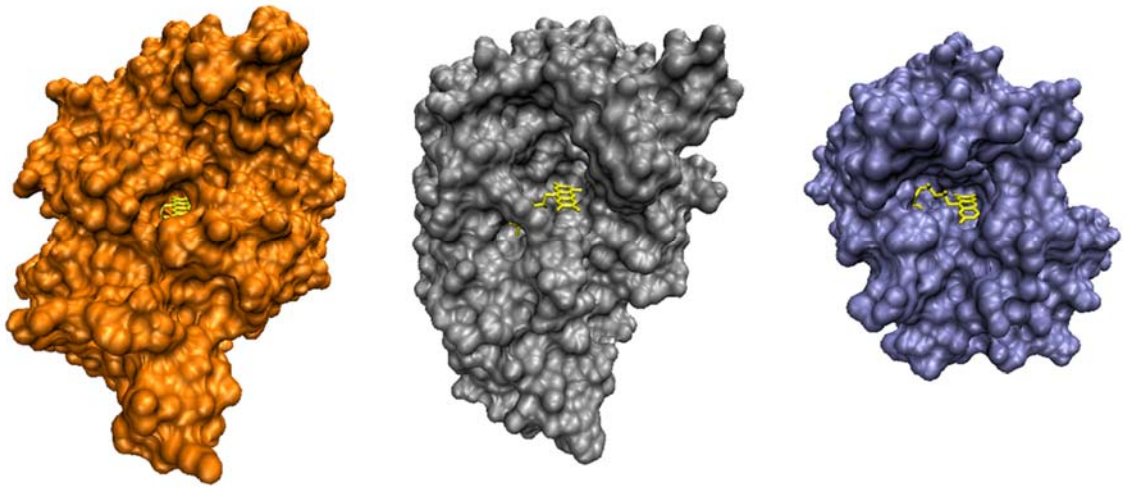

Figure 5.4 Substrate binding cavity comparison of OYE1 (PDB ID: 1OYB), XenA (PDB ID: 3L68) and NRentcl (PDB ID: 1KQB) (from left to right). Images rendered using Visual Molecular Dynamics (VMD).[41]

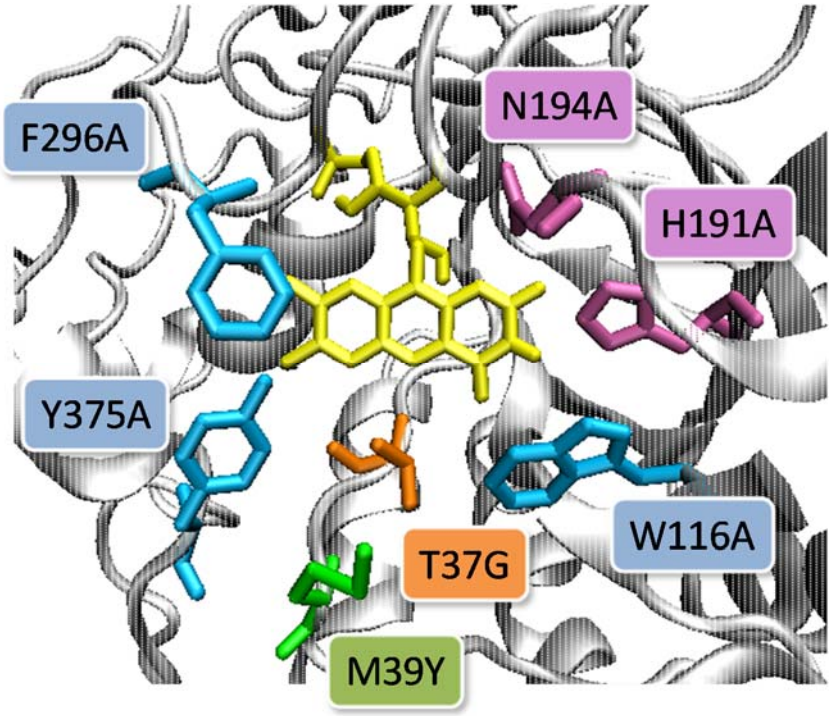

Figure 5.5 KYE1 crystal structure with mapped site-directed mutagenesis approach. Image rendered using Visual Molecular Dynamics (VMD).[41] Residues are colored according to the approach. orange: analogous to C25G in XenA; blue: increase binding pocket size; green: recover substrate interaction from loss of tyrosine (Y375); pink: eliminate ER activity.

Site-directed mutagenesis studies to confirm this hypothesis were focused on KYE1 as it has high similarity to OYE1. A homology structure of KYE1 was designed using ESyPred3D[178] with OYE1 (PDB ID: 1OYB), which shares an identity of 71.5%, as a template (Figure 5.5). Key residues were searched within 5 Å of the bound inhibitor *p*-hydroxybenzaldehyde. From this, F296 and Y375 were identified to block the active site entrance, and W116 was found to occupy a large amount of space in the substrate binding site. To minimize spatial constraints, each position was mutated to alanine. In addition, as Y375 is known to interact with the substrate through hydrogen bonding, two residues were selected for tyrosine mutations to compliment Y375A, in case the tyrosine is essential for substrate binding or catalysis.[125,207,208] M39Y was selected based on the analogous tyrosine at the identical position for XenA, and W116Y was selected based upon the proximity of the residue.

These single mutations were performed, and enzyme selectivity was measured by comparing specific activities towards ketoisophorone (KIP) for ER activity and 4-nitrobenzenesulfonamide (4-NBS) for NR activity. Most variants exhibited an increase in NR specific activity with Y375A as the best variant with a specific activity of 0.31 $U.mg^{-1}$ (Table 5.2, Figure 5.6).

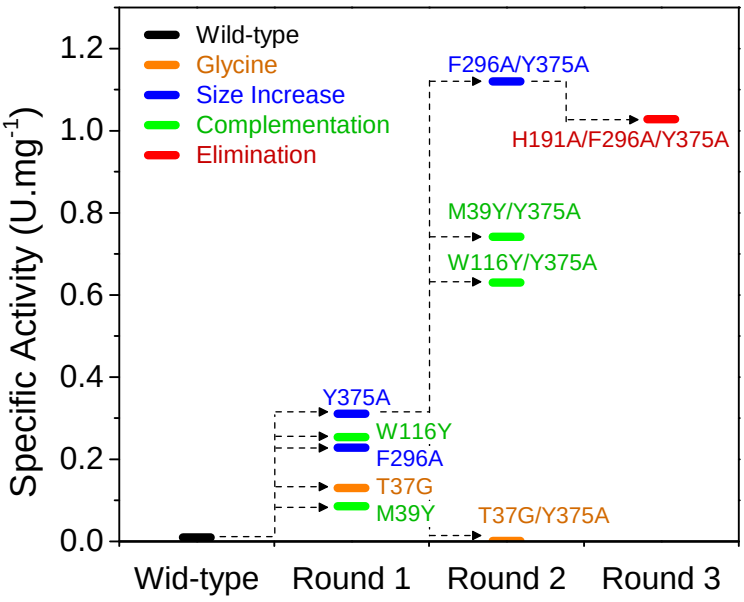

Figure 5.6 Iterative mutagenesis to increase NR activity with 4-NBS as a substrate.

Table 5.2 Summary of ER and NR specific activity. ER specific activity measured with 10 mM KIP, 0.2 mM NADPH and NR specific activity measure with 0.5 mM 4-NBS, 0.5mM NADPH. All reactions were performed with 0.5 µM enzyme in 50 mM NaP_i buffer (pH 7.5) at 25 °C. Activity ratios were calculated by assuming 0.01 $U.mg^{-1}$ for those with no detectable activity. Not detectable (N.D.)

Enzyme	ER ($U.mg^{-1}$)	NR ($U.mg^{-1}$)	$(NR)^2$/ER ratio
WT	2.27	0.01	0
T37G	-	0.13	N.D.
M39Y	1.97	0.08	0.003
W116Y	0.39	0.25	0.17
F296A	1.33	0.23	0.04
Y375A	0.09	0.31	1.12
T37G/Y375A	N.D.	N.D.	N.D.
M39Y/Y375A	0.37	0.74	1.49
W116Y/Y375A	N.D.	0.63	39.6
F296A/Y375A	0.12	1.12	10.3
H191A/F296A/Y375A	N.D.	1.03	106

5.3.4 Iterative mutagenesis for activity improvement

To study the additive and synergistic (i.e. better than additive) effects of the mutations, first round mutations were added to the Y375A variant. Among those, W116Y/Y375A showed additivity, while M39Y/Y375A and F296A/Y375A showed synergy from the coupled mutations (Figure 5.6). The highest achieved specific activity of 1.12 $U.mg^{-1}$ was two orders of magnitude higher than that of the wild-type. The variant T37G/Y375A showed a dramatic decrease in activity. This may be in relation to loss of substrate affinity, as both residues are near the N5 and C6 of the isoalloxazine ring. The extra space can increase the K_M^{4-NBS}, leading to a low specific activity at the studied substrate concentrations.

5.3.5 Elimination of ER activity

Full conversion of KYE1 ER to a NR was attempted by eliminating catalytic residues that were known to participate in alkene reduction, namely H191 and N194.[125] Previous studies on PETN reductase showed that mutation of residues 181 and 184 (which correspond to 191 and 194 in KYE1), can have a major impact on the enzyme selectivity.[209] Toogood et al. constructed a library through site-saturation mutagenesis and tested the reduction of nitrostyrenes. With some variants they were able to find an increase in oximes (product of nitro-reduction) and a decrease in alkanes (product of ene-reduction) in the product distribution. Among the variants, those that had alanine at position 181 or 184 exhibited the highest oxime to alkane ratio (8.3 for H181A 0.36 for H184A and 0.14 for wild-type).[209] Hence, mutations H191A and N194A were added as single and double mutations onto previously successful variants, M39Y/Y375A and

F296A/Y375A. In addition, single mutation variants were also generated to study their effect on NR activity.

The mutation N194A did not have a significant impact on ER activity elimination (Table E.2). However, any variant that included H191A showed no activity towards KIP. The triple variant H191A/F296A/Y375A also showed comparable specific activity (1.03 $U.mg^{-1}$) towards 4-NBS, showing the complete switch from ER to NR activity (Figure 5.6, Figure 5.7). The change in functionality was also characterized by taking a ratio of NR and ER activity. As this number alone will not be indicative of the absolute activity, $(NR)^2/ER$ was used compare variants (Table 5.2).

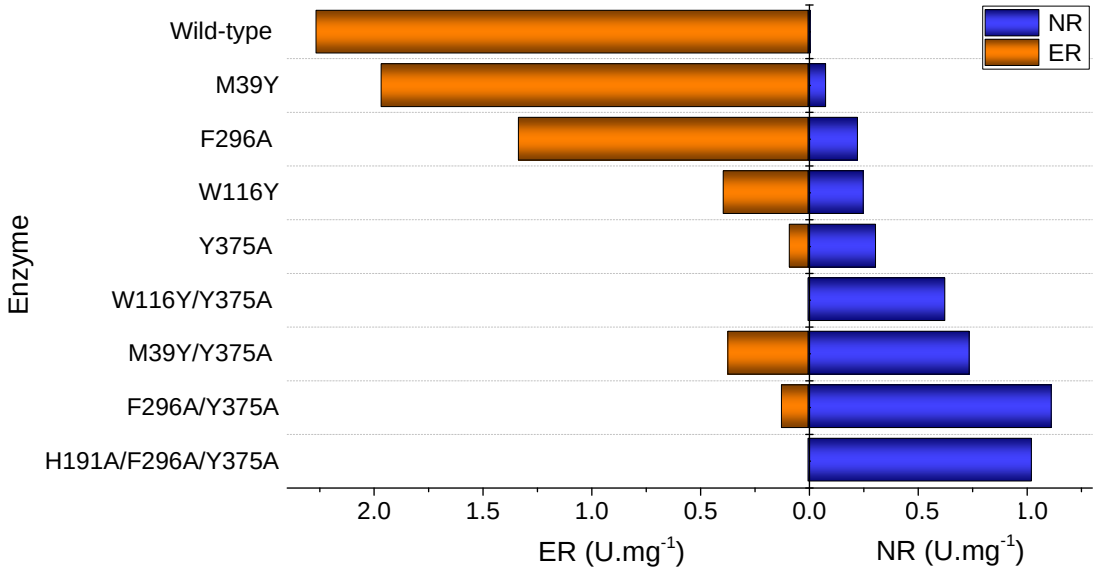

Figure 5.7 Switch of activity from ER to NR with KIP and 4-NBS as substrates, respectively.

5.3.6 Functional, kinetic and thermal characterization of variants

The variants with the highest NR specific activity (F296A/Y375A) and highest $(NR)^2/ER$ ratio (H191A/F296A/Y375A) were selected as the best variants, and further characterized in terms of their functional, kinetic and thermal properties.

Functionality of each enzyme was studied by reacting model substrates and determining the products. NR activity was confirmed by reducing 4-NBS and analyzing the reaction mixture *via* HPLC. Production of 4-hydroxylaminobenzenesulfonamide was confirmed for both variants (Figure E.1).

Table 5.3 Kinetic characterization of KYE1 wild-type and variants.

Enzyme	K_M^{NADPH} (μM)	K_M^{4-NBS} (μM)	k_{cat} (s^{-1})	k_{cat}/K_M^{4-NBS} ($s^{-1}.mM^{-1}$)
KYE1 Wild-type	43.5 ± 5.9	-	-	-
F296A/Y375A	< 10	317 ± 18	1.20 ± 0.02	3.8 ± 0.2
H191A/F296A/Y375A[a]	303 ± 61	115 ± 26	0.52 ± 0.03	4.5 ± 1.1

[a]apparent kinetic constants

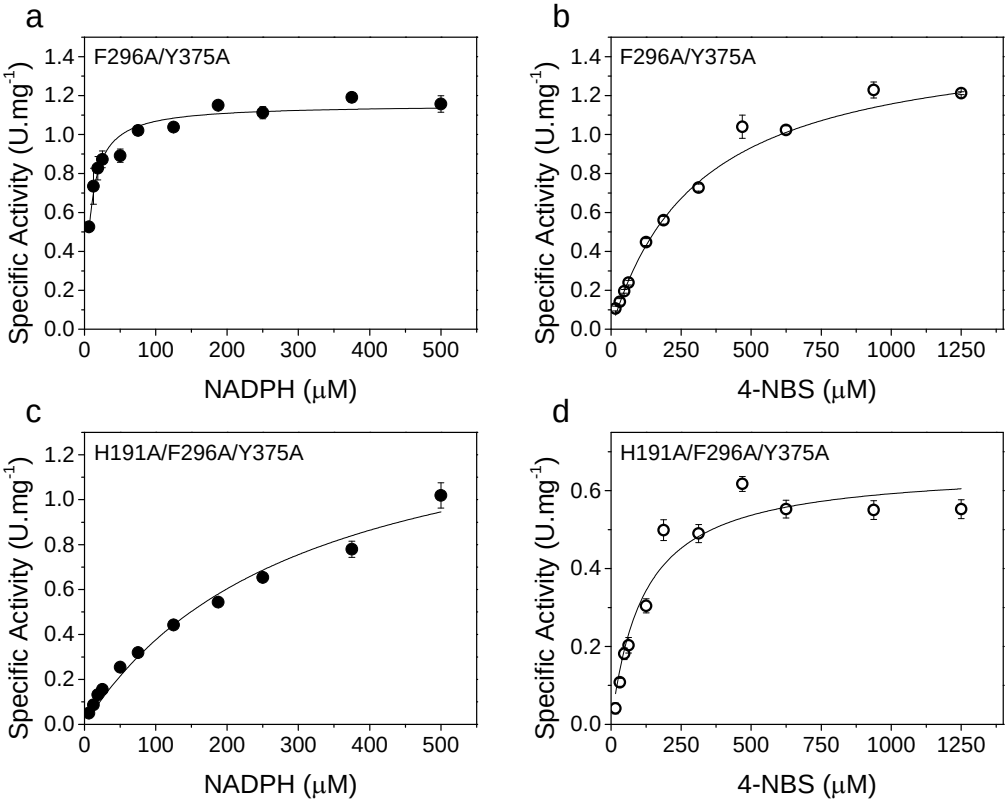

Figure 5.8 Kinetics of KYE1 variants in 50 mM NaP_i (pH 7.5) at 25 °C. (●): NADPH kinetics with 1 mM 4-NBS; (○): 4-NBS kinetics with 0.3 mM NADPH.

Kinetic parameters were measured while varying NADPH or 4-NBS, while keeping the other constant (Table 5.3). As oxygen is known as an electron acceptor for ene- and nitroreductases, NADPH oxidase activity was measured and subtracted in the absence of a nitro substrate. Variant F296A/Y375A showed an improvement in the K_m^{NADPH} (< 10 μM) compared to wild-type (43 μM). Turnover, k_{cat}, was measured to be 1.20 s^{-1} and the nitro substrate K_m was 317 μM. The introduction of H191A to this variant resulted in a loss of affinity for NADPH. Within the range that was studied (up to 0.5 mM), saturation of NADPH was not achieved. Measuring the NR activity at 0.3 mM NADPH yielded an apparent k_{cat} of 0.52 s^{-1} and k_{cat}/K_m of 4.5 $s^{-1}.mM^{-1}$. It is expected for the turnover to be similar to that of the variant F296A/Y375A at saturating conditions.

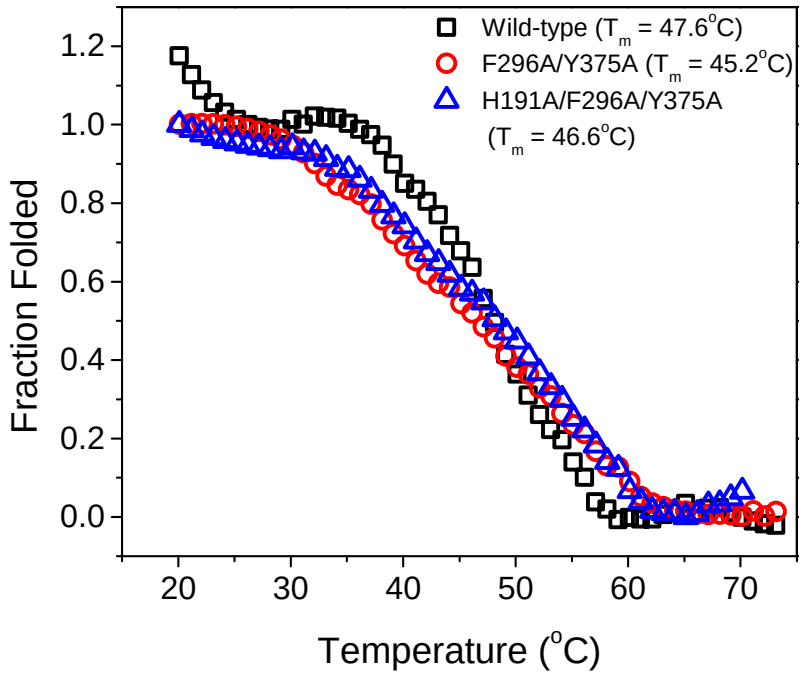

Figure 5.9 Temperature dependent unfolding of KYE1 wild-type and variants monitored using circular dichroism (CD) at 220 nm.

Table 5.4 Thermal characterization of KYE1 wild-type and variants.

Enzyme	T_m (°C)	ΔH_m (kJ.mol^{-1})
KYE1 Wild-type	47.5 ± 0.2	5.2 ± 0.3
F296A/Y375A	45.2 ± 0.3	2.8 ± 0.1
H191A/F296A/Y375A[a]	46.6 ± 0.3	3.0 ± 0.2

Circular dichroism (CD) experiments were performed to ensure that the mutations had no negative effects on their thermal stability. Wild-type and variants F296A/Y375A and H191A/ F296A/Y375A were subjected to a denaturation study with a thermal gradient of 1 °C.min^{-1} at 220 nm (Figure 5.9). The melting temperature (T_m) and melting enthalpy (ΔH_m) of each protein was determined by fitting the data to a van't Hoff equation assuming a two-state melting model. Compared to the wild-type (T_m = 47.5 °C), the T_m of both the double variant F296A/Y375A and triple variant H191A/ F296A/Y375A slightly decreased to 45.2 and 46.6 °C, respectively (Table 5.4). The decrease in ΔH_m was significant as the values for both variants were less 3 kJ.mol^{-1}.

5.3.7 Nitroreductase vs. ene-reductase functionality

It has been previously postulated by Jensen, that enzyme evolution does not occur through conversion of one specific functionality to another, but, rather, from promiscuous enzymes as starting points for advancement.[210] This concept has been further expanded by Khersonsky & Tawfik to define enzymes as 'specialists' and 'generalists', where 'specialists' catalyze a specific reaction and 'generalists' are those that are promiscuous.[211,212] Further, they discuss that directed evolution causes larger functionality trade-offs as the mutations commonly take place in the first shell (active site).[212] Here, by mapping the ER and NR activities of KYE1, it can be seen that this is

indeed the case for this study; the ER 'specialist' is converted to a NR with a fairly strong negative trade-off (Figure 5.10).

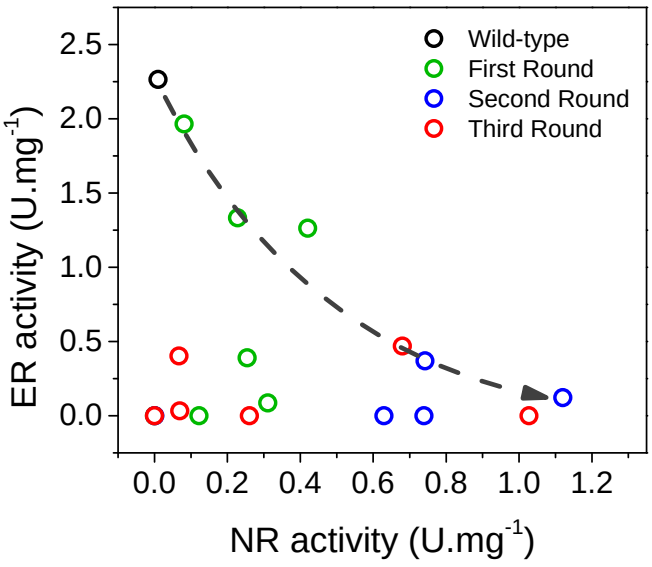

Figure 5.10 Evolutionary trade-off between ER and NR activity

The reasoning behind the functional selectivity has been questioned and investigated to some extent by Oberdorfer et al. with glycerol trinitrate reductase (NerA) from *Agrobacterium radiobacter* as a model enzyme.[213] However, in contrast to what was done in our study, the authors were focused on the comparison of aliphatic nitro reduction rather than aromatic. They compared NerA, OYE1, XenA and OPR-3 from *Arabidopsis thaliana* and attributed the difference in functionality, to the presence of a hydrophobic/hydrophilic patch in the binding pocket. Also, they discuss that the size and shape of the active site cavities have no clear relation with the functionality. However, as shown in their cavity representations, OYE1 has F297 and Y376 (equivalent to F296 and Y375 in KYE1) occupying a large amount of space (Figure 5.11). This observation leads

to the suggestion that the binding pocket size may indeed be important for aromatic nitro reduction functionality, but not aliphatic.

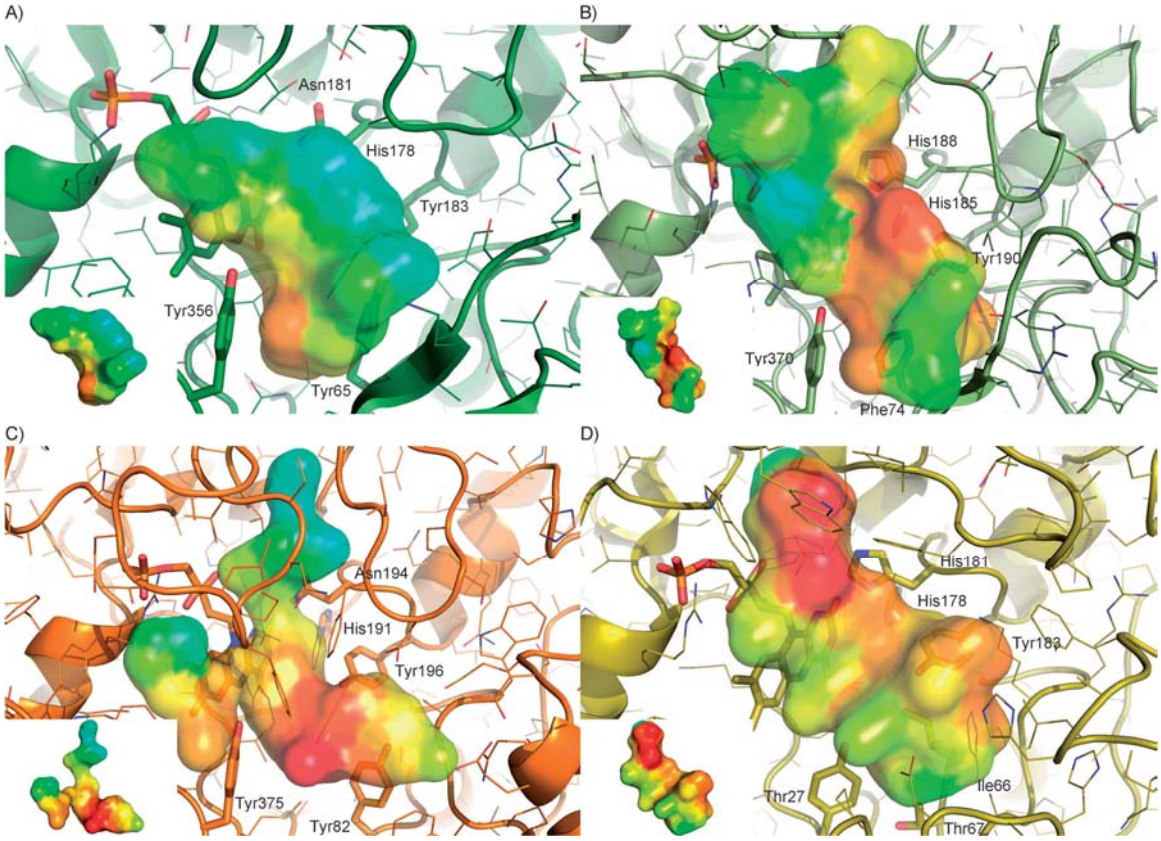

Figure 5.11 Active sites of A) NerA, B) OPR-3, C) OYE-1, and D) XenA. The colored, semi-transparent surfaces each represent the shape of the associated enzyme's active site cavity. The surfaces of the cavities are colored according to the hydrophobicity/hydrophilicity of the residues lining the active site (red hydrophobic, blue hydrophilic). The small insets in the lower left corners each show a cavity representation without the surrounding enzyme. Adapted from Oberdorfer et al.[213]

5.3.8 Universal application of mutations

Further studies were conducted to study whether these mutations could be universally applicable to other ERs with the expectance of a similar outcome. The equivalent residues of KYE1 H191, F296A and Y375 are H182, W276 and Y352 for YersER. The

combinations of YersER W276A/Y352A and H182/W276A/Y352A were created and studied for NR activity. However, these YersER variants did not yield the same results, indicating that the effect is not universal (data not shown).

5.4 Conclusion

In this work, a NR was successfully created from the ER KYE1 scaffold, through iterative site-directed mutagenesis based on rational design. With the hypothesis that increasing the binding site cavity volume would result in an increase of NR activity, we successfully created the variant F296A/Y375A. This enzyme showed to have more than a 100-fold increase in specific NR activity and catalyzed the reduction of 4-NBS at 1.20 s^{-1}. Further mutation of His 191 to Ala resulted in complete elimination of ER activity, but at the same time decreased the enzyme's affinity towards NADPH. The created monomeric form of these NRs can be extremely useful for immobilization applications such as two-step protein self-assembly with leucine zippers.[214]

CHAPTER 6

NAD(P)H OXIDASE V (NOXV) FROM *LACTOBACILLUS PLANTARUM* DISPLAYS ENHANCED OPERATIONAL STABILITY EVEN IN ABSENCE OF REDUCING AGENTS

6.1 Introduction

Enzymatic synthesis steps are used to produce active pharmaceutical ingredients (APIs) at higher yields, greater selectivity, and greater productivity than is possible through isolation of natural sources or chemically catalyzed routes. Interest in the nicotinamide cofactor aided production of rare sugars, namely L-nucleosides, for example L-ribose, L-mannose and L-gulose, has arisen for a number of L-nucleoside-based pharmaceutical compounds, such as the hepatitis B drug Emtriva® and the human immunodeficiency virus drug Clevudine®. A number of such rare sugar-based pharmaceuticals are currently approved or in clinical trials.[215] Another example of cofactor-assisted API synthesis is the production of keto acids, which are used to treat mild chronic renal insufficiency of hemodialysis patients and hyperphosphatemia.[216,217] Thus, α-ketoglutarate can be synthesized enzymatically from mono sodium L-glutamate (MSG) using L-glutamate dehydrogenase and a nicotinamide cofactor.[143]

High costs of nicotinamide cofactors (NAD^+: \$30/g; $NADP^+$: \$230/g from laboratory suppliers) rule out the option of adding equimolar amounts for large-scale processes. A regeneration system is mandatory for advantageous economics but also often alleviates product inhibition, and acts as the driving force to overcome thermodynamic equilibrium limitations.[144] Enzymatic, chemical, electrochemical,

photochemical, and biological methods have been proposed for cofactor regeneration.[144,218,219]

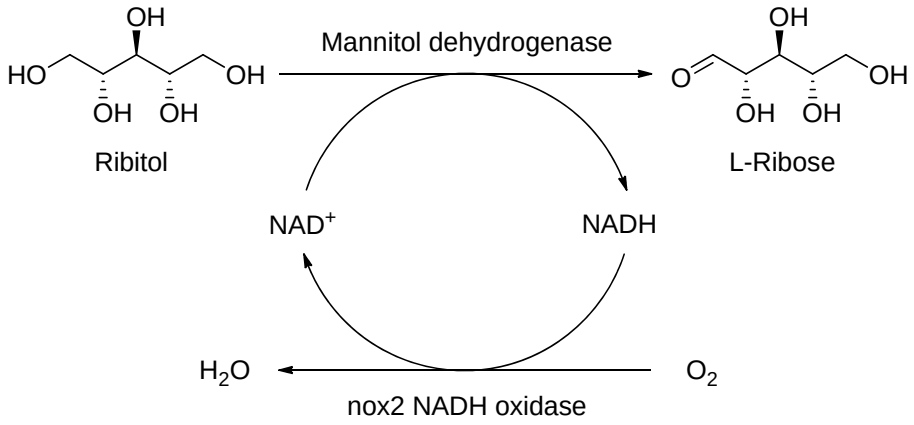

Figure 6.1 Schematic conversion of ribitol to L-ribose through mannitol dehydrogenase from *Apium graveolens* complemented with NADH cofactor regeneration using nox2 NADH oxidase.

Among different systems that can be chosen for cofactor regeneration, NAD(P)H oxidases feature a number of benefits, as they utilize only NAD(P)H and oxygen as co-substrates, both of which are available intracellularly (Figure 6.1) thus obviating exogenous addition, and, in the case of nox2 NAD(P)H oxidases, produce only water next to $NAD(P)^+$.[220] The reaction is carried out in a purely aqueous phase (in the absence of harsh solvents and metal catalysts).

The NoxV gene codes for an annotated NADH oxidase (NoxV) from *Lactobacillus plantarum* consisting of 1350 bp with a predicted size of 49 kDa. This study investigates the enzymatic properties of NoxV. A higher enzymatic productivity is achieved compared to its analogs, as evidenced by NoxV's higher TTN and increased stability against over-oxidation. Furthermore, while the wildtype enzyme solely accepts NADH as a substrate, we engineered the substrate binding pocket so that the enzyme also accepts and oxidizes NADPH.

6.2 Materials & Methods

6.2.1 Enzymes and other materials

The gene of NADH oxidase V (NoxV) from *Lactobacillus plantarum* 10S was obtained *via* gene probe from genomic DNA from the American Type Culture Collection (Manassas, VA), ATCC 10012. NADH and NADPH were obtained from Amresco (Solon, OH) and EMD chemicals (Gibbstown, NJ), respectively. MagicMedia^{TM} *Escherichia coli* Expression Medium was purchased from Invitrogen (Carlsbad, CA). Molecular biology reagents such as dithiothreitol (DTT) were obtained from JT Baker (Phillipsburg, NJ), all other materials such as various salts used for buffers, β-mercaptoethanol (BME) and NAD^+ were obtained from Sigma-Aldrich (St. Louis, MO). Oligonucleotides for cloning were purchased from Eurofins-MWG|Operon Biosciences (Huntsville, AL).

6.2.2 Cloning

The gene was cloned through PCR using the primers in Table C.2 The PCR product was gel purified with a Qiagen gel extraction kit and cloned into a pET-28a vector (Novagen; Darmstadt, Germany). The plasmid was then transformed into *E. coli* BL21(DE3)pLysS for expression. Constructs were confirmed with sequencing through Eurofins-MWG|Operon Biosciences (Huntsville, AL).

6.2.3 Site-directed mutagenesis

Single and double mutations were performed on residues G178 and L179 into K, R and K, R, H respectively, through overlap and Quikchange® PCR protocol using the primers in. Degenerate codons were used to generate multiple mutants with single transformations. ARR codes for amino acids R and K, and CRY codes H and R. The

DNA from PCR was transformed into *E. coli* XL1-blue. Colonies were picked from agar plates and sent for sequencing to Eurofins-MWG|Operon Biosciences (Huntsville, AL).

6.2.4 Overexpression

Growth and overexpression was carried out in MagicMedia™ *E. coli* Expression Medium (Invitrogen; Carlsbad, CA) with a final concentration of 30 $\mu g.mL^{-1}$ each of kanamycin and chloramphenicol. A dual temperature protocol was used for growth, starting out at 30 °C for 6 h, and then continued at room temperature (25±2 °C) for an additional 22 h. Cultures were harvested by centrifugation in a Beckman centrifuge at 4,050 g for 20 min in 50 mL conical tubes. The resulting cell pellet was either frozen, and stored at -80 °C or purified directly as described below.

6.2.5 Purification

Purification of NoxV was carried out at 4 °C or on ice to prevent denaturation of the enzyme. Cell pellets were resuspended in 15mL of 10 mM Tris-Cl buffer, pH 7.5 with 5 mM DTT (Buffer A) and sonicated at 14 W for 30 s nine times. Sonicated cells were centrifuged at 18,500 g for 30 min. The clarified cell lysate was then dialyzed against 250 mL of buffer A with 50% ammonium sulfate for 2 h. The dialysis membrane was transferred to fresh buffer and further dialyzed for 2 h. The solution was then centrifuged at 18,500 g for 30 min. The resulting supernatant was filtered through a 0.8 μm and 0.2 μm microfiltration membranes in series. The filtrate was loaded onto a HiPrep 16/10 butyl hydrophobic interaction column on an ÄKTAexplorer™. A gradient separation was performed starting from buffer A with 30% ammonium sulfate to 15%. The fractions with the highest activity were collected and dialyzed against buffer A for 2 h. After exchanging to fresh buffer the sample was dialyzed for an additional 2 h. The sample was

loaded on a HiPrep 16/10 DEAE weak anionic exchange column on the ÄKTAexplorer™. Separation was achieved with buffer A containing NaCl, a gradient of 150 to 250 mM. The resulting fractions were assayed and the ones with highest activity were collected as pure protein. The purified protein was either stored in 4 °C or in -20 °C with 25% glycerol.

6.2.6 Enzyme assay and protein determination

Standard assays to detect enzymatic activity were performed in 100 mM Triethanolamine (TEA) buffer pH 7.5 with 5 mM DTT in cuvettes with either 1 cm or 1 mm path length, depending on the concentration of substrate. Excluding studies of enzymatic activity and stability temperature dependence, all activity assays were performed with samples that were either pre-equilibrated to 25 °C, using a thermomixer (Eppendorf; Hamburg, Germany) or made and used directly at room temperature. Initial activity was measured by following the absorbance change using a Beckman Coulter DU 800 UV/Vis spectrophotometer at 340 nm. Activity of the enzyme was calculated using an extinction coefficient, ε, of NAD(P)H as 6,220 $M^{-1}.cm^{-1}$.[221] Unless otherwise noted, a substrate concentration of 0.2 mM NAD(P)H and enzyme concentration of 4 nM was used for assays. One unit (U) of activity is defined as μmol of $NAD(P)^+$ produced per minute.

The protein concentration was estimated by a Bradford assay.[163] BSA was used as standards and the absorbance was measured on a biophotometer (Eppendorf; Hamburg, Germany). SDS-PAGE analysis was performed to confirm the purity.

6.2.7 pH activity

Enzyme pH activity profiles were obtained at 25 °C using 100 mM buffers containing one of the following salts: sodium citrate from pH 4.0 to pH 6.5; sodium phosphate from

pH 6.0 to pH 8.0; TEA from pH 7.0 to pH 8.0; Tris-Cl from pH 7.0 to pH 9.0; glycine from pH 9.0 to pH 10.0.

6.2.8 Temperature activity

The dependence of the enzymatic activity on temperature was studied by preheating the buffer to different temperatures, and then adding the enzyme. After 1 min of incubation, the standard assay was carried out. A temperature range of 10 to 55 °C was chosen for this study.

6.2.9 Temperature stability

Temperature stability was studied by incubating the enzyme at various temperatures for 30 min. The enzyme solution was then cooled down and assayed at 25 °C. This study covered a range of 15 to 55 °C.

6.2.10 Kinetic parameters

Depending on the enzyme, a substrate concentration range from 1.5 μM up to 984 μM was investigated to determine the k_{cat} and K_m values for NAD(P)H. This was conducted at atmospheric concentrations of oxygen, 0.25 mM, present in the system. Doubly concentrated solutions were prepared by adding each the substrate and enzyme to 100 mM TEA buffer pH 7.5. The reaction was initiated by mixing the two solutions. The specific activity was measured, and the kinetic parameters were calculated from that data. Inhibition effects were measured by incubating the enzyme with NAD^+ for 30 minutes before the assay. A range of 0.2, 0.3, 0.4 and 0.6 mM were chosen and investigated.

6.2.11 Amplex Red Assay (H_2O_2 presence)

An Amplex Red Hydrogen Peroxide/Peroxidase Assay Kit (Invitrogen; Carlsbad, CA) was used to determine the amount of hydrogen peroxide (H_2O_2) produced during

turnover. The presence of H_2O_2 was determined by incubating the standard assay mixture with Amplex Red and peroxidase. Produced resorufin is detected with an extinction coefficient, ε, of 54,000 $M^{-1}.cm^{-1}$ via fluorescence spectroscopy with maximal emission at 587 nm and indicates H_2O_2 production with strict 1:1 stoichiometry. Various amounts of substrates were reacted and assayed to detect the presence of H_2O_2. The reactions were carried out in the provided 50 mM sodium phosphate buffer pH 7.4. Standards for the calibration curve were prepared with the same reaction buffer. Steady-state emission and excitation spectra were recorded with a PTI fluorimeter (Birmingham, NJ).

6.2.12 Total turnover number (TTN)

Standard kinetic assays at pH 7.5 and 25 °C in air-saturated solution were performed with 0.25, 0.5 and 1.0 nM of enzyme. 0.2 mM NAD(P)H substrate concentration was used. Assays were carried out for 2 to 3 h until there was no more enzymatic conversion of the substrate. Calculations of TTN were performed by dividing the change of NAD(P)H concentration until activity reached a standstill by the (necessarily very low) concentration of enzyme subunits that was used for each assay. As the stock solution of enzyme contained DTT, the buffer was exchanged to 10 mM Tris-Cl pH 7.5.

6.3 Results & Discussion

6.3.1 Cloning, expression, and purification

NoxV was identified through a sequence blast search. It has high similarity and identity levels with many other water-forming NADH oxidases (Table 6.1). The NoxV gene was cloned from genomic DNA of ATCC 10012 and inserted into a pET-28a vector using restriction sites NcoI and XhoI. Sequencing results of the gene showed a missense

mutation where the nucleotide at position 45 changed from C to T (accession number: Q88SH4).

NoxV was overexpressed in *E. coli* BL21(DE3)pLysS constituting 8% of cell protein. Purification of NoxV resulted in a yield of 14% of the total units and a 12.7-fold increase of specific activity to 167.5 $U.mg^{-1}$ (Table 6.2). The pure protein was identified as a single band at 49 kDa in sodium dodecyl sulfate polyacrylamide gel electrophoresis (SDS-PAGE) analysis (lane 5, Figure 6.2).

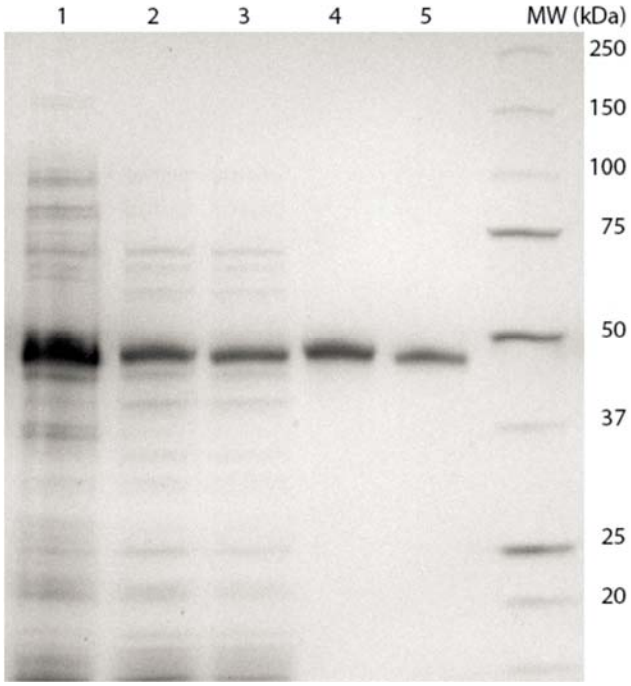

Figure 6.2 SDS-PAGE (12% gel) analysis of NoxV. Lane 1: 15 µg lysate, Lane 2-3: 6 and 3 µg, respectively, of dialyzed protein collected from HiPrep 16/10 Butyl column, Lane 4-5: 3 and 1 µg, respectively, of collected protein from HiPrep 16/10 DEAE column. The desired protein band is approximately 49 kDa.

Table 6.1 Sequence identity and similarity comparison of water forming NADH oxidases from different bacteria with respect to NoxV from *L. plantarum* (accession number: Q88SH4).

Bacteria	Identity (%)	Similarity (%)	Accession number	Ref.
Lactobacillus sanfranciscensis	59.4	72.2	Q9F1X5	[128]
Lactococcus lactis	33.1	56.1	A2RIB7	[134]
Lactobacillus brevis	64.0	74.2	Q8KRG4	[133]
Enterococcus faecalis	33.0	42.9	P37061	[132]
Streptococcus mutans	9.4	19.8	Q54453	[131]

Table 6.2 Table of purification. Lysate: clarified lysate; AS50 dia.: supernatant from centrifuged sample dialyzed against 50% ammonium sulfate; Butyl dia.: fractions collected from HiPrep 16/10 Butyl column dialyzed against 100 mM TEA pH 7.5 and 5 mM DTT; DEAE: fractions collected from HiPrep 16/10 DEAE column.

	Volume (ml)	Units (U)	Protein (mg)	Sp. ac. ($U.mg^{-1}$)	Purification Fold	Yield (%)
Lysate	20	1843.5	139.3	13.2	1.0	100
AS50 dia.	7	930.0	88.5	10.5	0.8	50
Butyl dia.	37.5	379.3	4.7	80.7	6.1	21
DEAE	20	261.9	1.6	167.5	12.7	14

6.3.2 Enzyme activity and stability

NAD(P)H oxidases are used exclusively in cofactor regeneration because their byproducts, water and hydrogen peroxide, are not of interest. As utility of NADH oxidases can only be derived through coupling with other enzymes, their operating conditions must be able to match those of the cofactor consuming enzyme. Consequently, studies of reaction conditions, especially in terms of pH value and temperature, are required to maximize production and stability of both enzymes.

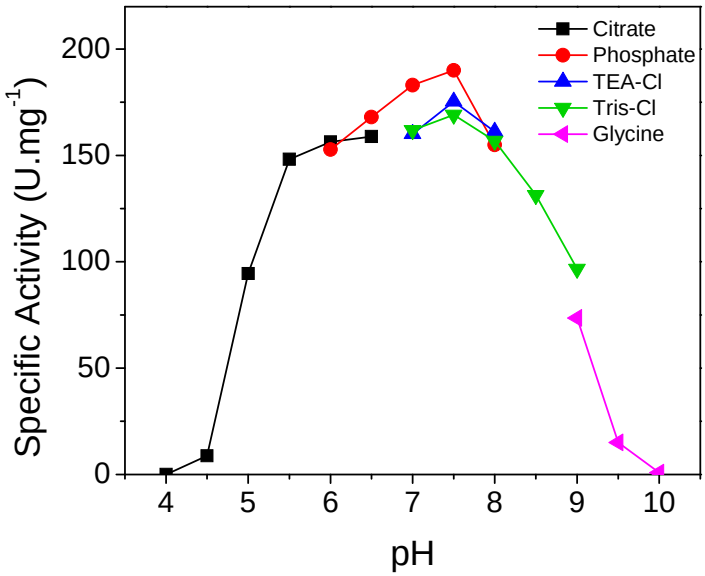

Figure 6.3 *L. plantarum* NoxV activity profile in different buffers (100 mM) at different pH values at 25 °C.

NoxV showed a rather broad pH activity range. Maximum activity was found at pH 7.5, independent of buffer type. The enzyme's optimal activity range was from pH 5.5 to 8.0, a common range for NAD(P)H oxidases (Figure 6.3). The upper limit is compatible with most dehydrogenases, so appropriate coupling seems feasible.

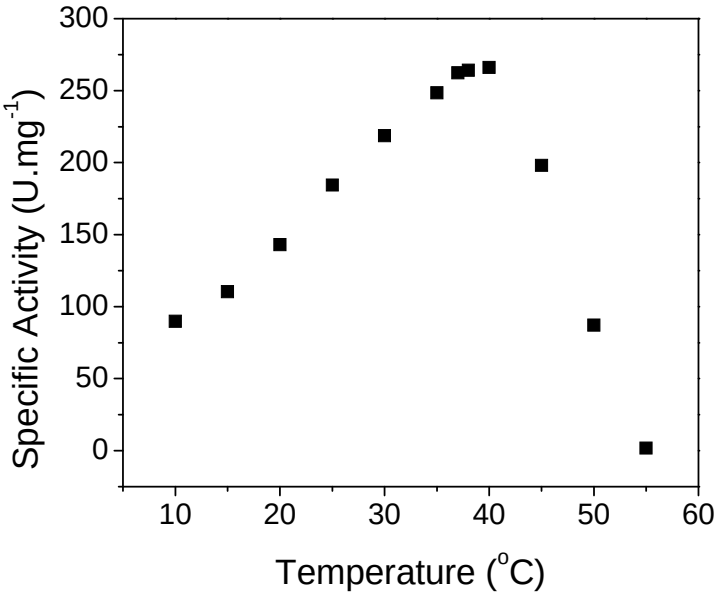

Figure 6.4 *L. plantarum* NoxV activity profile at various temperatures with 100 mM TEA buffer pH 7.5.

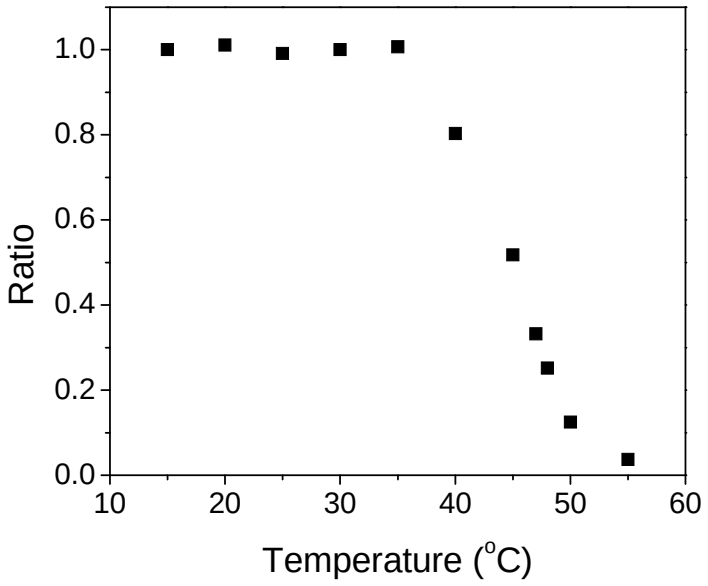

Figure 6.5 T_{50}^{30} plot to study stability of *L. plantarum* NoxV by incubating at different temperatures for 30 min each.

The temperature activity profile showed that maximum instantaneous activity was found at 40 °C, and the activity quickly declined to zero beyond that temperature (Figure 6.4). Using an Arrhenius model and data between 10 and 38 °C, the activation energy E_a was calculated as 32.7 kJ.mol^{-1}, and the deactivation energy (40-55 °C) E_d was calculated as -93.6 kJ.mol^{-1}. The temperature that exhibited half of the original activity after 30 minutes, T_{50}^{30}, was estimated to be 45 °C (Figure 6.5). At 55 °C the enzyme was completely inactive. The enthalpy of deactivation, ΔH_d, was calculated using the van't Hoff equation to be 5.0 kJ.mol^{-1} (Figure 6.5).

6.3.3 Kinetic parameters

Apparent kinetic data were obtained at constant oxygen concentration (air saturation) at 25 °C and pH 7.5 over a concentration range of NADH from 5 to 200 μM. The data were fitted with four different models (non-linear Michaelis-Menten, Lineweaver-Burk, Eadie-Hofstee, and Hanes-Woolf), all of which were in good agreement. Through non-linear fitting with a least squares approximation, the apparent k_{cat} and K_M^{NADH} values of the wild type were measured to be 211.6 s^{-1} and 50.2 μM, respectively, with an R^2 of 0.998 (Figure 6.6).

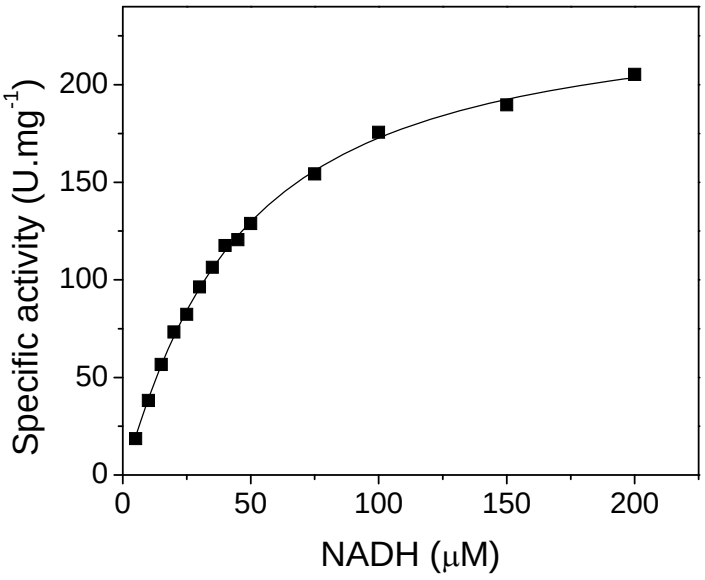

Figure 6.6 Nonlinear fitting to a Michaelis-Menten kinetic to determine the kinetic parameters k_{cat} and K_m at pH 7.5, 25 °C.

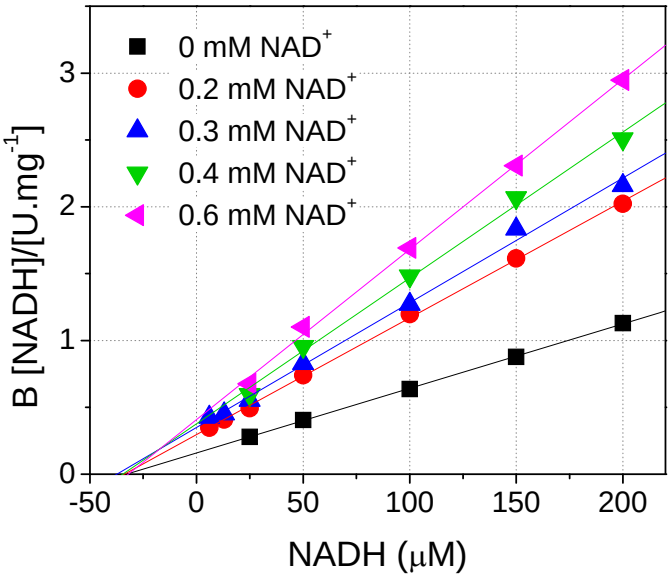

Figure 6.7 Hanes-Woolf plot to identify NAD^+ inhibition.

Possible product inhibition was investigated by incubating the enzyme with different concentrations of NAD^+. A non-competitive inhibition pattern was observed where the v_{max} value decreased with increasing inhibitor concentration, while $(K_M^{NADH})_{app}$ was constant. The product inhibition constant, $K_I^{NAD^+}$ was calculated to be 289 μM for NAD^+ (Figure 6.7). The apparent inhibition ratio $K_M^{NADH}/K_I^{NAD^+}$ is calculated to be 0.17. As this ratio is less than unity, it indicates that complete conversion is possible despite the non-competitive product inhibition.[222]

6.3.4 Water/H_2O_2 formation

The Amplex Red assay was performed to determine whether NoxV is a water- or hydrogen peroxide-producing enzyme. H_2O_2 was formed in 2.63% of the catalytic events, slightly higher than the analogs from *Lactobacillus sanfranciscensis* (0.2%) and *Lactococcus lactis* (0.4-0.7%), thus strongly suggesting that NoxV is a water-forming oxidase.[128,134]

6.3.5 Total turnover number (TTN)

Total turnover number (TTN) is a measure of catalyst productivity, defined as the total amount of product produced over the lifetime of an enzyme.[5] The TTN, in presence of DTT, was found to be approximately 168,000, at 25 °C and pH 7.5 (Figure 6.8).

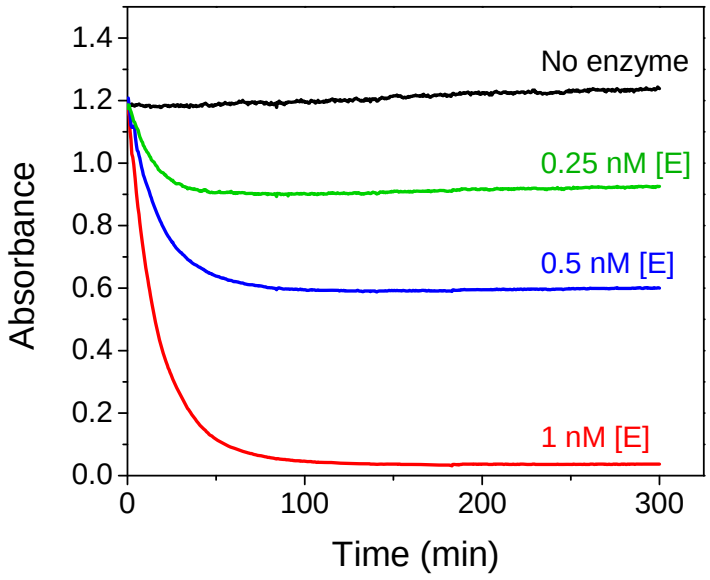

Figure 6.8 Total turnover number (TTN) analysis with different amounts of enzyme. The reaction was carried on until there was no consumption of substrate. ([E] = 0.25, 0.5 and 1.0 nM, 25 °C, pH 7.4)

Three potential causes of TTN limitation, which are commonly associated with enzyme deactivation, were investigated: i) thermal deactivation at 25 °C, ii) deactivation caused by H_2O_2, and iii) non-competitive product (NAD^+) inhibition in the system. Thermal stability at 25 °C (i) was measured by incubating the enzyme for extended periods of time. The enzyme was then assayed to determine the remaining activity. As there was no enzymatic activity loss after two hours (data not shown), which is longer than the reaction completion timescale (Figure 6.8), this study proved that the enzyme became catalytically inactive before it began to thermally deactivate. The effect of H_2O_2 was studied (ii) at 25 °C and pH 7.5 within a concentration range from 25 to 200 µM. Even at high concentrations of H_2O_2 the specific activity did not change over one hour (data not shown), thus demonstrating that the enzyme is indeed stable against H_2O_2. The

presence of NAD^+ inhibition (iii) and its pattern had been elucidated (Figure 6.7). However, as expected from the apparent inhibition ratio of 0.17, even at high concentrations of NAD^+ there was a reasonable amount of residual activity (data not shown), so it cannot be concluded that NAD^+ had inhibited the reaction completely. The cause of TTN-coupled deactivation is still not fully elucidated but it is not related to temperature nor either H_2O_2 or NAD^+ concentration.

Table 6.3 Comparison of TTN with and without DTT, for NADH oxidases from *L. plantarum*, *L.sanfranciscensis*, and *L. lactis*.

Organism	Enzyme	NADH		NADPH	
		TTN	TTN with DTT	TTN	TTN with DTT
L. plantarum	NoxV WT	128,000	168,000	-	-
	L179R	181,000	148,000		
	G178R/L179R	123,000	162,000	100,000	107,000
L. sanfranciscensis[143]	Nox2	5,000	112,500		
L. lactis[134]	Nox2	38,740	78,480	-	-

For all the TTN measurements the relative standard deviation (%RSD) was less than 5%, except for the TTN of mutant G178R/L179R with NADH, which was 12%.

To investigate the effect of reducing agents on the TTN, measurements were taken with and without reducing agents. The TTN without reducing agents, with 5 mM DTT, and with 5 mM BME were 128,000, 168,000, and 107,000 respectively. The presence of DTT had a positive effect but it was not as dramatic compared to the NADH oxidase from *L. sanfranciscensis*, which has an increase of over 20-fold.[143] However, addition of BME decreased the TTN by ~15%. The reason for the different influence of the reducing agents on the TTN is unknown, and will be assessed in future studies. One intriguing but speculative thought focuses on the different stoichiometry of the sulfenic

acid reduction for DTT and BME: a single molecule of DTT is capable of performing reduction, whereas two molecules of BME are required. In contrast, the first molecule of BME initiates thiol-disulfide interchange and occupies the water channel, thus blocking access to the second BME molecule and leaving the residue inactive.

NoxV has shown a higher TTN compared to previously studied NADH oxidases from *L. sanfranciscensis* and *L. lactis*, both with and without exogenously added reducing agents (Table 6.3). Such a higher TTN is an indication of improved intrinsic stability against overoxidation at the catalytically active cysteine residue because DTT, a known enhancer of TTN in the other NADH oxidases from *L. sanfranciscensis* and *L. lactis*, has little effect on the TTN in *L. plantarum*. As overoxidation of a catalytic cysteine is known as limiting catalysis over time in enzymes such as D-amino acid oxidase from *Trigonopsis variabilis* and xenobiotic reductase A (Xen A) from *Pseudomonas putida*, this increased intrinsic stability is of great interest.[203,223] The reason of decreased influence of reducing agents will be addressed in future works. Studying the exposure of the active cysteine in different enzymes would be of most interest to see if i) it is less accessible to the reducing agents or ii) protected from possible overoxidation factors, such as oxygen and H_2O_2.

The increased stability without reducing agents would be favorable since there are known inhibition effects of DTT on certain rare sugar- producing dehydrogenases, such as mannitol dehydrogenase from *Apium graveolens*.[224] Also, improved stability without reducing agents would be a significant advantage in industries where the use of reducing agents is avoided.

6.3.6 Mutation for NADPH activity

Wild type NoxV had activity exclusively towards NADH and not towards NADPH. To introduce NADPH activity, substrate binding pocket mutations were carried out. Homology modeling of the sequence of NoxV from *L. plantarum* onto the crystal structure of NAD(P)H oxidase from *L. sanfranciscensis* revealed electrostatic differences in the substrate binding pocket.[130] Nox2 from *L. sanfranciscensis* features histidine (His 181) to enable the negative charge accommodation of the NADPH 2′-phosphate, but NoxV consists of only small or hydrophobic residues in that area. Based on this knowledge, these residues were targeted for mutation with basic residues such as histidine, lysine and arginine.[225-227]

The single mutations of residues G178 and L179 into K, R and K, R, H, respectively, and double mutations 178/179 were performed and investigated for substrate specificity. The mutation of G178H was excluded because then two histidines would be positioned next to each other, causing steric hindrance within the binding pocket. The resulting mutants were expressed on small scale and assayed at the cell lysate level (Table 6.4). All the mutants showed activity with both NADH and NADPH as substrates. Among the single and double variants, L179R shows the highest specific activity at 25 °C and pH 7.5 with NADH (7.32 $U.mg^{-1}$) and G178R/L179R with NADPH (6.00 $U.mg^{-1}$), compared to wild-type at 10.0 $U.mg^{-1}$. We surmise that introduction of an additional positive charge at G178R stabilizes the positioning of L179R, decreasing the ability of free rotation of L179R side-chain bonds through hydrogen bonding. Arginine may be expected to provide the greatest NADPH activity because it has the most

positions for hydrogen bonding. The low activity of L179H can be rationalized by the presence of an adjacent proline causing steric hindrance.

Table 6.4 Cell lysate activity of mutants.

Mutant	NADH activity (U.mg^{-1})	NADPH activity (U.mg^{-1})
Wild Type	10.0	0.00
G178K	3.92	0.46
G178R	1.51	0.23
L179K	5.14	1.03
L179R	7.32	1.76
L179H	1.37	0.64
G178K/L179K	0.84	3.11
G178K/L179R	2.00	5.68
G178K/L179H	1.24	3.85
G178R/L179K	0.94	3.56
G178R/L179R	2.64	6.00
G178R/L179H	0.64	0.52

6.3.7 Study of variants L179R and G178R/L179R

L179R and G178R/L179R were selected for further purification and kinetic characterization (Table 6.5), and showed an FAD/enzyme ratio of 1.42 and 0.71, respectively (data not shown). The difference in flavin content seems to be due to spectral absorbance error from the low enzyme concentrations, and the FAD/enzyme ratio would most likely be close to one, which would be comparable to previous NOXs.[130] L179R was not as active as the wild-type (lower k_{cat}^{NADH}). However, the K_M^{NADH} value was also much lower, improving the specificity $(k_{cat}/K_M^{NADH})_{app}$ more than 4-fold. The mutant also showed NADPH activity but with a very high K_M^{NADPH} value. The double mutant G178R/L179R shows a trend similar to L179R: decreased $(k_{cat}^{NADH})_{app}$ and K_M^{NADH} values, resulting in an improved specificity $k_{cat,app}/K_{m,NADH}$ of 13.2 μM^{-1}.s^{-1}. For NADPH activity $(k_{cat}/K_M^{NADPH})_{app}$ was 11.7 μM^{-1}.s^{-1}. Overall, both variants yielded improved

specificities k_{cat}/K_M for both NADH and NADPH. The TTN of the two variants behaved similarly to the wild-type, in that the presence of reducing agents did not affect the processing stability (TTN) to a great extent (Table 6.3).

Table 6.5 Kinetic parameters of wild-type (WT) and mutant NAD(P)H oxidases. Data were fitted with least squares approximation to Michaelis-Menten kinetics with an R^2 of 0.96 or higher.

Enzyme	NADH			NADPH		
	k_{cat} (s^{-1})	K_M^{NADH} (μM)	k_{cat}/K_M^{NADH} ($\mu M^{-1}.s^{-1}$)	k_{cat} (s^{-1})	K_M^{NADPH} (μM)	k_{cat}/K_M^{NADPH} ($\mu M^{-1}.s^{-1}$)
WT	211.6	50.2	4.22	-	-	-
L179R	122.0	6.56	18.6	146.4	489.6	0.30
G178R/L179R	34.0	2.57	13.2	114.1	9.76	11.7

6.4 Conclusion

Starting from an annotated sequence, NADH oxidase V from *L. plantarum* (ATCC 10012) was developed and demonstrated to be a very active enzyme in air-saturated aqueous buffer at pH 7.5 and 25 °C ($k_{cat,app}$ = 212 s^{-1} and K_M^{NADH} = 50.2 μM). The temperature and pH optima, 45 °C and pH 5.5-8.0, respectively, overlap with relevant dehydrogenases that might be coupled for cofactor regeneration with NoxV. With total turnover numbers (TTN) of 128,000 and 168,000, respectively, in the absence and presence of DTT, *L. plantarum* NoxV demonstrated high processing stability regardless of the presence of reducing agents, a first among NADH oxidases.

After inspection of the homology model of *L. plantarum* NoxV on the structure of the *L. sanfranciscensis* analog, mutations in the substrate binding pocket to basic amino acid residues to accommodate the negative charge of the 2′-phosphate of NADPH were introduced to broaden the substrate specificity to NADPH. All single and double variants

G178K,R/L179K,R,H exhibited significant NADPH and NADH activity. Novel and more stable cofactor regeneration enzymes, in conjunction with novel methods of immobilization, such as on functionalized nanotubes , stand to further broaden the application of oxidative reactions with dehydrogenases/NADH oxidases.[228]

CHAPTER 7

RECOMMENDATIONS AND CONCLUSIONS

7.1 Recommendations

7.1.1 Enzymatic reduction of hydroxylamine

As shown in Chapter 2, nitroreductases (NRs) are capable of producing hydroxylamine, but not the amine. The exact reason why NRs do not reduce the –NHOH is unknown has yet to be determined. To complete the biocatalytic reduction from hydroxylamino to amino there two approaches can be proposed: engineering the current NR and altering its selectivity to produce amines or utilizing a different enzyme system that is capable of reducing hydroxylamimes and pairing it with NRs.

For NR engineering two possibilities can be proposed to overcome the lack of amine production. The first proposition is to engineer a NR to alter the redox potential of the bound flavin. Previously, Koder et al. has suggested that the last reduction step is improbable due to limitations in the flavin redox potential compared to the substrate.[40,229] Our collaborator Dr. Anne-Frances Miller's group at the University of Kentucky will investigate the possibility of lowering the flavin redox potential by changing the enzyme environment via protein engineering.

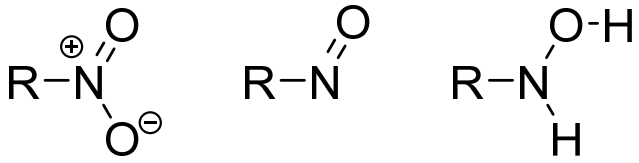

Figure 7.1 Comparison of nitro, nitroso, hydroxylamine moieties.

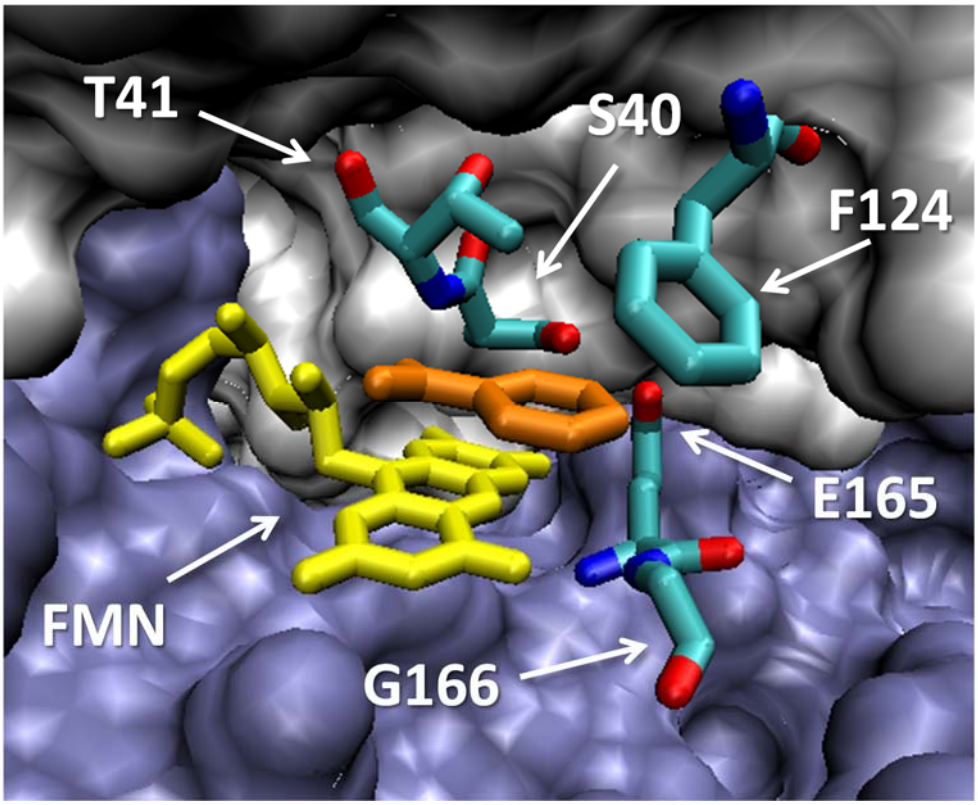

Figure 7.2 Crystal structure of NRentcl (PDB ID: IKQB) highlighted with FMN (yellow) and benzoate inhibitor (orange) and residues within 4 Å of benzoate at the dimer interface (monomers represented in blue and silver). Image rendered with Visual molecular dynamics (VMD).[41]

The second proposal is to modify the hydrogen bonding characteristics in the enzyme. Both nitro- and nitrosobenzene have several hydrogen bond acceptors, whereas hydroxylamines have hydrogen bond donors (Figure 7.1). These different characteristics could govern whether or not the substrate will bind for catalysis. As there is no reduced

NR crystal structure available with a bound inhibitor the oxidized form with benzoate bound as an inhibitor was studied for possible mutation sites. Mapping the active site with residues within 4 Å of benzoate yielded four amino acids as mutational candidates which were S40, T41, F124, and E165. Among these four, S40 and T41 should be investigated first as they are hydrogen bond donors in close proximity to the carboxyl group of benzoate. Steric considerations indicate that the best residues to replace these are glycine, alanine and valine. However, as the exact mechanism of interaction is unknown, directed evolution in combination with site-saturation mutagenesis may be beneficial.

An alternative biocatlytic route can also be considered for the final reduction step from hydroxylamine to amine. The use of a NADH cytochrome b5 reductase (CYB5R) and cytochrome b5 (CYB5) enzyme system has been published in the context of microsomal reduction of hydroxylamines in humans. Kurian et al. were able to show the substrates sulfamethoxazole hydroxylamine and dapsone hydroxylamine to their corresponding amines.[230] Catalysis is proposed to occur through the transfer of electrons from NADH to CYB5R (two-electrons), from CYB5R to CYB5 (one-electron), and from CYB5 to the hydroxylamine. As both NRs and CYB5R utilizes NADH as the electron donor there will be no need for an additional cofactor regeneration system. Therefore, the complete reaction can be conducted as a one-pot synthesis (Figure 7.3). This work will be continued in our lab by Lizzette M. Gómez Ramos.

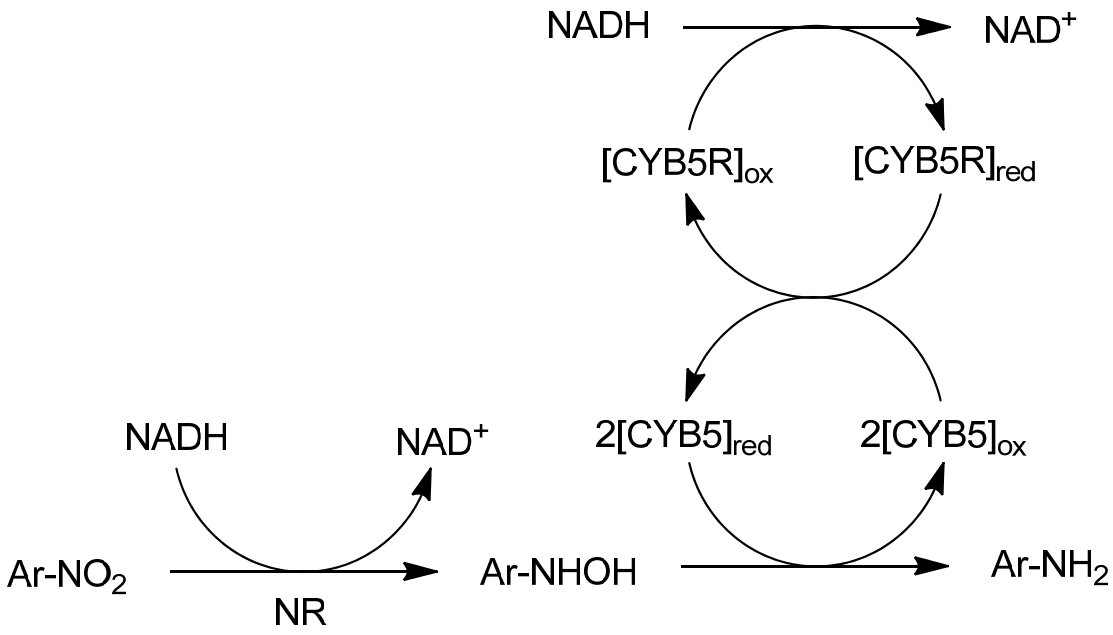

Figure 7.3 Proposed reaction scheme with a conjugated system of NRs and cytochrome enzymes (CYB5R and CYB5). Reduction of nitroaromatics (Ar-NO_2) to hydroxylamines (Ar-NHOH) are catalyzed with NRs and the subsequent reduction to amines (Ar-NH_2) is catalyzed by the cytochrome enzyme system.

7.1.2 High-throughput colorimetric assay

When generating a large number of enzyme variants through directed evolution (Section 7.1.1), it is necessary to have a quick and effective method to qualitatively analyze the occurring changes. As the goal is to alter the selectivity towards amine, the current assay that monitors the oxidation of NAD(P)H and relates that to substrate reduction is inadequate. The general rule of directed evolution is that "you get what you screen for" [231], thus, selecting variants based upon increased NAD(P)H oxidation rates will not necessarily translate into change in selectivity.

There are several fluorimetric and colorimetric assays that have been previously developed for the detection of amines including ninhydrin[232], fluorescamine[233], *o*-phthalaldehyde[234]. However, these assays cannot be utilized in biocatalytic assays due to

their affinity to the enzyme in the reaction solution. Further, many of these reagents react with the different redox states of nitrogen making it difficult to selectively quantify the amount of aromatic amine in solution.

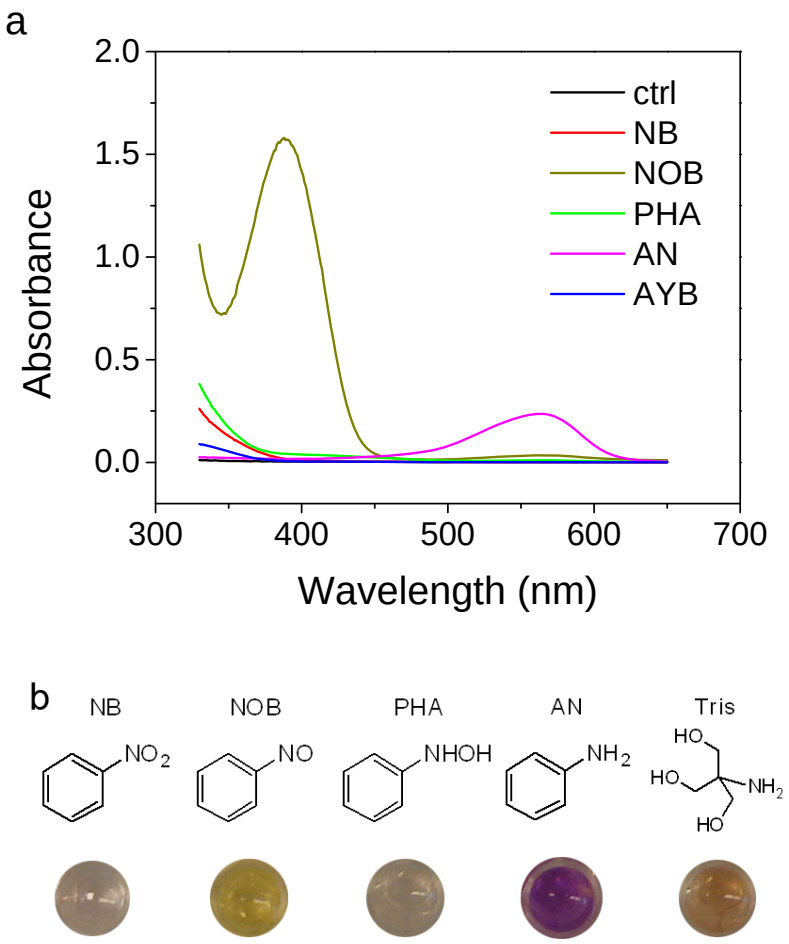

Figure 7.4 MBTH assay results. a) spectrum of the different redox states coupled with MBTH and b) color observed from 2 M substrate.

Pentacyanoammineferroate sodium salt (PCAF) and 3-methyl-2-benzothiazolinone hydrazone hydrochloride monohydrate (MBTH) were identified as candidates for the development of a colorimetric aromatic amine selective assay. PCAF

exhibited a fairly high extinction when reacted with aniline, but showed better affinity towards the PHA (data not shown). MBTH, which was initially developed as a phenol detection assay [235], selectively reacts with aniline under acidic conditions to produce a bright magenta color (**Figure 7.4**, for reaction details see Appendix F). Notably, NOB has a very strong signal that arises when associated with MBTH. This is problematic because over time the color even shifts towards the amine signal, making it difficult to resolve the two. One method to alleviate this problem is to conduct all experiments in anaerobic conditions. This has been tested and confirmed to work by one of our collaborators, John Hoben at the University of Kentucky. This will further eliminate the oxidation problems that are associated in the dual presence of hydroxylamines and molecular oxygen. Additionaly, color formation was also observed with Tris buffer which is an amine salt. Further work must be performed to investigate whether the selectivity holds in different reaction conditions, especially in the presence of cell lystate. If cell lystate proves to be detrimental a partial his-tag purification can be performed on nickel coated 96-plate well plates.

7.1.3 Overcoming low solubility

One of the major barriers that need to be addressed is the low solubility of many of the nitro aromatic substrates. The limitations in solubility are extreme to the extent that some substituted nitrobenzenes can only be dissolved up to 0.1 (w/w) % in aqueous solutions. Even with the enzymo-chemical synthesis developed in Chapter 4, the major bottleneck in synthesis is tied to low solubility.

To overcome this hurdle, the enzymo-chemical synthesis can be run in a continuous two-pot, two-step fashion. The hydroxylamine reduction step could then be

carried out in either a purely-aqueous or an aqueous-organic solvent. Although the concept of a two-pot, two-step system is straight-forward, it is unknown whether the reduction to amine with FSA will happen at similar levels. Another alternative can still be to run a one-pot, two-step system with the addition of organic solvents to increase the solubility or availability of substrates. For this system, possibilities include the use of both mono- and bi-phasic systems. However, to properly apply this technique, enzymes will either need to have high stability in solvents (monophasic option) or avoid contact with it (biphasic option). As flavoenzymes require the use of nicotinamide cofactors and a paired regeneration system, it will be difficult to perform reactions in solely organic solvents. High stability of enzymes in the presence of organic solvents can be attained by enzyme immobilization. Immobilization can be achieved through methods such as support binding, entrapment and cross-linking.[236] One concern that can arise for immobilization is the fact that NRs have its active site at the dimer interface. Depending on the immobilization method, the force could potentially make the monomers dissociate. To overcome such a problem, a monomeric NR, such as that developed in Chapter 5, could be used for immobilization.

7.2 Conclusions

The use of biocatalysis for synthesizing valuable molecules is an area where still much research can be done. This holds true for the application of nitroreductases (NRs) as well. Given the vast amount of known NRs and literature published on them, it is quite astonishing that there are still questions regarding their mechanism and product distribution. Although the goal of this thesis was not focused on identifying these aspects

the results obtained from Chapter 2 and 3 help understand these characteristics. Through the use of analytical tools, such as ^{15}N-NMR and HPLC, we were able to show that the enzymatic product from NB was PHA, not AN. Further, the reason for amine formation that is observed in limited examples was investigated to define whether this phenomenon is dependent on the enzyme and/or substrate. Comparison of the product spectrum of NRsalty and NRmycsm suggested that the selectivity is most likely related to the substrate features such as aromaticity and electron effects. Details on the nitro reduction mechanism were obtained while comparing these two enzymes and their pH dependencies. The transition in $\log[(k_{cat}/K_M^S) / (k_{cat}/K_M^S)_0]$ that NRmycsm exhibits, leads us to propose that enzyme is being heavily influenced by substrate binding or transition state stabilization depending on the substituent. Additional experiments to study the substrate binding kinetics have been proposed to obtain more insight on this matter. Most importantly, through the Hammett correlation we were able to develop a quantitative structure–activity relationship (QSAR) that indicates that substrates with more electron-withdrawing groups will be the best candidates for biocatalytical reduction.

As the desired amine was not produced through NRs, an attempt to further reduce the hydroxylamine was made. The first approach was through the establishment of an enzymo-chemical synthesis where NRs were paired with FSA to create a one-pot two-step synthesis. With the addition of the acidic reduction step we were able to obtain a 90.2% yield of 4-aminobenzoic acid starting from 4-nitrobenzoic acid. The second approach was to develop a high-throughput colorimetric assay to aid the alteration in

substrate specificity via directed evolution of NRs. An assay utilizing MBTH was developed but is still in the preliminary stages of application.

For the purpose of expanding the immobilization application possibilities, NRs were successfully created from monomeric ER KYE1 scaffolds. The best variant F296A/Y375A showed to have more than a 100-fold increase in specific NR activity and was able to catalyze the reduction of 4-NBS at 1.20 s^{-1}. Another variant H191A/F296A/Y375A had no reactivity towards KIP while maintaining comparable NR activity to the double variant

A different type of enzyme, NADH oxidase V (NoxV) from *Lactobacillus plantarum*, was characterized and developed for nicotinamide cofactor regeneration. This enzyme demonstrated to not only be very active ($k_{cat,app}$ = 212 s^{-1} and K_M^{NADH} = 50.2 μM), but it showed to have a superior TTN compared to other Noxs, especially in the absence of reducing agents (TTN = 128,000). This high processing stability regardless of the presence of reducing agents is a first among NADH oxidases. Further, protein engineering was performed to alter the substrate specificity and accommodate NADPH. The variants L179R and G178R/L179R exhibited significant NADPH and NADH oxidase activity and maintained high TTN.

This dissertation investigated a number of flavoenzyme applications for active pharmaceutical ingredient (API) production. In some cases it was through direct participation in the reaction of interest, whereas in other cases it was by fulfilling a supporting role. Regardless of the function, the value in the target molecules and the constraints set in the field of production make these biocatalytic pathways worthwhile investigating.

Appendix A

ENZYME NOMENCLATURE

The use of enzyme nomenclature can show inconsistencies in many cases. This is also the case for nitroreductase names. Below are some examples.

A.1 The gene is called both by *nfnA* (*nfsA*) and *nfnB* (*nfsB*), and the enzyme as NfsA, NfsB or NTR.[162]

A.2 The nitroreductase from *E. cloacae* is known as NR, which here is the universal nomenclature for Nitroreductase.[40]

A.3 Change in name due to change in publishing group. "Classical" nitroreductase (Cnr) and NRSal are identical enzymes.[39,237]

A.4 GlNR1 from *Giardia lamblia* is deposited in Genbank as Fd-NR2.[238]

To avoid these complications, in this document we propose a systematic nomenclature for naming nitroreductases, where all NRs shall be named in conjunction to their species name. For example, a NR from *Escherichia coli* will be named with the first three letters of the first word and two letters of the second word, NRescco. The use of multiple characters is necessary as it will be impossible to distinguish *E. coli* and *Enterobacter cloacae* if they are abbreviated as "ec". Again, this is for convenience and clarity of this thesis. To avoid confusion, the enzymes will be documented in their original names in the Introduction and phylogenetic tree (Appendix B)

Appendix B

PHYLOGENETIC TREE

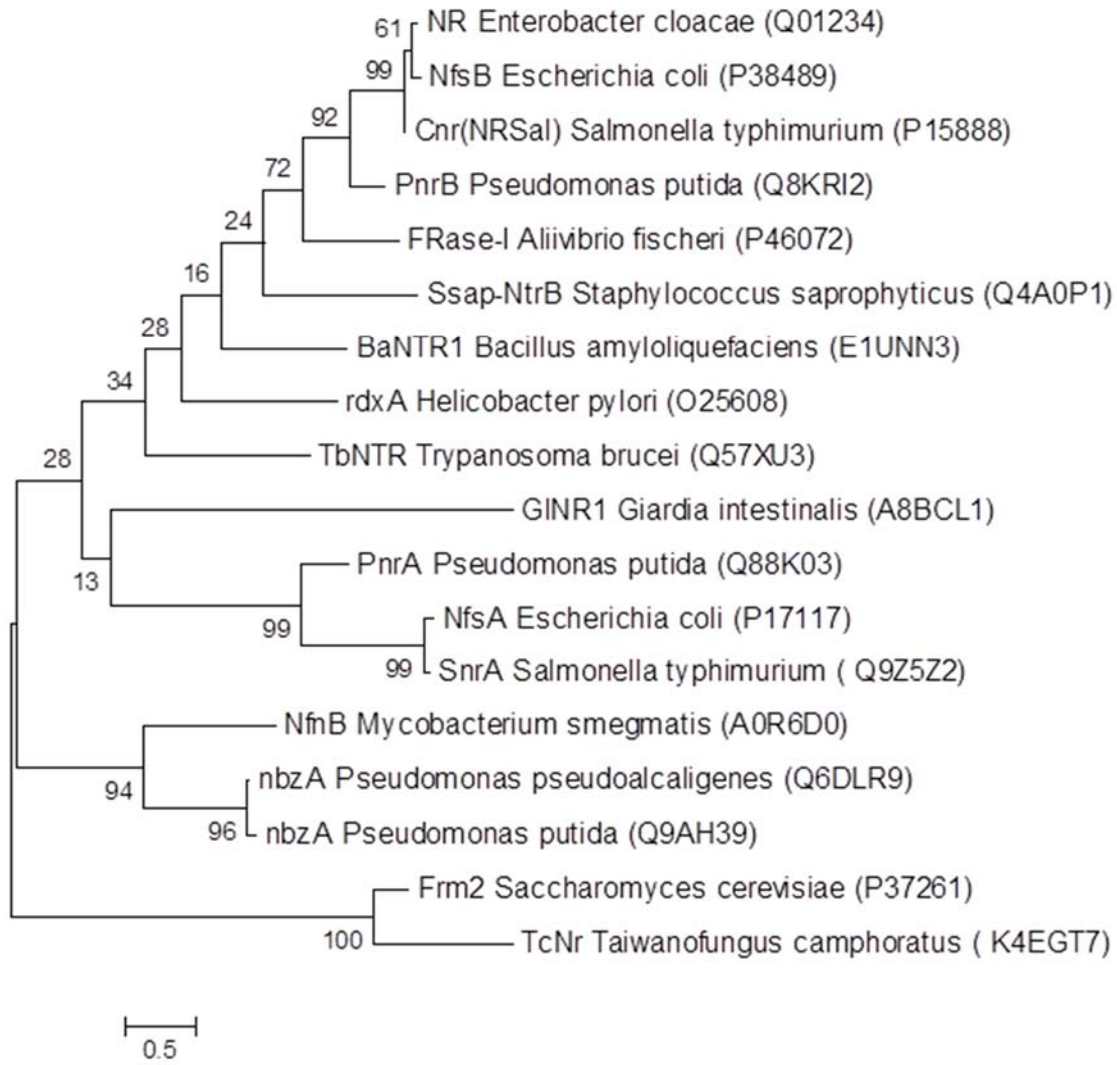

Figure B.1 NR phylogenetic tree created with Maximum Likelihood (ML) method with a bootstrap test (500 replicates) using MEGA6 software[239] Accession numbers given in parentheses.

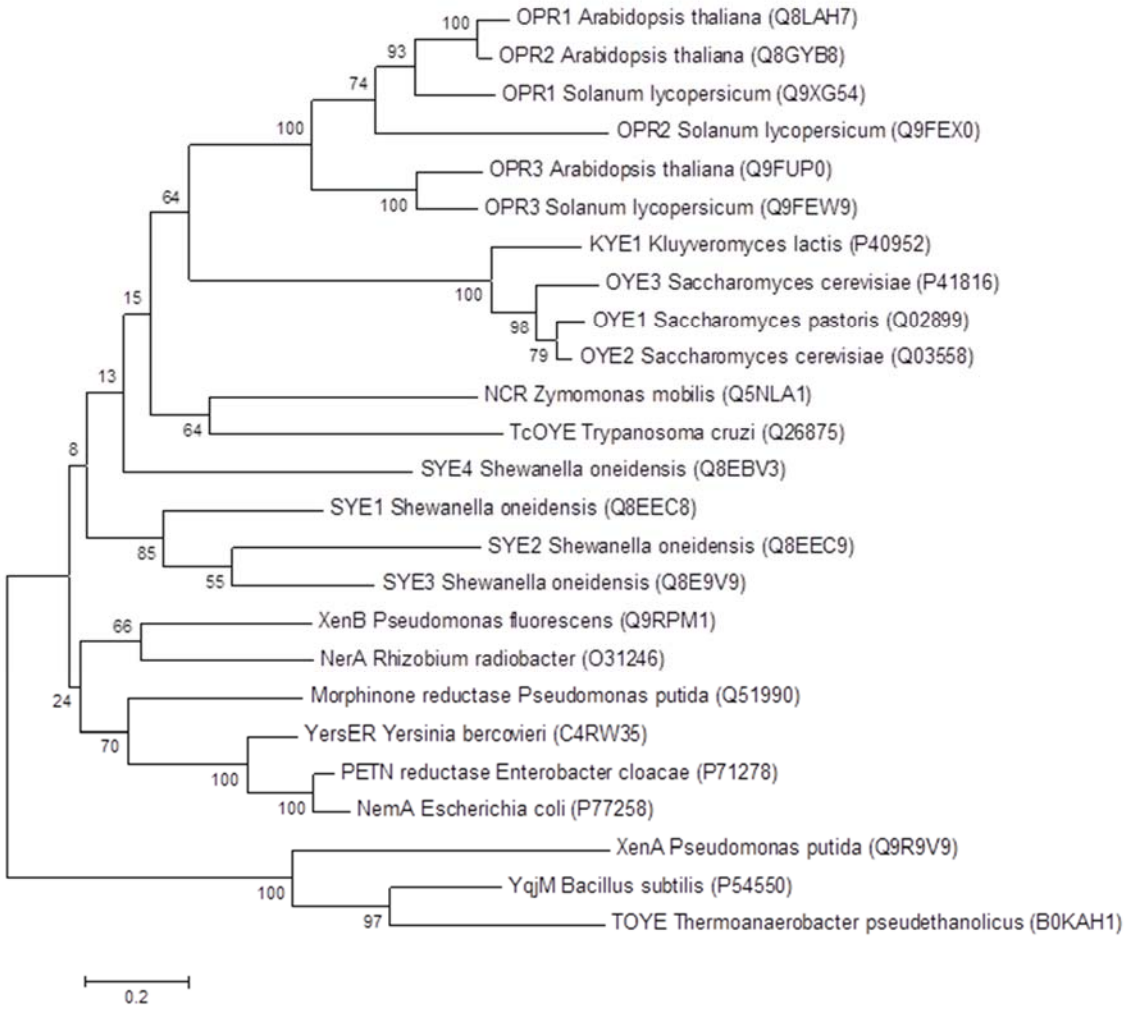

Figure B.2 ER phylogenetic tree created with Maximum Likelihood (ML) method with a bootstrap test (500 replicates) using MEGA6 software[239] Accession numbers given in parentheses.

Figure B.3 Sequence alignment of ERs and NRs. gray: identity (%); white: similarity (%).

%	OYE1 (Q02899)	KYE1 (P40952)	PETN (P71278)	YersER (C4RW35)	XenA (Q9R9V9)	NRsatly (P15888)	NRentcl (Q01234)	NRescco (P38489)	NRmycsm (A0R6D0)
OYE1	-	80.5	45.4	47.7	34.3	15.3	14.3	17.2	18.0
KYE1	71.5	-	47.0	46.8	32.8	17.8	15.6	18.8	17.3
PETN	34.3	35.8	-	83.0	37.7	18.1	18.4	18.6	21.0
YersER	36.0	34.3	74.5	-	38.3	19.4	20.2	19.9	21.3
XenA	22.4	22.3	24.6	24.2	-	19.0	19.0	17.9	22.0
NRsatly	9.3	10.3	11.5	12.4	10.5	-	92.2	90.8	30.4
NRentcl	8.0	10.3	11.0	11.5	9.6	88.9	-	90.3	30.4
NRescco	9.7	12.0	11.5	12.4	11.6	88.5	88.0	-	29.1
NRmycsm	10.5	11.3	13.4	12.9	12.4	16.9	15.6	15.6	-

Appendix C

CONSTRUCTS & PRIMERS

Table C.1 Construct information

Enzyme	Organism	Accession Number	Vector	Restriction sites	Tags
NRsalty	*S. typhimurium*	P15888	pET-28a	NcoI/XhoI	none
NRentcl	*E. cloacae*	Q01234	pET-24d	NcoI/XhoI	none
NRentcl-TRX	*E. cloacae*	Q01234	pET-32a	NcoI/XhoI	TRX, TEV, N-His
NRentcl-his	*E. cloacae*	Q01234	pET-28a	NdeI/XhoI	N-His
NRmycsm	*M. smegmatis*	A0R6D0	pET-28a	NdeI/XhoI	N-His, C-His
XenA	*P. Putida*	Q9R9V9	pET-27b	NdeI/HindIII	none
KYE1	*K. lactis*	P40952	pET-28a	NdeI/XhoI	N-His, TEV
YersER	*Y. bercovieri*	C4RW35	pET-28a	NdeI/HindIII	N-His
NoxV	*L. plantarum*	Q88SH4	pET-28a	NcoI/XhoI	none

Table C.2 Primer design for NoxV variants. Mutated residues are colored gray and the affected codons are underlined

Enzyme	Mutatation	Sequence (5′ to 3′)
NoxV	forward	TGCATGCATGCCATGGTTATGAAAGTTATTGTAATT GGTTGTACCCA
	reverse	CCGCCGCCGCCGCTCGAGTTATTCAGTGACAGCTTC GGCC
	G178ARR	GCAAGGTAAGGAAGTCACACTAATTGATARRTTACC ACGGATTTTAAATAAATACTTAGACAA
	L179CRY	AGGTAAGGAAGTCACACTAATTGATGGTCRYCCACG GATTTTAAATAAATACTTAGACAAAG
	L179K	AGGTAAGGAAGTCACACTAATTGATGGTAAACCAC GGATTTTAAATAAATACTTAGACAAA
	G178ARR/L179CRY	GCAAGGTAAGGAAGTCACACTAATTGATARRCRYCC ACGGATTTTAAATAAATACTTAGACAAAG
	G178ARR/L179K	GCAAGGTAAGGAAGTCACACTAATTGATARRAAAC CACGGATTTTAAATAAATACTTAGACAAA

Table C.3 ER to NR site-directed mutagenesis primer forward sequence. Mutated residues are colored gray and the affected codon is underlined

Enzyme	Mutatation	Sequence (5′ to 3′)
KYE1	T37G	GGGTTGTCATGCCTGCATTGGGTAGAATGAGAGCGTTGC ATCCAG
	M39Y	TTGTCATGCCTGCATTGACAAGATATAGAGCGTTGCATC CAGGCAA
	W116A	CAACAAGTCTTTTGTTTGGGTACAATTGGCGGTTCTAGGT AGACAAGCTTTTGCTGATA
	W116Y	CAACAAGTCTTTTGTTTGGGTACAATTGTATGTTCTAGGT AGACAAGCTTTTGCTGATAA
	H191A	CTGGTGCAGATGGTGTTGAAATCGCTTCCGCTAACGGTT ATTTGTTGA
	N194A	GGTGTTGAAATCCATTCCGCTGCCGGTTATTTGTTGAATC AATTCCTAGA
	F296A	GAACCTCGTGTCACATCGCCAGCCCAACCGGAATTTGAA GGCTG
	Y375A	CATTGAATCAATACGATAGACCCTCTTTCGCCAAAATGT CTGCGGAAGGGTATATC
	H191A/N194A	TGGTGCAGATGGTGTTGAAATCGCTTCCGCTGCCGGTTA TTTGTTGAATCAATTCCTAG
YersER	T27G	CGCGTATTTATGGCACCACTGGGTCGCTTACGCAGTATT GAGCC
	H182A	GAAGCGGGTTTTGACTATATCGAACTCGCTGCCGCCCAT GGTTATTTGC
	W276 A	CCTGCACATCTCCGAGCCAGATGCGGCCGGTGGTAAACC TTACTCAGAG
	Y352A	AATGAGCCTGATGGCGAAACATTCGCCGGCGGCGGTGCT AAGG

Table C.4 Primer design for NRentcl library Mutated residues are colored gray and the affected codon is underlined

Enzyme	Mutatation	Sequence (5′ to 3′)
NRentcl	T41N	GCAGTACAGCCCGTCCAGCAACAACTCCCAGCCGTGGCA
	T41Q	GCAGTACAGCCCGTCCAGCCAGAACTCCCAGCCGTGGCACT
	S40NNK	GCTGCAGTACAGCCCGTCCNNKACCAACTCCCAGCCGTGG
	T41NNK	GCAGTACAGCCCGTCCAGCNNKAACTCCCAGCCGTGGCACT
	T41S	GTACAGCCCGTCCAGCAGCAACTCCCAGCCGTGG
	S40N/T41S	GCAGTACAGCCCGTCCAACTCCAACTCCCAGCCGTG

Appendix D

NRMYCSM CHARACTERIZATION

D.1 Materials and Methods

D.1.1 Influence of pH and temperature on enzyme activity

Initial specific activity measurements were conducted on a DU 800 spectrophotometer (Beckman Coulter; Brea, CA). Oxidation of the cofactor NADH was monitored at 370 nm (ε_{370} = 2,660 $M^{-1}.cm^{-1}$).[176] Enzyme pH activity profiles were obtained at 25 °C with 0.1 μM enzyme, 0.5 mM NADH, and 0.1 mM 2,4-DNT. 100 mM buffers containing one of the following salts: sodium citrate (pH 4-6.5), NaP_i buffer (pH 6-8), Tris-Cl (pH 7-9) and glycine (pH 9-10).

The dependence of the enzymatic activity on temperature was studied with 100 mM NaP_i buffer (pH 7), 0.1 μM enzyme, 0.5 mM NADH, and 0.1 mM 2, 4-DNT. The buffer was equilibrated to the target temperature and the enzyme was added. After 1 min of incubation, the assay was initiated with addition of the substate. Measurements were conducted over a temperature range of 10 to 55 °C.

D.1.2 Circular dichroism (CD)

Since the imidazole which is added during the purification has a high absorbance at the used wavelength spectra is was removed by size exclusion chromatography (PD-10 Desalting Column, GE Healthcare). The ellipticity was measured with a Jasco J-810 circular dichroism (CD) spectrophotometer (Easton, MD) equipped with a Peltier temperature controller. The temperature was increased at a rate of 1 °C min^{-1} with a range

of 10-90 °C at 220 nm. The protein concentration was 0.675 mg.mL^{-1} in 10 mM NaP_i buffer (pH 7).

D.2 Results and Discussion

D.2.1 Characterization of NRmycsm

Characterization of NRmycsm according to its activity dependence on pH and temperature were determined. The highest activity is achieved at pH 7 with phosphate buffer.

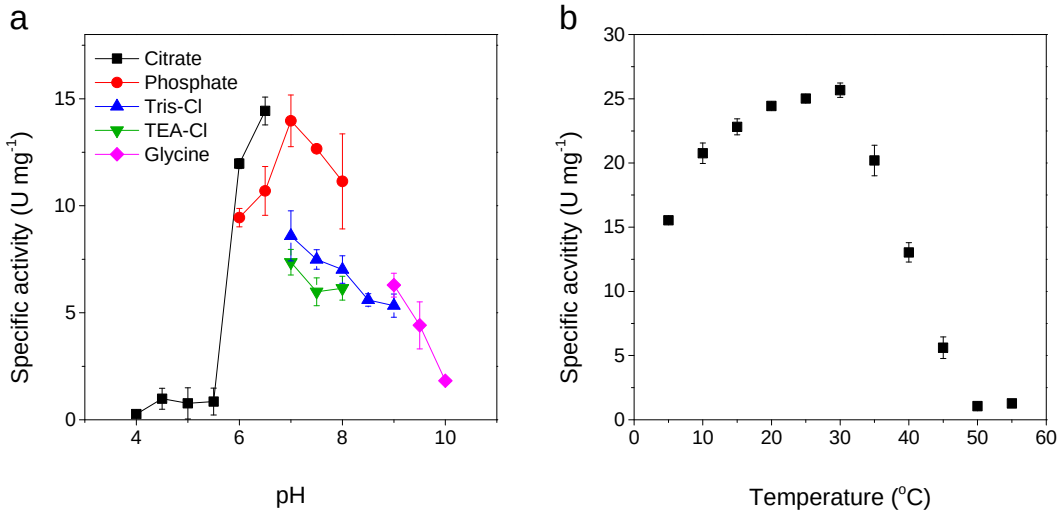

Figure D.1 NRmycsm activity profile a) in different buffers (100 mM) at different pH values at 25 °C and b) at various temperatures with 50 mM NaP_i buffer (pH 7.0).

The pH-activity curve shows an activity maximum of 14.4 U.mg^{-1} at pH 6.5 with citrate buffer and of 13.9 U.mg^{-1} at pH 7 with phosphate buffer. The activity with Tris-Cl and TEA-Cl was significantly lower at similar pH values compared to phosphate buffer, which indicates that the activity is also buffer dependent (**Figure D.1**a). This was different from other nitroreductases like NRsalty from *Salmonella typhimurium* which showed higher activity with Tris-Cl than in phosphate buffer. However, the pH-optimum of NRmycsm is similar to NRsalty.[39]

The temperature-activity curve shows a temperature optimum at 30 °C where the specific activity is 25.6 $U.mg^{-1}$. Interestingly the activity of NfnB decreases only by 18.9 % to 20.7 $U.mg^{-1}$ at 10 °C compared to 30 °C (**Figure D.1**b). Using an Arrhenius relation for the temperature range from 10 to 30 °C gives an activation energy, E_A, of 22.6 $J.mol^{-1}$. The relatively low activation energy and the low temperature optimum might be the reason for better expression at room temperature compared to 37 °C. The unusual phenomena of low activation energy and temperature optimum was recently descript for a Nitroreductase from *Staphylococcus saprophyticus*.[31]

D.2.2 Thermal stability of NRmycsm

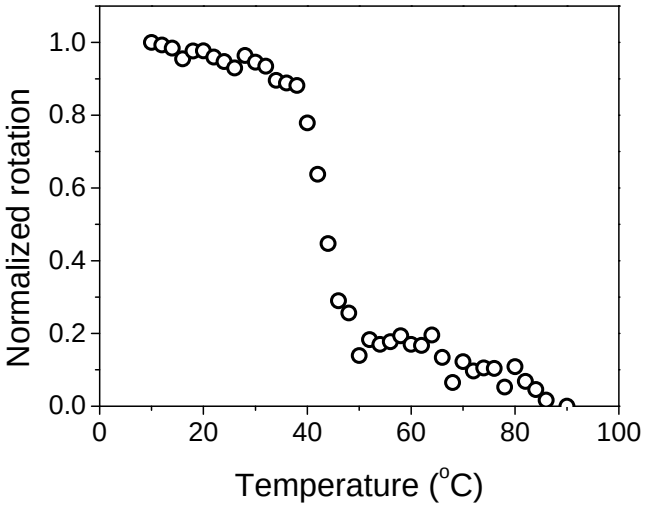

Figure D.2 Thermal denaturation of NRmycsm in 10 mM NaP_i (pH 7.0)

The melting temperature (T_m) of proteins can be determined by measuring the change in ellipticity as a function of temperature. When heated the protein denatures and loses its ordered structure such as α-helices and β-sheets. The loss of ordered structure contributes to the change in ellipticity. The normalized ellipticity as a function of temperature reveals

a single stage unfolding of NfnB and the melting temperature can be calculated from the midpoint of the transition with 43.4 °C (Figure D.2).

Appendix E

SUPPLEMENTARY INFORMATION FOR CHAPTER 5

Table E.1 Growth conditions for KYE variants

Variant	Temperature (°C)	IPTG (mM)
WT	37	0.5
T37G	37	0.5
M39Y	18	0.5
W116A	18	0.1
W116Y	30	0.5
H191A	30	0.5
N194A	30	0.5
F296A	37	0.1
Y375A	37	0.1
T37G/Y375A	37	0.5
M39Y/Y375A	30	0.5
F296A/Y375A	18	0.5
W116Y/Y375A	30	0.5
T37G/M39Y/Y375A	30	0.5
T37G/W116Y/Y375A	18	0.5
T37G/H191A/Y375A	37	0.5
M39Y/H191A/Y375A	18	0.5
M39Y/N194A/Y375A	18	0.5
H191A/F296A/Y375A	30	0.5
N194A/F296A/Y375A	18	0.5
H191A/N194A/F296A/Y375A	18	1.0
H191A/N194A	30	0.5

Table E.2 Summary of KYE1 variants activity comparison

Enzyme	ER ($U.mg^{-1}$)	NR ($U.mg^{-1}$)	NR/ER ratio
WT	2.27	0.01	0.00
T37G	-	0.13	-
M39Y	1.97	0.08	0.003
H191A	N.D.	0.12	1.49
N194A	1.26	0.42	0.14
W116A	N.D.	0.00	0.00
W116Y	0.39	0.25	0.17
F296A	1.33	0.23	0.04
Y375A	0.09	0.31	1.12
T37G/Y375A	N.D.	N.D.	0.00
M39Y/Y375A	0.37	0.74	1.49
W116Y/Y375A	N.D.	0.63	39.6
F296A/Y375A	0.12	1.12	10.3
H191A/N194A	N.D.	0.74	54.6
T37G/M39Y/Y375A	0.40	0.07	0.01
T37G/W116Y/Y375A	0.03	0.07	0.14
M39Y/H191A/Y375A	N.D.	0.26	6.79
M39Y/N194A/Y375A	N.D.	N.D.	-
H191A/F296A/Y375A	N.D.	1.03	106
N194A/F296A/Y375A	0.47	0.68	0.98
H191A/N194A/F296A/Y37A	N.D.	N.D.	-

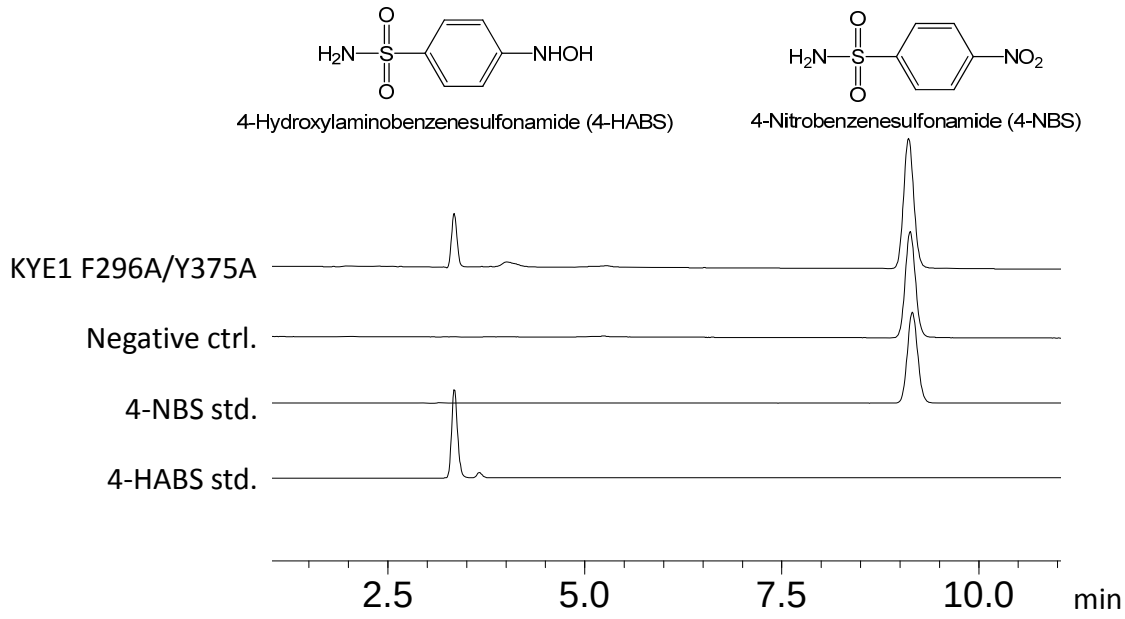

Figure E.1 Enzymatic production of 4-HABS from 4-NBS. 1 mM 4-NBS with glucose dehydrogenase (GDH) recycling system (2.4 $U.mL^{-1}$ GDH, 0.1 mM $NADP^{+}$, 10 mM dextrose) at 25 °C.

Appendix F

COLORIMETRIC ASSAY METHODS

F.1 MBTH assay

F.1.1 Chemicals

3-Methyl-2-benzothiazolinone hydrazone hydrochloride monohydrate (MBTH) and ammonium cerium(IV) sulfate dehydrate (ACS) were purchased from Sigma-Aldrich (St. Louis, MO)

F.1.2 Color development

Experimental procedures were developed based on previously published methods.[235,240,241] Stock solutions of 0.1% (w/v) MBTH was prepared in water (4.28 mM) and 0.2% (w/v) ACS was dissolved in acidified water (0.4% (v/v) sulfuric acid in water) (3.16 mM). Substrates were initially dissolved in DMSO (1 M) then diluted 4 mM in 250 μL of water. To this solution, 250 μL of the MBTH and ACS stock solutions were added. This was incubated over 10 mins and the spectra were recorded using a DU 800 spectrophotometer (Beckman Coulter; Brea, CA).

REFERENCES

[1] Faber, K. *Biotransformations in organic chemistry : a textbook*; 6th rev. and corr. ed.; Springer: Heidelberg ; New York, 2011.

[2] Adlercreutz, P.; Straathof, A. J. J. *Applied biocatalysis*; 2nd ed.; Harwood Academic Publishers: Amsterdam, 2000.

[3] Snider, M. J.; Wolfenden, R., "The rate of spontaneous decarboxylation of amino acids", *J Am Chem Soc*, **2000**, *122*, 11507.

[4] Wolfenden, R.; Snider, M. J., "The depth of chemical time and the power of enzymes as catalysts", *Accounts Chem Res*, **2001**, *34*, 938.

[5] Bommarius, A. S.; Riebel, B. R. *Biocatalysis*; Wiley-VCH: Weinheim ; Cambridge, 2004.

[6] Chotani, G.; Dodge, T.; Hsu, A.; Kumar, M.; LaDuca, R.; Trimbur, D.; Weyler, W.; Sanford, K., "The commercial production of chemicals using pathway engineering", *Bba-Protein Struct M*, **2000**, *1543*, 434.

[7] Blyth, A. W., "LVI.—The composition of cows' milk in health and disease", *Journal of the Chemical Society, Transactions*, **1879**, *35*, 530.

[8] Massey, V., "The chemical and biological versatility of riboflavin", *Biochem Soc T*, **2000**, *28*, 283.

[9] Edwards, A.; Royal Society of Chemistry: London, UK: 2006; Vol. 6, p 1.

[10] Hemmerich, P.; Massey, V.; Fenner, H., "Flavin and 5-Deazaflavin - Chemical Evaluation of Modified Flavoproteins with Respect to Mechanisms of Redox Biocatalysis", *Febs Lett*, **1977**, *84*, 5.

[11] Palmer, G.; Reedijk, J., "Nomenclature of Electron-Transfer Proteins - Recommendations 1989", *European Journal of Biochemistry*, **1991**, *200*, 599.

[12] Merrill, A. H.; Lambeth, J. D.; Edmondson, D. E.; Mccormick, D. B., "Formation and Mode of Action of Flavoproteins", *Annu Rev Nutr*, **1981**, *1*, 281.

[13] Walsh, C. *Enzymatic reaction mechanisms*; W. H. Freeman: San Francisco, 1979.

[14] Mason, R. P.; Holtzman, J. L., "The role of catalytic superoxide formation in the O2 inhibition of nitroreductase", *Biochemical and biophysical research communications*, **1975**, *67*, 1267.

[15] Peterson, F. J.; Mason, R. P.; Hovsepian, J.; Holtzman, J. L., "Oxygen-Sensitive and Oxygen-Insensitive Nitroreduction by Escherichia-Coli and Rat Hepatic Microsomes", *Journal of Biological Chemistry*, **1979**, *254*, 4009.

[16] Angermaier, L.; Simon, H., "On Nitroaryl Reductase Activities in Several Clostridia", *H-S Z Physiol Chem*, **1983**, *364*, 1653.

[17] Zenno, S.; Koike, H.; Kumar, A. N.; Jayaraman, R.; Tanokura, M.; Saigo, K., "Biochemical characterization of NfsA, the Escherichia coli major nitroreductase exhibiting a high amino acid sequence homology to Frp, a Vibrio harveyi flavin oxidoreductase", *Journal of bacteriology*, **1996**, *178*, 4508.

[18] Zenno, S.; Koike, H.; Tanokura, M.; Saigo, K., "Gene cloning, purification, and characterization of NfsB, a minor oxygen-insensitive nitroreductase from Escherichia coli, similar in biochemical properties to FRase I, the major flavin reductase in Vibrio fischeri", *J Biochem-Tokyo*, **1996**, *120*, 736.

[19] Bryant, C.; Deluca, M., "Purification and Characterization of an Oxygen-Insensitive Nad(P)H Nitroreductase from Enterobacter-Cloacae", *Journal of Biological Chemistry*, **1991**, *266*, 4119.
[20] Watanabe, M.; Ishidate, M., Jr.; Nohmi, T., "Nucleotide sequence of Salmonella typhimurium nitroreductase gene", *Nucleic Acids Research*, **1990**, *18*, 1059.
[21] Nokhbeh, M. R.; Boroumandi, S.; Pokorny, N.; Koziarz, P.; Paterson, E. S.; Lambert, I. B., "Identification and characterization of SnrA, an inducible oxygen-insensitive nitroreductase in Salmonella enterica serovar Typhimurium TA1535", *Mutat Res-Fund Mol M*, **2002**, *508*, 59.
[22] Somerville, C. C.; Nishino, S. F.; Spain, J. C., "Purification and characterization of nitrobenzene nitroreductase from *Pseudomonas pseudoalcaligenes* JS45", *Journal of bacteriology*, **1995**, *177*, 3837.
[23] Riefler, R. G.; Smets, B. F., "NAD(P)H : flavin mononucleotide oxidoreductase inactivation during 2,4,6-trinitrotoluene reduction", *Appl Environ Microb*, **2002**, *68*, 1690.
[24] Goodwin, A.; Kersulyte, D.; Sisson, G.; van Zanten, S. J. O. V.; Berg, D. E.; Hoffman, P. S., "Metronidazole resistance in Helicobacter pylori is due to null mutations in a gene (rdxA) that encodes an oxygen-insensitive NADPH nitroreductase", *Molecular microbiology*, **1998**, *28*, 383.
[25] Park, H. S.; Kim, H. S., "Identification and characterization of the nitrobenzene catabolic plasmids pNB1 and pNB2 in Pseudomonas putida HS12", *Journal of bacteriology*, **2000**, *182*, 573.
[26] Caballero, A.; Lazaro, J. J.; Ramos, J. L.; Esteve-Nunez, A., "PnrA, a new nitroreductase-family enzyme in the TNT-degrading strain Pseudomonas putida JLR11", *Environ Microbiol*, **2005**, *7*, 1211.
[27] Kutty, R.; Bennett, G. N., "Biochemical characterization of trinitrotoluene transforming oxygen-insensitive nitroreductases from Clostridium acetobutylicum ATCC 824", *Arch Microbiol*, **2005**, *184*, 158.
[28] Muller, J.; Wastling, J.; Sanderson, S.; Muller, N.; Hemphill, A., "A novel Giardia lamblia nitroreductase, GlNR1, interacts with nitazoxanide and other thiazolides", *Antimicrobial agents and chemotherapy*, **2007**, *51*, 1979.
[29] Manina, G.; Bellinzoni, M.; Pasca, M. R.; Neres, J.; Milano, A.; Ribeiro, A. L. D. L.; Buroni, S.; Skovierova, H.; Dianiskova, P.; Mikusova, K.; Marak, J.; Makarov, V.; Giganti, D.; Haouz, A.; Lucarelli, A. P.; Degiacomi, G.; Piazza, A.; Chiarelli, L. R.; De Rossi, E.; Salina, E.; Cole, S. T.; Alzari, P. M.; Riccardi, G., "Biological and structural characterization of the Mycobacterium smegmatis nitroreductase NfnB, and its role in benzothiazinone resistance", *Molecular microbiology*, **2010**, *77*, 1172.
[30] Hall, B. S.; Wu, X. H.; Hu, L. Q.; Wilkinson, S. R., "Exploiting the Drug-Activating Properties of a Novel Trypanosomal Nitroreductase", *Antimicrobial agents and chemotherapy*, **2010**, *54*, 1193.
[31] Celik, A.; Yetis, G., "An unusually cold active nitroreductase for prodrug activations", *Bioorgan Med Chem*, **2012**, *20*, 3540.
[32] Bang, S. Y.; Kim, J. H.; Lee, P. Y.; Bae, K. H.; Lee, J. S.; Kim, P. S.; Lee, D. H.; Myung, P. K.; Parka, B. C.; Park, S. G., "Confirmation of Frm2 as a novel

nitroreductase in Saccharomyces cerevisiae", *Biochemical and biophysical research communications*, **2012**, *423*, 638.
[33] Yang, J.; Xie, B.; Bai, J.; Yang, Q., "Purification and characterization of a nitroreductase from the soil bacterium Streptomyces mirabilis", *Process Biochem*, **2012**, *47*, 720.
[34] Chauviac, F. X.; Bommer, M.; Yan, J.; Parkin, G.; Daviter, T.; Lowden, P.; Raven, E. L.; Thalassinos, K.; Keep, N. H., "Crystal Structure of Reduced MsAcg, a Putative Nitroreductase from Mycobacterium smegmatis and a Close Homologue of Mycobacterium tuberculosis Acg", *Journal of Biological Chemistry*, **2012**, *287*, 44372.
[35] Chen, C. C.; Ken, C. F.; Wen, L.; Chang, C. F.; Lin, C. T., "Taiwanofungus camphorata nitroreductase: cDNA cloning and biochemical characterisation", *Food Chem*, **2012**, *135*, 2708.
[36] Voak, A. A.; Gobalakrishnapillai, V.; Seifert, K.; Balczo, E.; Hu, L. Q.; Hall, B. S.; Wilkinson, S. R., "An Essential Type I Nitroreductase from Leishmania major Can Be Used to Activate Leishmanicidal Prodrugs", *Journal of Biological Chemistry*, **2013**, *288*, 28466.
[37] Nguyen-Tran, H. H.; Zheng, G. W.; Qian, X. H.; Xu, J. H., "Highly selective and controllable synthesis of arylhydroxylamines by the reduction of nitroarenes with an electron-withdrawing group using a new nitroreductase BaNTR1", *Chem Commun*, **2014**, *50*, 2861.
[38] Bryant, D. W.; Mccalla, D. R.; Leeksma, M.; Laneuville, P., "Type-I Nitroreductases of Escherichia-Coli", *Can J Microbiol*, **1981**, *27*, 81.
[39] Yanto, Y.; Hall, M.; Bommarius, A. S., "Nitroreductase from Salmonella typhimurium: characterization and catalytic activity", *Organic & biomolecular chemistry*, **2010**, *8*, 1826.
[40] Koder, R. L., Jr.; Miller, A.-F., "Steady state kinetic mechanism, stereospecificity, substrate and inhibitor specificity of Enterobacter cloacae nitroreductase", *Biochim. Biophys. Acta*, **1998**, *1387*, 394.
[41] Humphrey, W.; Dalke, A.; Schulten, K., "VMD: Visual molecular dynamics", *J Mol Graph Model*, **1996**, *14*, 33.
[42] Haynes, C. A.; Koder, R. L., Jr.; Miller, A.-F.; Rodgers, D. W., "Structures of Nitroreductase in Three States: Effects of Inhibitor Binding and Reduction.", *J. Biol. Chem.*, **2002**, *277*, 11513.
[43] Parkinson, G. N.; Skelly, J. V.; Neidle, S., "Crystal structure of FMN-dependent nitroreductase from *Escherichia coli* B: a prodrug-activating enzyme.", *J. Med. Chem.*, **2000**, *43*, 3624.
[44] Lovering, A. L.; Hyde, E. I.; Searle, P. F.; White, S. A., "The structure of *Escherichia coli* nitroreductase complexed with nicotinic acid: Three crystal forms at 1.7 Å, 108Å and 2.4 Å resolution.", *J. Mol. Biol.*, **2001**, *309*, 203.
[45] Hecht, H. J.; Erdmann, H.; Park, H. J.; Sprinzl, M.; Schmid, R. D., "Crystal-Structure of Nadh Oxidase from Thermus-Thermophilus", *Nat Struct Biol*, **1995**, *2*, 1109.
[46] Tanner, J. J.; Lei, B. F.; Tu, S. C.; Krause, K. L., "Flavin reductase P: Structure of a dimeric enzyme that reduces flavin", *Biochemistry*, **1996**, *35*, 13531.

[47] Koike, H.; Sasaki, H.; Kobori, T.; Zenno, S.; Saigo, K.; Murphy, M. E. P.; Adman, E. T.; Tanokura, M., "1.8 angstrom crystal structure of the major NAD(P)H : FMN oxidoreductase of a bioluminescent bacterium, Vibrio fischeri: Overall structure, cofactor and substrate-analog binding, and comparison with related flavoproteins", *Journal of molecular biology*, **1998**, *280*, 259.

[48] Zenno, S. H.; Koike, H.; Tanokura, M.; Saigo, K., "Conversion of NfsB, a minor Escherichia coli nitroreductase, to a flavin reductase similar in biochemical properties to FRase I, the major flavin reductase in Vibrio fischeri, by a single amino acid substitution", *Journal of bacteriology*, **1996**, *178*, 4731.

[49] Whiteway, J.; Koziarz, P.; Veall, J.; Sandhu, N.; Kumar, P.; Hoecher, B.; Lambert, I. B., "Oxygen-insensitive nitroreductases: Analysis of the roles of nfsA and nfsB in development of resistance to 5-nitrofuran derivatives in Escherichia coli", *Journal of bacteriology*, **1998**, *180*, 5529.

[50] Grove, J. I.; Lovering, A. L.; Guise, C.; Race, P. R.; Wrighton, C. J.; White, S. A.; Hyde, E. I.; Searle, P. F., "Generation of Escherichia coli nitroreductase mutants conferring improved cell sensitization to the prodrug CB1954", *Cancer research*, **2003**, *63*, 5532.

[51] Guise, C. P.; Grove, J. I.; Hyde, E. I.; Searle, P. F., "Direct positive selection for improved nitroreductase variants using SOS triggering of bacteriophage lambda lytic cycle", *Gene Ther*, **2007**, *14*, 690.

[52] Jarrom, D.; Jaberipour, M.; Guise, C. P.; Daff, S.; White, S. A.; Searle, P. F.; Hyde, E. I., "Steady-State and Stopped-Flow Kinetic Studies of Three Escherichia coli NfsB Mutants with Enhanced Activity for the Prodrug CB1954", *Biochemistry*, **2009**, *48*, 7665.

[53] Christofferson, A.; Wilkie, J., "Mechanism of CB1954 reduction by Escherichia coli nitroreductase", *Biochem Soc T*, **2009**, *37*, 413.

[54] Snape, J. R.; Walkley, N. A.; Morby, A. P.; Nicklin, S.; White, G. F., "Purification, properties, and sequence of glycerol trinitrate reductase from Agrobacterium radiobacter", *Journal of bacteriology*, **1997**, *179*, 7796.

[55] French, C. E.; Nicklin, S.; Bruce, N. C., "Sequence and properties of pentaerythritol tetranitrate reductase from Enterobacter cloacae PB2", *Journal of bacteriology*, **1996**, *178*, 6623.

[56] Spain, J. C., "Biodegradation of Nitroaromatic Compounds", *Annu Rev Microbiol*, **1995**, *49*, 523.

[57] Roldan, M.; Perez-Reinado, E.; Castillo, F.; Moreno-Vivian, C., "Reduction of polynitroaromatic compounds: the bacterial nitroreductases", *Fems Microbiol Rev*, **2008**, *32*, 474.

[58] Nishino, S. F.; Spain, J. C., "Degradation of Nitrobenzene by a Pseudomonas-Pseudoalcaligenes", *Appl Environ Microb*, **1993**, *59*, 2520.

[59] Spiess, T.; Desiere, F.; Fischer, P.; Spain, J. C.; Knackmuss, H. J.; Lenke, H., "A new 4-nitrotoluene degradation pathway in a Mycobacterium strain", *Appl Environ Microb*, **1998**, *64*, 446.

[60] Roldan, M. D.; Blasco, R.; Caballero, F. J.; Castillo, F., "Degradation of p-nitrophenol by the phototrophic bacterium Rhodobacter capsulatus", *Arch Microbiol*, **1998**, *169*, 36.

[61] Yin, H.; Wood, T. K.; Smets, B. F., "Reductive transformation of TNT by Escherichia coli: pathway description", *Appl Microbiol Biot*, **2005**, *67*, 397.
[62] Stenuit, B.; Eyers, L.; Rozenberg, R.; Habib-Jiwan, J. L.; Agathos, S. N., "Aerobic growth of Escherichia coli with 2,4,6-trinitrotoluene (TNT) as the sole nitrogen source and evidence of TNT denitration by whole cells and cell-free extracts", *Appl Environ Microb*, **2006**, *72*, 7945.
[63] Zarlpov, S. A.; Naumov, A. V.; Abdrakhmanova, J. F.; Garusov, A. V.; Naumma, R. P., "Models of 2,4,6-trinitrotoluene (TNT) initial conversion by yeasts", *Fems Microbiol Lett*, **2002**, *217*, 213.
[64] Kim, H. Y.; Bennett, G. N.; Song, H. G., "Degradation of 2,4,6-trinitrotoluene by Klebsiella sp isolated from activated sludge", *Biotechnol Lett*, **2002**, *24*, 2023.
[65] Oh, B. T.; Shea, P. J.; Drijber, R. A.; Vasilyeva, G. K.; Sarath, G., "TNT biotransformation and detoxification by a Pseudomonas aeruginosa strain", *Biodegradation*, **2003**, *14*, 309.
[66] Park, C.; Kim, T. H.; Kim, S.; Kim, S. W.; Lee, J.; Kim, S. H., "Optimization for biodegradation of 2,4,6-trinitrotoluene (TNT) by Pseudomonas putida", *J Biosci Bioeng*, **2003**, *95*, 567.
[67] Kim, H. Y.; Song, H. G., "Transformation and mineralization of 2,4,6-trinitrotoluene by the white rot fungus Irpex lacteus", *Appl Microbiol Biot*, **2003**, *61*, 150.
[68] Jain, M. R.; Zinjarde, S. S.; Deobagkar, D. D.; Deobagkar, D. N., "2,4,6-Trinitrotoluene transformation by a tropical marine yeast, Yarrowia lipolytica NCIM 3589", *Mar Pollut Bull*, **2004**, *49*, 783.
[69] Borch, T.; Inskeep, W. P.; Harwood, J. A.; Gerlach, R., "Impact of ferrihydrite and anthraquinone-2,6-disulfonate on the reductive transformation of 2,4,6-trinitrotoluene by a gram-positive fermenting bacterium", *Environ Sci Technol*, **2005**, *39*, 7126.
[70] Hoehamer, C. F.; Wolfe, N. L.; Eriksson, K. E. L., "Biotransformation of 2,4,6-trinitrotoluene (tnt) by the fungus Fusarium oxysporum", *Int J Phytoremediat*, **2006**, *8*, 95.
[71] Claus, H.; Bausinger, T.; Lehmler, I.; Perret, N.; Fels, G.; Dehner, U.; Preuss, J.; Konig, H., "Transformation of 2,4,6-trinitrotoluene (TNT) by Raoultella terrigena", *Biodegradation*, **2007**, *18*, 27.
[72] Anlezark, G. M.; Melton, R. G.; Sherwood, R. F.; Coles, B.; Friedlos, F.; Knox, R. J., "The Bioactivation of 5-(Aziridin-1-Yl)-2,4-Dinitrobenzamide (Cb1954) .1. Purification and Properties of a Nitroreductase Enzyme from Escherichia-Coli - a Potential Enzyme for Antibody-Directed Enzyme Prodrug Therapy (Adept)", *Biochemical pharmacology*, **1992**, *44*, 2289.
[73] Knox, R. J.; Friedlos, F.; Jarman, M.; Davies, L. C.; Goddard, P.; Anlezark, G. M.; Melton, R. G.; Sherwood, R. F., "Virtual Cofactors for an Escherichia-Coli Nitroreductase Enzyme - Relevance to Reductively Activated Prodrugs in Antibody-Directed Enzyme Prodrug Therapy (Adept)", *Biochemical pharmacology*, **1995**, *49*, 1641.
[74] Hay, M. P.; Wilson, W. R.; Denny, W. A., "A Novel Enediyne Prodrug for Antibody-Directed Enzyme Prodrug Therapy (Adept) Using Escherichia-Coli-B Nitroreductase", *Bioorg Med Chem Lett*, **1995**, *5*, 2829.

[75] Hay, M. P.; Wilson, W. R.; Denny, W. A., "Nitrobenzyl carbamate prodrugs of enediynes for nitroreductase gene-directed enzyme prodrug therapy (GDEPT)", *Bioorg Med Chem Lett*, **1999**, *9*, 3417.
[76] Denny, W. A., "Nitroreductase-based GDEPT", *Curr Pharm Design*, **2002**, *8*, 1349.
[77] Helsby, N. A.; Ferry, D. M.; Patterson, A. V.; Pullen, S. M.; Wilson, W. R., "2-Amino metabolites are key mediators of CB 1954 and SN 23862 bystander effects in nitroreductase GDEPT", *Brit J Cancer*, **2004**, *90*, 1084.
[78] McNeish, I. A.; Green, N. K.; Gilligan, M. G.; Ford, M. J.; Mautner, V.; Young, L. S.; Kerr, D. J.; Searle, P. F., "Virus directed enzyme prodrug therapy for ovarian and pancreatic cancer using retrovirally delivered E-coli nitroreductase and CB1954", *Gene Ther*, **1998**, *5*, 1061.
[79] Palmer, D. H.; Mautner, V.; Mirza, D.; Oliff, S.; Gerritsen, W.; van der Sijp, J. R. M.; Hubscher, S.; Reynolds, G.; Bonney, S.; Rajaratnam, R.; Hull, D.; Horne, M.; Ellis, J.; Mountain, A.; Hill, S.; Harris, P. A.; Searle, P. F.; Young, L. S.; James, N. D.; Kerr, D. J., "Virus-directed enzyme prodrug therapy: Intratumoral administration of a replication-deficient adenovirus encoding nitroreductase to patients with resectable liver cancer", *J Clin Oncol*, **2004**, *22*, 1546.
[80] Hoogenraad, M.; van der Linden, J. B.; Smith, A. A.; Hughes, B.; Derrick, A. M.; Harris, L. J.; Higginson, P. D.; Pettman, A. J., "Accelerated process development of pharmaceuticals: Selective catalytic hydrogenations of nitro compounds containing other functionalities", *Org Process Res Dev*, **2004**, *8*, 469.
[81] Haber, F., "Elektrolytische Darstellung von Phenyl-β-Hydroxylamin", *Zeitschrift für Elektrochemie*, **1898**, *5*, 77.
[82] Corma, A.; Concepcion, P.; Serna, P., "A different reaction pathway for the reduction of aromatic nitro compounds on gold catalysts", *Angew Chem Int Edit*, **2007**, *46*, 7266.
[83] Hornback, J. M. *Organic chemistry*; 2nd ed.; Thomson: Belmont, CA, 2005.
[84] Carey, F. A. *Organic chemistry*; 6th ed.; McGraw-Hill: Dubuque, IA, 2006.
[85] Haber, F., "Über die elektrolytische Reduction der Nitrokörper", *Angewandte Chemie*, **1900**, *13*, 433.
[86] Cornils, B.; Herrmann, W. A. *Applied homogeneous catalysis with organometallic compounds*; VCH Weinheim etc., 1996; Vol. 2.
[87] Corma, A.; Serna, P., "Chemoselective hydrogenation of nitro compounds with supported gold catalysts", *Science*, **2006**, *313*, 332.
[88] Rylander, P. N. *Catalytic hydrogenation in organic syntheses*; Academic Press: New York, 1979.
[89] Schabel, T.; Belger, C.; Plietker, B., "A Mild Chemoselective Ru-Catalyzed Reduction of Alkynes, Ketones, and Nitro Compounds", *Org Lett*, **2013**, *15*, 2858.
[90] Tafesh, A. M.; Weiguny, J., "A review of the selective catalytic reduction of aromatic nitro compounds into aromatic amines, isocyanates, carbamates, and ureas using CO", *Chem Rev*, **1996**, *96*, 2035.
[91] Nishimura, S. *Handbook of heterogeneous catalytic hydrogenation for organic synthesis*; J. Wiley: New York, 2001.

[92] Corma, A.; Serna, P.; Concepcion, P.; Calvino, J. J., "Transforming nonselective into chemoselective metal catalysts for the hydrogenation of substituted nitroaromatics", *J Am Chem Soc*, **2008**, *130*, 8748.
[93] Wienhofer, G.; Sorribes, I.; Boddien, A.; Westerhaus, F.; Junge, K.; Junge, H.; Llusar, R.; Beller, M., "General and Selective Iron-Catalyzed Transfer Hydrogenation of Nitroarenes without Base", *J Am Chem Soc*, **2011**, *133*, 12875.
[94] Khan, F. A.; Dash, J.; Sudheer, C.; Gupta, R. K., "Chemoselective reduction of aromatic nitro and azo compounds in ionic liquids using zinc and ammonium salts", *Tetrahedron Lett*, **2003**, *44*, 7783.
[95] Imai, H.; Nishiguchi, T.; Fukuzumi, K., "Homogeneous Catalytic Reduction of Aromatic Nitro-Compounds by Hydrogen Transfer", *Chem Lett*, **1976**, 655.
[96] Watanabe, Y.; Ohta, T.; Tsuji, Y.; Hiyoshi, T.; Tsuji, Y., "Ruthenium Catalyzed Reduction of Nitroarenes and Azaaromatic Compounds Using Formic-Acid", *B Chem Soc Jpn*, **1984**, *57*, 2440.
[97] Bentaleb, A.; Jenner, G., "Synthesis of Aminoarenes in Homogeneously Catalyzed Nitroarene Methyl Formate Reactions", *J Mol Catal*, **1994**, *91*, L149.
[98] Sharma, U.; Kumar, P.; Kumar, N.; Kumar, V.; Singh, B., "Highly Chemo- and Regioselective Reduction of Aromatic Nitro Compounds Catalyzed by Recyclable Copper(II) as well as Cobalt(II) Phthalocyanines", *Adv Synth Catal*, **2010**, *352*, 1834.
[99] Jagadeesh, R. V.; Surkus, A. E.; Junge, H.; Pohl, M. M.; Radnik, J.; Rabeah, J.; Huan, H. M.; Schunemann, V.; Bruckner, A.; Beller, M., "Nanoscale Fe2O3-Based Catalysts for Selective Hydrogenation of Nitroarenes to Anilines", *Science*, **2013**, *342*, 1073.
[100] Alsante, K. M.; Huynh-Ba, K. C.; Baertschi, S. W.; Reed, R. A.; Landis, M. S.; Furness, S.; Olsen, B.; Mowery, M.; Russo, K.; Iser, R., "Recent Trends in Product Development and Regulatory Issues on Impurities in Active Pharmaceutical Ingredient (API) and Drug Products. Part 2: Safety Considerations of Impurities in Pharmaceutical Products and Surveying the Impurity Landscape", *AAPS PharmSciTech*, **2013**, 1.
[101] use, C. f. m. p. f. h. *Guideline on the Specification Limit for Residues of Metal Catalysts or Metal Reagents, Doc. No*, EMEA/CHMP/SWP/4446/2000, European Medicines Agency, London, UK, 2008.
[102] Stuermer, R.; Hauer, B.; Hall, M.; Faber, K., "Asymmetric bioreduction of activated C=C bonds using enoate reductases from the old yellow enzyme family", *Current opinion in chemical biology*, **2007**, *11*, 203.
[103] Hall, M.; Yanto, Y.; Bommarius, A. S.; Flickinger, M. C. In *Encyclopedia of Industrial Biotechnology*; John Wiley & Sons, Inc.: 2009.
[104] Warburg, O.; Christian, W., "Ein zweites sauerstoffübertragendes Ferment und sein Absorptionsspektrum", *Naturwissenschaften*, **1932**, *20*, 688.
[105] Saito, K.; Thiele, D. J.; Davio, M.; Lockridge, O.; Massey, V., "The Cloning and Expression of a Gene Encoding Old Yellow Enzyme from Saccharomyces-Carlsbergensis", *Journal of Biological Chemistry*, **1991**, *266*, 20720.
[106] Stott, K.; Saito, K.; Thiele, D. J.; Massey, V., "Old Yellow Enzyme - the Discovery of Multiple Isozymes and a Family of Related Proteins", *Journal of Biological Chemistry*, **1993**, *268*, 6097.

[107] Niino, Y. S.; Chakraborty, S.; Brown, B. J.; Massey, V., "A New Old Yellow Enzyme of Saccharomyces-Cerevisiae", *Journal of Biological Chemistry*, **1995**, *270*, 1983.
[108] French, C. E.; Bruce, N. C., "Purification and Characterization of Morphinone Reductase from Pseudomonas-Putida M10", *Biochem J*, **1994**, *301*, 97.
[109] Miura, K.; Tomioka, Y.; Suzuki, H.; Yonezawa, M.; Hishinuma, T.; Mizugaki, M., "Molecular cloning of the nemA gene encoding N-ethylmaleimide reductase from Escherichia coli", *Biol Pharm Bull*, **1997**, *20*, 110.
[110] Blehert, D. S.; Fox, B. G.; Chambliss, G. H., "Cloning and sequence analysis of two Pseudomonas flavoprotein xenobiotic reductases", *Journal of bacteriology*, **1999**, *181*, 6254.
[111] Kubata, B. K.; Kabututu, Z.; Nozaki, T.; Munday, C. J.; Fukuzumi, S.; Ohkubo, K.; Lazarus, M.; Maruyama, T.; Martin, S. K.; Duszenko, M.; Urade, Y., "A key role for old yellow enzyme in the metabolism of drugs by Trypanosoma cruzi", *J Exp Med*, **2002**, *196*, 1241.
[112] Schaller, F.; Hennig, P.; Weiler, E. W., "12-oxophytodienoate-10,11-reductase: Occurrence of two isoenzymes of different specificity against stereoisomers of 12-oxophytodienoic acid", *Plant Physiol*, **1998**, *118*, 1345.
[113] Strassner, J.; Schaller, F.; Frick, U. B.; Howe, G. A.; Weiler, E. W.; Amrhein, N.; Macheroux, P.; Schaller, A., "Characterization and cDNA-microarray expression analysis of 12-oxophytodienoate reductases reveals differential roles for octadecanoid biosynthesis in the local versus the systemic wound response", *Plant J*, **2002**, *32*, 585.
[114] Fitzpatrick, T. B.; Amrhein, N.; Macheroux, P., "Characterization of YqjM, an old yellow enzyme homolog from Bacillus subtilis involved in the oxidative stress response", *Journal of Biological Chemistry*, **2003**, *278*, 19891.
[115] Brige, A.; Van den Hemel, D.; Carpentier, W.; De Smet, L.; Van Beeumen, J. J., "Comparative characterization and expression analysis of the four Old Yellow Enzyme homologues from Shewanella oneidensis indicate differences in physiological function", *Biochem J*, **2006**, *394*, 335.
[116] Chaparro-Riggers, J. F.; Rogers, T. A.; Vazquez-Figueroa, E.; Polizzi, K. M.; Bommarius, A. S., "Comparison of three enoate reductases and their potential use for biotransformations", *Adv Synth Catal*, **2007**, *349*, 1521.
[117] Muller, A.; Hauer, B.; Rosche, B., "Asymmetric alkene reduction by yeast old yellow enzymes and by a novel Zymomonas mobilis reductase", *Biotechnol Bioeng*, **2007**, *98*, 22.
[118] Adalbjornsson, B. V.; Toogood, H. S.; Fryszkowska, A.; Pudney, C. R.; Jowitt, T. A.; Leys, D.; Scrutton, N. S., "Biocatalysis with Thermostable Enzymes: Structure and Properties of a Thermophilic 'ene'-Reductase related to Old Yellow Enzyme", *Chembiochem*, **2010**, *11*, 197.
[119] Opperman, D. J.; Piater, L. A.; van Heerden, E., "A novel chromate reductase from Thermus scotoductus SA-01 related to old yellow enzyme", *Journal of bacteriology*, **2008**, *190*, 3076.
[120] Banner, D. W.; Bloomer, A. C.; Petsko, G. A.; Phillips, D. C.; Pogson, C. I.; Wilson, I. A.; Corran, P. H.; Furth, A. J.; Milman, J. D.; Offord, R. E.; Priddle, J. D.; Waley, S. G., "Structure of Chicken Muscle Triose Phosphate Isomerase

Determined Crystallographically at 2.5a Resolution Using Amino-Acid Sequence Data", *Nature*, **1975**, *255*, 609.
[121] Vaz, A. D. N.; Chakraborty, S.; Massey, V., "Old Yellow Enzyme - Aromatization of Cyclic Enones and the Mechanism of a Novel Dismutation Reaction", *Biochemistry*, **1995**, *34*, 4246.
[122] Knowles, W. S., "Asymmetric hydrogenations (Nobel lecture)", *Angew Chem Int Edit*, **2002**, *41*, 1999.
[123] Noyori, R., "Asymmetric catalysis: Science and opportunities (Nobel lecture)", *Angew Chem Int Edit*, **2002**, *41*, 2008.
[124] Messiha, H. L.; Bruce, N. C.; Sattelle, B. M.; Sutcliffe, M. J.; Munro, A. W.; Scrutton, N. S., "Role of active site residues and solvent in proton transfer and the modulation of flavin reduction potential in bacterial morphinone reductase", *Journal of Biological Chemistry*, **2005**, *280*, 27103.
[125] Brown, B. J.; Deng, Z.; Karplus, P. A.; Massey, V., "On the active site of old yellow enzyme - Role of histidine 191 and asparagine 194", *Journal of Biological Chemistry*, **1998**, *273*, 32753.
[126] Kohli, R. M.; Massey, V., "The oxidative half-reaction of old yellow enzyme - The role of tyrosine 196", *Journal of Biological Chemistry*, **1998**, *273*, 32763.
[127] Higuchi, M.; Shimada, M.; Yamamoto, Y.; Hayashi, T.; Koga, T.; Kamio, Y., "Identification of two distinct NADH oxidases corresponding to H2O2-forming oxidase and H2O-forming oxidase induced in Streptococcus mutans", *Journal of general microbiology*, **1993**, *139*, 2343.
[128] Riebel, B. R.; Gibbs, P. R.; Wellborn, W. B.; Bommarius, A. S., "Cofactor regeneration of NAD(+) from NADH: Novel water-forming NADH oxidases", *Adv Synth Catal*, **2002**, *344*, 1156.
[129] Ahmed, S. A.; Claiborne, A., "The Streptococcal Flavoprotein Nadh Oxidase .1. Evidence Linking Nadh Oxidase and Nadh Peroxidase Cysteinyl Redox Centers", *Journal of Biological Chemistry*, **1989**, *264*, 19856.
[130] Lountos, G. T.; Jiang, R. R.; Wellborn, W. B.; Thaler, T. L.; Bommarius, A. S.; Orville, A. M., "The crystal structure of NAD(P)H oxidase from Lactobacillus sanfranciscensis: Insights into the conversion of O-2 into two water molecules by the flavoenzyme", *Biochemistry*, **2006**, *45*, 9648.
[131] Matsumoto, J.; Higuchi, M.; Shimada, M.; Yamamoto, Y.; Kamio, Y., "Molecular cloning and sequence analysis of the gene encoding the H2O-forming NADH oxidase from Streptococcus mutans", *Biosci Biotech Bioch*, **1996**, *60*, 39.
[132] Ross, R. P.; Claiborne, A., "Molecular-Cloning and Analysis of the Gene Encoding the Nadh Oxidase from Streptococcus-Faecalis 10c1 - Comparison with Nadh Peroxidase and the Flavoprotein Disulfide Reductases", *Journal of molecular biology*, **1992**, *227*, 658.
[133] Hummel, W.; Riebel, B., "Isolation and biochemical characterization of a new NADH oxidase from Lactobacillus brevis", *Biotechnol Lett*, **2003**, *25*, 51.
[134] Jiang, R. R.; Riebel, B. R.; Bommarius, A. S., "Comparison of alkyl hydroperoxide reductase (AhpR) and water-forming NADH oxidase from Lactococcus lactis ATCC 19435", *Adv Synth Catal*, **2005**, *347*, 1139.

[135] Kleiger, G.; Eisenberg, D., "GXXXG and GXXXA motifs stabilize FAD and NAD(P)-binding Rossmann folds through C-alpha-H center dot center dot center dot O hydrogen bonds and van der Waals interactions", *Journal of molecular biology*, **2002**, *323*, 69.
[136] Geueke, B.; Riebel, B.; Hummel, W., "NADH oxidase from Lactobacillus brevis: a new catalyst for the regeneration of NAD", *Enzyme and Microbial Technology*, **2003**, *32*, 205.
[137] Gibson, C. M.; Mallett, T. C.; Claiborne, A.; Caparon, M. G., "Contribution of NADH oxidase to aerobic metabolism of Streptococcus pyogenes", *Journal of bacteriology*, **2000**, *182*, 448.
[138] Mande, S. S.; Parsonage, D.; Claiborne, A.; Hol, W. G. J., "Crystallographic Analyses of Nadh Peroxidase Cys42ala and Cys42ser Mutants - Active-Site Structures, Mechanistic Implications, and an Unusual Environment of Arg-303", *Biochemistry*, **1995**, *34*, 6985.
[139] Claiborne, A.; Yeh, J. I.; Mallett, T. C.; Luba, J.; Crane, E. J.; Charrier, V.; Parsonage, D., "Protein-sulfenic acids: Diverse roles for an unlikely player in enzyme catalysis and redox regulation", *Biochemistry*, **1999**, *38*, 15407.
[140] Mallett, T. C.; Claiborne, A., "Oxygen reactivity of an NADH oxidase C42S mutant: Evidence for a C(4a)-peroxyflavin intermediate and a rate-limiting conformational change", *Biochemistry*, **1998**, *37*, 8790.
[141] Poole, L. B.; Claiborne, A., "The Non-Flavin Redox Center of the Streptococcal Nadh Peroxidase .2. Evidence for a Stabilized Cysteine-Sulfenic Acid", *Journal of Biological Chemistry*, **1989**, *264*, 12330.
[142] Stehle, T.; Ahmed, S. A.; Claiborne, A.; Schulz, G. E., "Refined Structure of Nadh Peroxidase from Streptococcus-Faecalis 10c1 at 2.16 a Resolution", *Faseb Journal*, **1991**, *5*, A1560.
[143] Odman, P.; Wellborn, W. B.; Bommarius, A. S., "An enzymatic process to alpha-ketoglutarate from L-glutamate: the coupled system L-glutamate dehydrogenase/NADH oxidase", *Tetrahedron-Asymmetry*, **2004**, *15*, 2933.
[144] Chenault, H. K.; Whitesides, G. M., "Regeneration of Nicotinamide Cofactors for Use in Organic-Synthesis", *Applied Biochemistry and Biotechnology*, **1987**, *14*, 147.
[145] Weckbecker, A.; Groger, H.; Hummel, W., "Regeneration of Nicotinamide Coenzymes: Principles and Applications for the Synthesis of Chiral Compounds", *Adv Biochem Eng Biot*, **2010**, *120*, 195.
[146] Wu, H.; Tian, C. Y.; Song, X. K.; Liu, C.; Yang, D.; Jiang, Z. Y., "Methods for the regeneration of nicotinamide coenzymes", *Green Chem*, **2013**, *15*, 1773.
[147] Paul, C. E.; Arends, I. W. C. E.; Hollmann, F., "Is Simpler Better? Synthetic Nicotinamide Cofactor Analogues for Redox Chemistry", *Acs Catal*, **2014**, *4*, 788.
[148] Bommarius, B.; Au, S. K.; Markou, G. C.; Bommarius, A. S. In *Zing Biocatalysis* Xcaret, Mexico, 2012, December
[149] Schutte, H.; Flossdorf, J.; Sahm, H.; Kula, M. R., "Purification and Properties of Formaldehyde Dehydrogenase and Formate Dehydrogenase from Candida-Boidinii", *European Journal of Biochemistry*, **1976**, *62*, 151.

[150] Allen, S. J.; Holbrook, J. J., "Isolation, Sequence and Overexpression of the Gene Encoding Nad-Dependent Formate Dehydrogenase from the Methylotrophic Yeast Candida-Methylica", *Gene*, **1995**, *162*, 99.
[151] Nanba, H.; Takaoka, Y.; Hasegawa, J., "Purification and characterization of an alpha-haloketone-resistant formate dehydrogenase from Thiobacillus sp strain KNK65MA, and cloning of the gene", *Biosci Biotech Bioch*, **2003**, *67*, 2145.
[152] Bright, J. R.; Byrom, D.; Danson, M. J.; Hough, D. W.; Towner, P., "Cloning, Sequencing and Expression of the Gene Encoding Glucose-Dehydrogenase from the Thermophilic Archaeon Thermoplasma-Acidopilum", *European Journal of Biochemistry*, **1993**, *211*, 549.
[153] Vazquez-Figueroa, E.; Chaparro-Riggers, J.; Bommarius, A. S., "Development of a thermostable glucose dehydrogenase by a structure-guided consensus concept", *Chembiochem*, **2007**, *8*, 2295.
[154] Okuno, H.; Nagata, K.; Nakajima, H., "Purification and properties of glucose-6-phosphate dehydrogenase from Bacillus stearothermophilus", *Journal of applied biochemistry*, **1985**, *7*, 192.
[155] Naylor, C. E.; Gover, S.; Basak, A. K.; Cosgrove, M. S.; Levy, H. R.; Adams, M. J., "NADP(+) and NAD(+) binding to the dual coenzyme specific enzyme Leuconostoc mesenteroides glucose 6-phosphate dehydrogenase: different interdomain hinge angles are seen in different binary and ternary complexes", *Acta Crystallogr D*, **2001**, *57*, 635.
[156] Drewke, C.; Ciriacy, M., "Overexpression, Purification and Properties of Alcohol Dehydrogenase-Iv from Saccharomyces-Cerevisiae", *Biochim Biophys Acta*, **1988**, *950*, 54.
[157] Adolph, H. W.; Maurer, P.; Schneiderbernlohr, H.; Sartorius, C.; Zeppezauer, M., "Substrate-Specificity and Stereoselectivity of Horse Liver Alcohol-Dehydrogenase - Kinetic Evaluation of Binding and Activation Parameters Controlling the Catalytic Cycles of Unbranched, Acyclic Secondary Alcohols and Ketones as Substrates of the Native and Active-Site-Specific Co(Ii)-Substituted Enzyme", *European Journal of Biochemistry*, **1991**, *201*, 615.
[158] vanIersel, M. F. M.; Eppink, M. H. M.; vanBerkel, W. J. H.; Rombouts, F. M.; Abee, T., "Purification and characterization of a novel NADP-dependent branched-chain alcohol dehydrogenase from Saccharomyces cerevisiae", *Appl Environ Microb*, **1997**, *63*, 4079.
[159] Keinan, E.; Hafeli, E. K.; Seth, K. K.; Lamed, R., "Thermostable Enzymes in Organic-Synthesis .2. Asymmetric Reduction of Ketones with Alcohol-Dehydrogenase from Thermoanaerobium-Brockii", *J Am Chem Soc*, **1986**, *108*, 162.
[160] Johannes, T. W.; Woodyer, R. D.; Zhao, H. M., "Directed evolution of a thermostable phosphite dehydrogenase for NAD(P)H regeneration", *Appl Environ Microb*, **2005**, *71*, 5728.
[161] Johannes, T. W.; Woodyer, R. D.; Zhao, H. M., "Efficient regeneration of NADPH using an engineered phosphite dehydrogenase", *Biotechnol Bioeng*, **2007**, *96*, 18.
[162] Race, P. R.; Lovering, A. L.; Green, R. M.; Ossor, A.; White, S. A.; Searle, P. F.; Wrighton, C. J.; Hyde, E. I., "Structural and mechanistic studies of Escherichia

coli nitroreductase with the antibiotic nitrofurazone. Reversed binding orientations in different redox states of the enzyme", *The Journal of biological chemistry*, **2005**, *280*, 13256.
[163] Bradford, M. M., "Rapid and Sensitive Method for Quantitation of Microgram Quantities of Protein Utilizing Principle of Protein-Dye Binding", *Anal Biochem*, **1976**, *72*, 248.
[164] Chapman, S. K.; Reid, G. A. *Flavoprotein protocols*; Springer, 1999; Vol. 131.
[165] Bauer, H.; Rosenthal, S. M., "4-hydroxylaminobenzenesulfonamide, its acetyl derivatives and diazotization reaction", *J Am Chem Soc*, **1944**, *66*, 611.
[166] Corbett, M. D.; Wei, C.-i.; Corbett, B. R., "Nitroreductase-dependent mutagenicity of p-nitrophenythydroxylamine and its N-acetyl and N-formyl hydroxamic acids", *Carcinogenesis*, **1985**, *6*, 727.
[167] Corbett, M. D.; Corbett, B. R., "Effect of Ring Substituents on the Transketolase-Catalyzed Conversion of Nitroso Aromatics to Hydroxamic Acids", *Biochemical pharmacology*, **1986**, *35*, 3613.
[168] Kuhn, R.; Weygand, F., "o-und p-Nitro-phenylhydroxylamin", *Berichte der deutschen chemischen Gesellschaft (A and B Series)*, **1936**, *69*, 1969.
[169] Bamberger, E., "Ueber das Phenylhydroxylamin", *Berichte der deutschen chemischen Gesellschaft*, **1894**, *27*, 1548.
[170] Ogata, Y.; Sawaki, Y.; Mibae, J.; Morimoto, T., "Kinetics of the Autoxidation of Phenylhydroxylamines to Azoxybenzenes in Methanol", *J Am Chem Soc*, **1964**, *86*, 3854.
[171] White, R. C.; Selvam, T.; Ihmels, H.; Adam, W., "Photolysis of N-phenylhydroxylamine: a novel photochemical disproportionation reaction in N-O bond cleavage assisted by hydrogen bonding", *J Photoch Photobio A*, **1999**, *122*, 7.
[172] Channon, H. J.; Mills, G. T.; Williams, R. T., "The metabolism of 2 : 4 : 6-trinitrotoluene (alpha-TNT)", *Biochem J*, **1944**, *38*, 70.
[173] Pitsawong, W.; Hoben, J. P.; Miller, A. F., "Understanding the Broad Substrate Repertoire of Nitroreductase Based on its Kinetic Mechanism", *The Journal of biological chemistry*, **2014**.
[174] Xie, B.; Yang, J.; Yang, Q., "Isolation and characterization of an efficient nitro-reducing bacterium, Streptomyces mirabils DUT001, from soil", *World J Microb Biot*, **2010**, *26*, 855.
[175] Mccormick, N. G.; Feeherry, F. E.; Levinson, H. S., "Microbial Transformation of 2,4,6-Trinitrotoluene and Other Nitroaromatic Compounds", *Appl Environ Microb*, **1976**, *31*, 949.
[176] Koder, R. L.; Miller, A. F., "Overexpression, isotopic labeling, and spectral characterization of Enerobacter cloacae nitroreductase", *Protein Expres Purif*, **1998**, *13*, 53.
[177] Michaelis, L.; Menten, M. L., "Die kinetik der invertinwirkung", *Biochem. z*, **1913**, *49*, 352.
[178] Lambert, C.; Leonard, N.; De Bolle, X.; Depiereux, E., "ESyPred3D: Prediction of proteins 3D structures", *Bioinformatics*, **2002**, *18*, 1250.
[179] version 11.02 ed.; Advanced Chemistry Development, Inc., Toronto, On, Canada, www.acdlabs.com: 2014.

[180] Li, F.; Cui, J. N.; Qian, X. H.; Zhang, R., "A novel strategy for the preparation of arylhydroxylamines: chemoselective reduction of aromatic nitro compounds using bakers' yeast", *Chem Commun*, **2004**, 2338.
[181] Hansch, C.; Leo, A.; Hoekman, D. H. *Exploring QSAR*; American Chemical Society: Washington, DC, 1995.
[182] Hansch, C.; Leo, A.; Taft, R. W., "A Survey of Hammett Substituent Constants and Resonance and Field Parameters", *Chem Rev*, **1991**, *91*, 165.
[183] Hammett, L. P., "Some relations between reaction rates and equilibrium constants", *Chem Rev*, **1935**, *17*, 125.
[184] Hammett, L. P., "The effect of structure upon the reactions of organic compounds benzene derivatives", *J Am Chem Soc*, **1937**, *59*, 96.
[185] Alexandre, F. R.; Pantaleone, D. P.; Taylor, P. P.; Fotheringham, I. G.; Ager, D. J.; Turner, N. J., "Amine-boranes: effective reducing agents for the deracemisation of DL-amino acids using L-amino acid oxidase from Proteus myxofaciens", *Tetrahedron Lett*, **2002**, *43*, 707.
[186] Schnapperelle, I.; Hummel, W.; Groger, H., "Formal Asymmetric Hydration of Non-Activated Alkenes in Aqueous Medium through a "Chemoenzymatic Catalytic System"", *Chem-Eur J*, **2012**, *18*, 1073.
[187] Wang, Z.; Chinoy, Z. S.; Ambre, S. G.; Peng, W. J.; McBride, R.; de Vries, R. P.; Glushka, J.; Paulson, J. C.; Boons, G. J., "A General Strategy for the Chemoenzymatic Synthesis of Asymmetrically Branched N-Glycans", *Science*, **2013**, *341*, 379.
[188] Powell, B. F.; Overberger, C. G.; Anselme, J. P., "Chemistry of Azo-Compounds .53. Hydrosulfite Reduction of N-Nitroso-1,2,3,4-Tetrahydroisoquinolines and Oxidation of N-Amino-1,2,3,4-Tetrahydroisoquinolines", *J Heterocyclic Chem*, **1983**, *20*, 121.
[189] Audrieth, L. F.; Sveda, M., "Preparation and properties of some N-substituted sulfamic acids", *J Org Chem*, **1944**, *9*, 89.
[190] Fox, J. L., "Sodium Dithionite Reduction of Flavin", *Febs Lett*, **1974**, *39*, 53.
[191] Kolker, P. L.; Waters, W. A., "Radical-Anions of Para-Substituted Aromatic Nitrocompounds", *J Chem Soc*, **1964**, 1136.
[192] Morello, J. A.; Forster, R. E.; Craw, M. R.; Constantine, H. P., "Rate of Reaction of Dithionite Ion with Oxygen in Aqueous Solution", *J Appl Physiol*, **1964**, *19*, 522.
[193] Huang, S.-L.; Chen, T.-Y., "Reduction of Organic Compounds with Thiourea Dioxide II. The Reduction of Organic Nitrogen Compounds", *Journal of the Chinese Chemical Society*, **1975**, *22*, 91.
[194] Hutchins, R. O.; Learn, K.; Nazer, B.; Pytlewski, D.; Pelter, A., "Amine Boranes as Selective Reducing and Hydroborating Agents - a Review", *Org Prep Proced Int*, **1984**, *16*, 337.
[195] Lane, C. F., "Sodium Cyanoborohydride - Highly Selective Reducing Agent for Organic Functional Groups", *Synthesis-Stuttgart*, **1975**, 135.
[196] Zhou, L.; Lu, X. Y.; Shao, J. Z.; Chen, Y. N., "Study on Thiourea Dioxide's Reducing Capacity and Its Reactivity with Reactive Dyes", *Adv Mater Res-Switz*, **2012**, *396-398*, 1174.

[197] Nakagawa, K.; Minami, K., "Reduction of Organic Compounds with Thiourea Dioxide .1. Reduction of Ketones to Secondary Alcohols", *Tetrahedron Lett*, **1972**, 343.
[198] Nakagawa, K.; Mineo, S.; Kawamura, S.; Minami, K., "Reduction of Organic-Compounds with Thiourea Dioxide .2. Reduction of Aromatic Nitro-Compounds and Syntheses of Hydrazo Compounds", *Yakugaku Zasshi*, **1977**, *97*, 1253.
[199] SHANGXIANG, G.; KALING, Y.; ZIJIE, H.; JIGUI, W., "Study on reduction of organic compounds with thiourea dioxide", *Chin. J. Org. Chem.*, **1998**, *18*, 157.
[200] Toogood, H. S.; Gardiner, J. M.; Scrutton, N. S., "Biocatalytic Reductions and Chemical Versatility of the Old Yellow Enzyme Family of Flavoprotein Oxidoreductases", *Chemcatchem*, **2010**, *2*, 892.
[201] Oberdorfer, G.; Steinkellner, G.; Stueckler, C.; Faber, K.; Gruber, K., "Stereopreferences of Old Yellow Enzymes: Structure Correlations and Sequence Patterns in Enoate Reductases", *Chemcatchem*, **2011**, *3*, 1562.
[202] Williams, R. E.; Rathbone, D. A.; Scrutton, N. S.; Bruce, N. C., "Biotransformation of explosives by the old yellow enzyme family of flavoproteins", *Appl Environ Microb*, **2004**, *70*, 3566.
[203] Yanto, Y.; Yu, H. H.; Hall, M.; Bommarius, A. S., "Characterization of xenobiotic reductase A (XenA): study of active site residues, substrate spectrum and stability", *Chem Commun*, **2010**, *46*, 8809.
[204] Yanto, Y.; Winkler, C. K.; Lohr, S.; Hall, M.; Faber, K.; Bommarius, A. S., "Asymmetric Bioreduction of Alkenes Using Ene-Reductases YersER and KYE1 and Effects of Organic Solvents", *Org Lett*, **2011**, *13*, 2540.
[205] Griese, J. J.; Jakob, R. P.; Schwarzinger, S.; Dobbek, H., "Xenobiotic reductase A in the degradation of quinoline by Pseudomonas putida 86: Physiological function, structure and mechanism of 8-hydroxycoumarin reduction", *Journal of molecular biology*, **2006**, *361*, 140.
[206] Spiegelhauer, O.; Mende, S.; Dickert, F.; Knauer, S. H.; Ullmann, G. M.; Dobbek, H., "Cysteine as a Modulator Residue in the Active Site of Xenobiotic Reductase A: A Structural, Thermodynamic and Kinetic Study", *Journal of molecular biology*, **2010**, *398*, 66.
[207] Fox, K. M.; Karplus, P. A., "Old Yellow Enzyme at 2-Angstrom Resolution - Overall Structure, Ligand-Binding, and Comparison with Related Flavoproteins", *Structure*, **1994**, *2*, 1089.
[208] Kitzing, K.; Fitzpatrick, T. B.; Wilken, C.; Sawa, J.; Bourenkov, G. P.; Macheroux, P.; Clausen, T., "The 1.3 A crystal structure of the flavoprotein YqjM reveals a novel class of Old Yellow Enzymes", *Journal of Biological Chemistry*, **2005**, *280*, 27904.
[209] Toogood, H. S.; Fryszkowska, A.; Hulley, M.; Sakuma, M.; Mansell, D.; Stephens, G. M.; Gardiner, J. M.; Scrutton, N. S., "A Site-Saturated Mutagenesis Study of Pentaerythritol Tetranitrate Reductase Reveals that Residues 181 and 184 Influence Ligand Binding, Stereochemistry and Reactivity", *Chembiochem*, **2011**, *12*, 738.
[210] Jensen, R. A., "Enzyme Recruitment in Evolution of New Function", *Annu Rev Microbiol*, **1976**, *30*, 409.

[211] Khersonsky, O.; Roodveldt, C.; Tawfik, D. S., "Enzyme promiscuity: evolutionary and mechanistic aspects", *Current opinion in chemical biology*, **2006**, *10*, 498.
[212] Khersonsky, O.; Tawfik, D. S., "Enzyme promiscuity: a mechanistic and evolutionary perspective", *Annual review of biochemistry*, **2010**, *79*, 471.
[213] Oberdorfer, G.; Binter, A.; Wallner, S.; Durchschein, K.; Hall, M.; Faber, K.; Macheroux, P.; Gruber, K., "The Structure of Glycerol Trinitrate Reductase NerA from Agrobacterium radiobacter Reveals the Molecular Reason for Nitro- and Ene-Reductase Activity in OYE Homologues", *Chembiochem*, **2013**, *14*, 836.
[214] Park, W. M.; Champion, J. A., "Two-Step Protein Self-Assembly in the Extracellular Matrix", *Angew Chem Int Edit*, **2013**, *52*, 8098.
[215] Woodyer, R. D.; Wymer, N. J.; Racine, F. M.; Khan, S. N.; Saha, B. C., "Efficient production of L-ribose with a recombinant Escherichia coli biocatalyst", *Appl Environ Microb*, **2008**, *74*, 2967.
[216] Riedel, E.; Nundel, M.; Hampl, H., "alpha-Ketoglutarate application in hemodialysis patients improves amino acid metabolism", *Nephron*, **1996**, *74*, 261.
[217] Teplan, V.; Schuck, O.; Votruba, M.; Poledne, R.; Kazdova, L.; Skibova, J.; Maly, J., "Metabolic effects of keto acid - amino acid supplementation in patients with chronic renal insufficiency receiving a low-protein diet and recombinant human erythropoietin - A randomized controlled trial", *Wiener Klinische Wochenschrift*, **2001**, *113*, 661.
[218] Leonida, M. D., "Redox enzymes used in chiral syntheses coupled to coenzyme regeneration", *Current Medicinal Chemistry*, **2001**, *8*, 345.
[219] van der Donk, W. A.; Zhao, H. M., "Recent developments in pyridine nucleotide regeneration", *Curr Opin Biotech*, **2003**, *14*, 421.
[220] Higuchi, M.; Yamamoto, Y.; Poole, L. B.; Shimada, M.; Sato, Y.; Takahashi, N.; Kamio, Y., "Functions of two types of NADH oxidases in energy metabolism and oxidative stress of Streptococcus mutans", *Journal of bacteriology*, **1999**, *181*, 5940.
[221] Dawson, R. M. C. *Data for biochemical research*; 3rd ed.; Clarendon Press: Oxford, 1986.
[222] Lee, L. G.; Whitesides, G. M., "Preparation of Optically-Active 1,2-Diols and Alpha-Hydroxy Ketones Using Glycerol Dehydrogenase as Catalyst - Limits to Enzyme-Catalyzed Synthesis Due to Noncompetitive and Mixed Inhibition by Product", *J Org Chem*, **1986**, *51*, 25.
[223] Slavica, A.; Dib, I.; Nidetzky, B., "Single-site oxidation, cysteine 108 to cysteine sulfinic acid, in D-amino acid oxidase from Trigonopsis variabilis and its structural and functional consequences", *Appl Environ Microb*, **2005**, *71*, 8061.
[224] Stoop, J. M. H.; Williamson, J. D.; Conkling, M. A.; MacKay, J. J.; Pharr, D. M., "Characterization of NAD-dependent mannitol dehydrogenase from celery as affected by ions, chelators, reducing agents and metabolites", *Plant Science*, **1998**, *131*, 43.
[225] Bubner, P.; Klimacek, M.; Nidetzky, B., "Structure-guided engineering of the coenzyme specificity of Pseudomonas fluorescens mannitol 2-dehydrogenase to

enable efficient utilization of NAD(H) and NADP(H)", *Febs Lett*, **2008**, *582*, 233.
[226] Woodyer, R.; van der Donk, W. A.; Zhao, H. M., "Relaxing the nicotinamide cofactor specificity of phosphite dehydrogenase by rational design", *Biochemistry*, **2003**, *42*, 11604.
[227] May, O. Presentation at Biocat 2010, Hamburg, Germany.
[228] Wang, L. A.; Wei, L.; Chen, Y. A.; Jiang, R. R., "Specific and reversible immobilization of NADH oxidase on functionalized carbon nanotubes", *J Biotechnol*, **2010**, *150*, 57.
[229] Koder, R. L.; Haynes, C. A.; Rodgers, M. E.; Rodgers, D. W.; Miller, A.-F., "Flavin thermodynamics explain the oxygen insensitivity of enteric nitroreductases.", *Biochemistry*, **2002**, *41*, 14197.
[230] Kurian, J. R.; Bajad, S. U.; Miller, J. L.; Chin, N. A.; Trepanier, L. A., "NADH cytochrome b5 reductase and cytochrome b5 catalyze the microsomal reduction of xenobiotic hydroxylamines and amidoximes in humans", *Journal of Pharmacology and Experimental Therapeutics*, **2004**, *311*, 1171.
[231] Schmidt-Dannert, C.; Arnold, F. H., "Directed evolution of industrial enzymes", *Trends in biotechnology*, **1999**, *17*, 135.
[232] Samejima, K.; Dairman, W.; Stone, J.; Udenfrie.S, "Condensation of Ninhydrin with Aldehydes and Primary Amines to Yield Highly Fluorescent Ternary Products .2. Application to Detection and Assay of Peptides, Amino Acids, Amines, and Amino Sugars", *Anal Biochem*, **1971**, *42*, 237.
[233] Udenfriend, S.; Stein, S.; Boehlen, P.; Dairman, W.; Leimgruber, W.; Weigele, M., "Fluorescamine: a reagent for assay of amino acids, peptides, proteins, and primary amines in the picomole range", *Science*, **1972**, *178*, 871.
[234] Benson, J. R.; Hare, P., "O-phthalaldehyde: fluorogenic detection of primary amines in the picomole range. Comparison with fluorescamine and ninhydrin", *Proceedings of the National Academy of Sciences*, **1975**, *72*, 619.
[235] Pospisilova, M.; Svobodova, D.; Gasparic, J.; Machacek, M., "Investigation of the Color-Reaction of Phenols with Mbth .2. Properties of the Isolated Products of the Reaction with Phenol, 2,6-Dimethylphenol and 4-Methylphenol", *Mikrochim Acta*, **1990**, *3*, 117.
[236] Sheldon, R. A., "Enzyme immobilization: The quest for optimum performance", *Adv Synth Catal*, **2007**, *349*, 1289.
[237] Watanabe, M.; Nishino, T.; Takio, K.; Sofuni, T.; Nohmi, T., "Purification and characterization of wild-type and mutant "Classical" nitroreductases of Salmonella typhimurium - L33R mutation greatly diminishes binding of FMN to the nitroreductase of S-typhimurium", *Journal of Biological Chemistry*, **1998**, *273*, 23922.
[238] Nillius, D.; Muller, J.; Muller, N., "Nitroreductase (GlNR1) increases susceptibility of Giardia lamblia and Escherichia coli to nitro drugs", *J Antimicrob Chemoth*, **2011**, *66*, 1029.
[239] Tamura, K.; Stecher, G.; Peterson, D.; Filipski, A.; Kumar, S., "MEGA6: Molecular Evolutionary Genetics Analysis Version 6.0", *Mol Biol Evol*, **2013**, *30*, 2725.

[240] Elkommos, M. E.; Emara, K. M., "Spectrophotometric Determination of Certain Local-Anesthetics Using 3-Methylbenzothiazolin-2-One Hydrazone", *Analyst*, **1987**, *112*, 1253.
[241] Lui, A. E., "Engineering of aniline dioxygenase for bioremediation and industrial applications", **2007**.

VITA

JONATHAN TAEJOO PARK

Jonathan was born in Boston, Massachusetts. After seven years, he moved to Exton, PA with his family where he attended Uwchlan Hills Elementary School. When he was nine, he moved back to South Korea and spent his school years in Korea. Jonathan was accepted to the Chemical Engineering program at Hanyang University where he graduated with Honors. He then pursued a doctoral degree at Georgia Institute of Technology within the school of Chemical & Biomolecular Engineering. Jonathan is married to Hyea Kim whom he met during graduate school and has a son, Aaron Park.